AFGL-TR-88-0203

AD-A210 109

Studies of the Cosmic Ray Penumbra

David J. Cooke

University of Utah
Physics Department
Salt Lake City, Utah 84112

1 August 1988

Final Report
9 September 1980-30 September 1985

APPROVED FOR PUBLIC RELEASE; DISTRIBUTION UNLIMITED

AIR FORCE GEOPHYSICS LABORATORY
AIR FORCE SYSTEMS COMMAND
UNITED STATES AIR FORCE
HANSCOM AIR FORCE BASE, MASSACHUSETTS 01731-5000

Contractor:	University of Utah
Principal Investigator:	David J. Cooke, Research Associate Professor Department of Physics
Prepared For:	Air Force Geophysics Laboratory
Contract Monitor:	Don F. Smart

Objectives of the Contract: To elucidate the detailed form and characteristics of the cosmic ray penumbra in order to establish the potential value of cosmic ray observations in the checking and improvement of current mathematical models of the geomagnetic field.

"This technical report has been reviewed and is approved for publication"

Don F. Smart
Contract Manager

E. G. Mullen
Chief, Space Particles Environment Branch

FOR THE COMMANDER

Rita C. Sagalyn
Director, Space Physics Division

This report has been reviewed by the ESD Public Affairs Office (PA) and is releasable to the National Technical Information Service (NTIS).

Qualified requestors may obtain additional copies from the Defense Technical Information Center. All others should apply to the National Technical Information Service.

If your address has changed, or if you wish to be removed from the mailing list, or if the addressee is no longer employed by your organization, please notify AFGL/DAA, Hanscom AFB, MA 01731. This will assist us in maintaining a current mailing list.

Do not return copies of this report unless contractual obligations or notices on a specific contract require that it be returned.

Unclassified
SECURITY CLASSIFICATION OF THIS PAGE

REPORT DOCUMENTATION PAGE

1a. REPORT SECURITY CLASSIFICATION Unclassified	1b. RESTRICTIVE MARKINGS
2a. SECURITY CLASSIFICATION AUTHORITY	3. DISTRIBUTION / AVAILABILITY OF REPORT Approved for public release; Distribution unlimited
2b. DECLASSIFICATION / DOWNGRADING SCHEDULE	
4. PERFORMING ORGANIZATION REPORT NUMBER(S)	5. MONITORING ORGANIZATION REPORT NUMBER(S) AFGL-TR-88-0203
6a. NAME OF PERFORMING ORGANIZATION University of Utah 6b. OFFICE SYMBOL (If applicable)	7a. NAME OF MONITORING ORGANIZATION Air Force Geophysics Laboratory
6c. ADDRESS (City, State, and ZIP Code) Physics Department Salt Lake City, Utah 84112	7b ADDRESS (City, State, and ZIP Code) Hanscom AFB Massachusetts 01731-5000
8a. NAME OF FUNDING / SPONSORING ORGANIZATION 8b OFFICE SYMBOL (If applicable)	9. PROCUREMENT INSTRUMENT IDENTIFICATION NUMBER F19628-81-K-0020
8c. ADDRESS (City, State, and ZIP Code)	10. SOURCE OF FUNDING NUMBERS PROGRAM ELEMENT NO. 61102F; PROJECT NO. 2311; TASK NO. G1; WORK UNIT ACCESSION NO. AP

11. TITLE (Include Security Classification)

Studies of the Cosmic Ray Penumbra

12. PERSONAL AUTHOR(S)
David J. Cooke

13a. TYPE OF REPORT	13b. TIME COVERED	14. DATE OF REPORT (Year, Month, Day)	15. PAGE COUNT
FINAL REPORT	FROM 9/9/80 TO 9/30/85	1988 August 1	110

16. SUPPLEMENTARY NOTATION

17. COSATI CODES			18. SUBJECT TERMS (Continue on reverse if necessary and identify by block number)
FIELD	GROUP	SUB-GROUP	Cosmic rays, Cutoff, Penumbra, Penumbral Island, Trajectory parameterization, Cyclic
08	14		
22	01		

19. ABSTRACT (Continue on reverse if necessary and identify by block number)

The "penumbra" is the term used to refer to the interval of space which lies, for any given particle rigidity, between the solid angle zone within which all such particles have free access, and the region within which particle access is completely forbidden. The term is also used to refer, in a specific direction, to the rigidity interval between the lowest rigidity for which any particle may enter in the given direction, and the rigidity below which particle access is completely forbidden in the same direction. Typically the penumbra consists of a mixture of allowed and forbidden trajectories.

This question of access of charged primary cosmic rays to points within the magnetic field of a planet is of great interest in numbers of areas of physics. It is very difficult, however, to map the allowed and forbidden regions of access, because of the time-consuming nature of the calculations involved. The present research has involved a systematic study of the nature of the characteristic zones of access in order to produce techniques by which information about the cosmic ray penumbra may efficiently be derived. The work has then focussed on the mapping and study of the phenomenology of the penumbra. Keywords: /

20. DISTRIBUTION / AVAILABILITY OF ABSTRACT ☐ UNCLASSIFIED/UNLIMITED ☐ SAME AS RPT. ☐ DTIC USERS	21. ABSTRACT SECURITY CLASSIFICATION Unclassified
22a. NAME OF RESPONSIBLE INDIVIDUAL Don F. Smart	22b. TELEPHONE (Include Area Code) 22c. OFFICE SYMBOL AFGL/PHG

DD FORM 1473, 84 MAR 83 APR edition may be used until exhausted. All other editions are obsolete.

SECURITY CLASSIFICATION OF THIS PAGE
Unclassified

CONTENTS

CHAPTER 1: THE PHENOMENOLOGY AND TERMINOLOGY OF COSMIC RAY ACCESS

1.1 PREFACE

This chapter presents a summary of the current understanding of the phenomenology of cosmic ray cutoffs. A list of terms is presented by which cosmic ray cutoffs, and access generally, may be discussed. The text, which originally constituted an as yet unpublished paper "Cosmic Ray Cutoffs Within Planetary Magnetic Fields - An Examination of the Phenomenology and Terminology" prepared by the author of this report and eight other researchers (listed below), grew out of the papers "On the Terminology of the Penumbra" by Cooke, Shea and Smart, 1981; and "Re-evaluation of Cosmic Ray Cutoff Terminology" by Cooke et al. (the same nine researchers), 1985.

1. D. J. Cooke, Physics Department, University of Utah, Salt Lake City, Utah, U.S.A.
2. J. E. Humble, Physics Department, University of Tasmania, Hobart, Tasmania, Australia
3. M. A. Shea and D. F. Smart, Air Force Geophysics Laboratory, Hanscom AFB, Bedford, Massachusetts, U.S.A.
4. N. Lund, I.L. Rasmussen and B. Byrnak, Danish Space Research Institute, Lundtoftevej, Lyngby, Denmark
5. P. Goret and N. Petrou, Section d'Astrophysique, Centre d'Etudes Nucleaires de Saclay, Saclay, France

1.2 INTRODUCTION

The question of charged particle access to points within the geomagnetic field has been a topical one throughout the entire history of cosmic ray physics. Results obtained from theoretical investigations into the phenomenology of charged particle access have been instrumental in aiding the interpretation of a wide range of experimental investigations. These studies have ranged from examination of the aurora, through attempts to account for the observed directional asymmetries detected in the primary and secondary cosmic ray fluxes, cosmic ray astronomy, the determination of primary-secondary cosmic ray relationships, to the utilization of specific access properties of the geomagnetic field for the determination of cosmic ray isotopic abundances.

There is a growing interest in the question of access of cosmic rays into the magnetospheres of other planets (Jupiter is of particular interest at this time), specifically in regard to the charged particle fluxes likely to be encountered by spacecraft in the vicinity of the planets, and in the interpretation of the detail of the flux distributions actually measured, and the information these yield on the characteristics of the magnetospheres.

The early workers who researched the question of charged primary cosmic ray particle access to positions within the geomagnetic field recognised that the general equation of charged particle motion in a magnetic field does not have a solution in closed form, and developed alternative techniques for investigating the access problem. The initial papers in this area were published by Stormer (1930), Bouckaert (1934), Lemaitre et al (1935)* and Lemaitre and Vallarta (1936a,b)*. The attentions of those authors were directed towards the need to systematically distinguish between directions of arrival along which a particle from interplanetary space could reach a given location (allowed directions) and those directions not accessible to such particles (forbidden directions).

The approach of these pioneering investigators took advantage of the

fact that the magnetic field of the Earth could be approximated by that of a simple dipole. In such an axially symmetric field, bound periodic orbits are especially significant in delimiting and characterizing the different access regions. (The bound periodic orbits, which are those totally constrained to remain within the magnetic field, possess a regular periodicity. This periodicity is manifested as cyclic variations in altitude, latitude, and longitude along the trajectory.)

Experimental investigations of the access problem were carried out by, amongst others, Malmfors (1946), Brunberg (1953), and Brunberg and Dattner (1953). These authors used experiments in which the motion of electrons in the proximity of a charged terella was used to model cosmic ray motion in the geomagnetic field.

With the advent of fast digital computers it became practicable to establish the extent of significant allowed and forbidden regions by systematic direct checking of access of individual trajectories calculated using high order simulations of the geomagnetic field. The technique was immediately applied to computations which were beyond the practical capability of the early investigators, such as determination of asymptotic cones of acceptance for the world wide network of cosmic ray stations (McCracken et al., 1962, 1965, 1968) and calculation of a world wide grid of vertical cosmic ray cutoff rigidities (Shea et al., 1968).

In these initial digital computer studies it was unnecessary to correlate the position or extent of the allowed and forbidden access regions with the associated trajectory characteristics. As a result, for many years there was little effort to relate the real field access patterns to those predicted for the simple axially symmetric field, or to look into the role, if any, that bound periodic orbits play in defining the allowed and forbidden regions in the real field. Nevertheless, the terms used in the dipole case to refer to the access regions were carried over into the numerical calculations, although, as noted by Cooke (1981) and Gall (1981), often in an imprecise way. Whereas the early theoretical workers viewed access conditions in what may be called a "direction picture", describing the directions from which particles of a specific rigidity could or could

not arrive, the later computer calculations have usually used a "rigidity picture" in which accessibility is considered as a function of particle rigidity in a single arrival direction. The use of the old geometric terms, appropriate to the direction picture, has caused considerable confusion in the rigidity picture studies.

It is believed that a reexamination at this time of the characteristics of the access regions distinguished by Stormer and by Lemaitre and Vallarta, together with a comparison between the properties of these analytically distinguished regions and those detected by the digital computer method, will be useful for further progress in the understanding of the cosmic ray access problem.

Additionally, the developing interest in examining the characteristics of the cosmic ray fluxes within other planetary magnetospheres has spurred interest in transposing the new techniques and insights across from the terrestrial work.

This chapter reviews the past and present work, and then presents a set of definitions which, it is hoped, will meet present needs in relation to the consideration of access to locations within the magnetic field of any planet.

1.3: HISTORICAL PERSPECTIVE

1.3.1 Magnetic Field Alone

Stormer (1930), later summarized by Stormer (1955), considered the matter of access from the point of view of fully forbidden, rather than fully allowed, directions of arrival. In addition to establishing some of the important general properties of charged particle trajectories in the geomagnetic field, he showed analytically that at any point in a magnetic dipole field there exists a right circular conical shell of directions of arrival, within which all access is forbidden to particles of a specified magnetic rigidity approaching from infinity.

The opening angle of this cone is a function of particle rigidity, and its axis is perpendicular to the dipole axis and also to the radius vector from the dipole center to the point concerned. In terrestrial terms the axis of the cone is horizontal at this point and is directed east-west. The existence of this cone, which is often called the Stormer cone and which encloses forbidden directions of arrival, is purely a property of an axially symmetric field, and is independent of the presence or absence of a solid body, such as the Earth, which might envelop the source of the field.

For positively charged cosmic rays, all directions to the east of the Stormer cone are populated only by particles in bound periodic orbits. As particle rigidity increases, the opening angle of the cone decreases. For any given direction, a particular rigidity value exists for which the Stormer cone lies in that direction. At this rigidity value, and at all lower values, all access from infinity in the given direction is forbidden. In the rigidity picture this limiting, or "cutoff", rigidity value is termed the "Stormer cutoff rigidity", or simply the "Stormer cutoff".

It is essential to note that there has been a change in the usage of the term "Stormer cone" since it was first introduced. Early authors (e.g. Lemaitre and Vallarta, 1936b; Hutner, 1939a) used the term to identify the boundary between fully inaccessible and partly accessible solid angles of particle arrival on the direction sphere. The usage changed from this definition of a shell-like boundary to one incorporating the solid angle containing all arrival directions which are not expressly forbidden by Stormer theory (Alpher, 1950; Kasper, 1959; Vallarta, 1961, 1971). With the advent of digital computer-based calculations the usage became reversed to represent the solid angle which is fully forbidden (e.g. Schwartz, 1959). Great care must therefore be taken when consulting the literature on this matter. To alleviate further confusion the term "Stormer cone" will be used throughout this report in its original, shell-like, sense, and the term "forbidden cone" (section 1.5) will be used to describe the solid angle within which all access is forbidden to charged particles of a specified rigidity and sign. In figure 1.1 the forbidden cone for positively charged particles is the solid angle region which is open towards the east. Stormer theory, pertaining as it does only to the matter

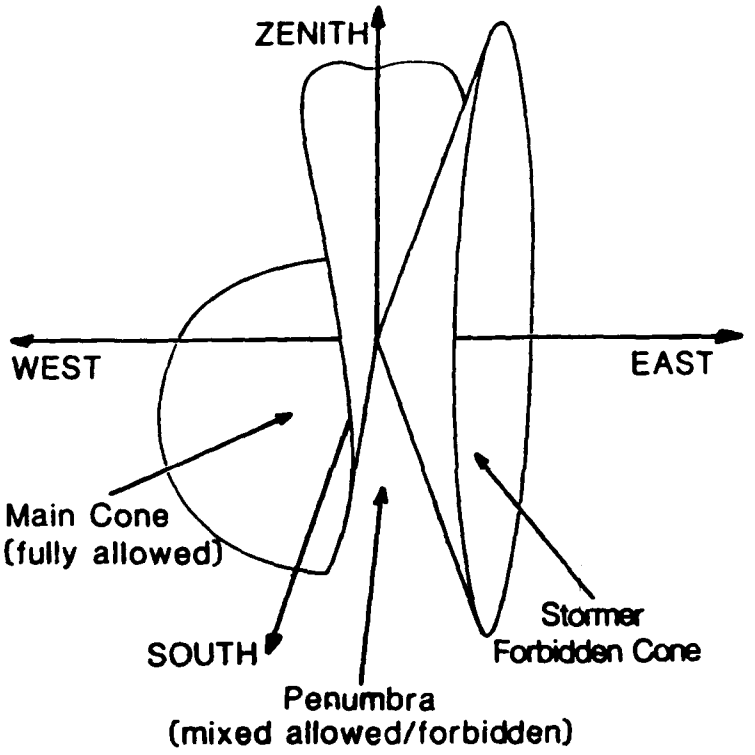

FIGURE 1.1

Notional spatial relations of the allowed cone, main cone, penumbra, Stormer cone, and forbidden cone for positively charged cosmic ray nuclei with an arbitrary rigidity value at an arbitrary location in a magnetic dipole field.

of forbidden access, makes no predictions about the important question of accessibility in directions outside the forbidden cone. The essential point is that on one side of the Stormer cone charged particle access is forbidden for all directions, whereas on the other side of the cone charged particle access may occur in certain directions.

Although Stormer's original work was done for a dipole field, the theory applies equally well to any other axially symmetric field, and other investigators have looked into the characteristics of the forbidden cone for more complex representation of the Earth's field. In each case an additional complexity was introduced into the axially symmetric field in order to represent the field in what was perceived to be a more realistic way (e.g.: a dipole plus ring current - Trieman, 1953; dipole plus quadrupole - Quenby and Webber, 1959; and dipole plus uniform field - Obayashi and Hakura, 1960). The field of Jupiter has also proven to be essentially dipolar in form (although the higher order terms are found to be basically dipolar in form (although the higher order terms are found to be somewhat higher relative to those in the geomagnetic field), and so the Stormer theory can be applied to the study of the cutoffs for Jupiter (see for example, Cooke, 1974).

1.3.2 Effect of the Solid Planet

Stormer's work was of profound importance for determining the filtering effect of a dipole field on the incoming cosmic radiation, but it did not take into account an effect which turned out to be extremely important for cosmic ray research carried out close to the surface of the earth: the presence of the solid earth itself, together with its atmosphere (or more generally, the presence of the solid planet within its magnetosphere). At rigidities marginally above the Stormer cutoff, the trajectories followed by incoming charged particles in a dipolar (or almost dipolar) field like that of the earth are often very complex, going through a number of altitude oscillations. In the case of the earth, if the particle dives deep into the atmosphere during one of these oscillations, it is lost by interaction with atmospheric nuclei and cannot then be

observed further along its theoretical track. (This track, which we refer to later in this report as a "virtual trajectory", is the track which the particle would have followed had the planet not been present and had the trajectory been controlled solely by the magnetic field.) In practice the presence of the earth excludes from observation most of the particles with arrival directions immediately to the west of the Stormer cone. Therefore, to successfully model the cutoff distribution pattern which actually exists in the vicinity of a planet, it is necessary to consider the much more complex problem of "magnetic field plus solid body".

It was Lemaitre and Vallarta (1936a,b), later summarized by Vallarta (1961), who first developed a solution to the problem in terms of allowed, rather than forbidden, access, in relation to the geomagnetic field. For a given rigidity, they realized that in the absence of the Earth, trajectories which are asymptotic to the simplest bound periodic orbits form the generators of a cone, within which all possible directions of arrival are accessible to charged particle entering the field from infinity. Lemaitre and Vallarta took account of the presence of the earth by introducing as additional delimiters, within the cone of allowed directions, trajectories which are at some point tangential to the Earth's surface and whose directions of approach to the point concerned lie within both sets of delimiters (Lemaitre and Vallarta, 1936b), and which, therefore, are allowed under both considerations. Lemaitre and Vallarta also used, at various times, the terms "main cone" and "region of full light" to refer, apparently synonymously, to this cone.

We note that, unlike the Stormer cone, the main cone was initially defined as a solid quantity. However, as in the case of the Stormer cone, but rather less seriously, some slightly inconsistent usages have appeared in the literature. To clarify this situation, and to prepare for the symmetric set of definitions which appears in section 5, we shall, for the remainder of this report, use the phrase "allowed cone" to describe the solid angle region of full light, as defined by Lemaitre and Vallarta, and will reserve the term "Main cone" to describe the boundary of the allowed cone. The use of the word "cone" can be misleading, since the main cone can be of very convoluted shape, and can even break into two or more

separate solid angle regions (or cones) in some situations.

The allowed cone is a very useful geometric concept. For any given rigidity and location in a magnetic field, a solid angle region can be determined within which cosmic ray particles have free access from outside the field. For decreasing values of rigidity the size of the allowed cone diminishes, until at some lower value it vanishes.

Lemaitre and Vallarta (1936b) used a mechanical analogue computer to calculate trajectories by a numerical integration development of the initial value problem. The assumption of axial symmetry in the magnetic field allowed them (like Stormer before them) to restrict their calculations to those involved with tracing particle motion in the meridian plane. Use of the Stormer length parameter

(where e is the charge of the particle, M is the dipole magnetic moment, m is the particle mass, and v its velocity) permitted generalization of their results from a limited number of traces of trajectories asymptotic to bound periodic orbits. Having thus investigated the behavior of the families of asymptotic trajectories, Lemaitre and Vallarta were able to deduce the form of the allowed cone as a function of latitude and rigidity. Later work which incorporated quadrupole terms did not alter this generality.

When the question of cosmic ray access to a specific location is considered in terms of the effect in a given direction, it is evident that charged particles with rigidities in excess of a certain limiting value will have free access to that point. This limiting rigidity value corresponds to that of the main cone in the direction concerned and has been termed the "main cone cutoff rigidity" (Shea et al., 1965). A particle arriving in this direction with this rigidity value will have traveled along a path which either is asymptotic to a bound periodic orbit or which grazes the top of the atmosphere (in the case of the Earth). The Stormer cone and the main cone can never overlap, although at low latitudes they can, in principle, come into contact over a limited range of direction.

Figure 1.1 shows, conceptually, the spatial relationship between the allowed cone, the main cone, the Stormer cone, the forbidden cone, and the cosmic ray penumbra. The latter is the solid angle zone which lies between the main cone and the Stormer cone, and is in general a region of alternating allowed and forbidden bands of directions of arrival.

Cosmic ray access to the penumbral region cannot easily be evaluated, and so the properties of the terrestrial penumbra have been studied intensively in an attempt to find discernable characteristics by which access can be defined. The method of Lemaitre and Vallarta was applied to the study of the larger scale forbidden band structures in the terrestrial penumbra by later investigators, such as Hutner (1939a,b); Schremp (1938a,b); Kasper (1959) and Schwartz (1959). Their work showed the penumbra to possess a very complex structure of allowed and forbidden bands of varying rigidity widths. Each individual forbidden band is the manifestation of particular low altitude points which, for a given family of trajectories, intersect the surface of the Earth (or other planet) over a finite domain of rigidity. It was not until the advent of high speed digital computers that this matter could be further investigated.

1.4 CLASSICAL TERMINOLOGY AS APPLIED TO DIGITAL COMPUTER RESULTS

The digital computer-based studies determine the access of cosmic rays to particular locations by tracing trajectories, using numerical integration, through the planetary field as represented by a high order mathematical model. As the arrival location is given at the outset, the trajectory actually traced is of a negatively charged particle leaving the location in the direction concerned. This trajectory is identical to that of an inbound positive particle arriving at the site from the same direction. If a particular outbound trajectory is unable to escape from the magnetic field (due to periodic orbit trapping, or due to the intersection with the surface of the planet) then clearly a particle from infinity is unable to traverse the same path in the reverse direction, and this arrival direction is forbidden.

In the trajectory-tracing technique, the form of the allowed and forbidden access regions relating to any point in the field may be sampled over any of one or more parameters (rigidity*; latitude, longitude, and altitude of location; and zenith and azimuth angles of arrival) by calculating sets of trajectory traces with incrementally spaced values of the given parameter. For example, where it is desired to deduce the penumbral structure in a given direction for a certain location as a function of rigidity, a series of trajectories would be calculated at spaced intervals of rigidity, over the total range extending from a value sufficiently high that free access is ensured, through to a low value at which it may confidently be assumes that access would be forbidden. The size of the rigidity increment chosen depends on the particular requirement in hand - relatively large increments are employed where only gross details of the penumbra are required, and fine increments if more detailed information is sought (at the expense of a proportionate increase in computer run time).

The majority of recent studies, both of cut-offs and penumbral features in the geomagnetic field, have employed rigidity as the parameter, leading automatically to considerations of particle access in a particular direction. As noted in section 1 we intend to call this the rigidity picture, in contrast to the directional picture used by the early investigators in their studies of particle access as a function of arrival direction at a particular rigidity. This and the following section discuss access from the rigidity viewpoint, whilst section 5 provides definitions appropriate to each point of view.

The difference between the reference frames used in the earlier analytic and later digital computer-based work has led to confusion. Not having, at the time, a full realization of the distinction between the two viewpoints, the initial users of the digital computer technique applied the

* Rigidity - momentum per unit charge is a more convenient unit to use than is energy, since the results obtained are then independent of the particle species.

1.5 PRESENT UNDERSTANDING OF THE PHENOMENOLOGY OF PARTICLE ACCESS TO POINTS IN A PLANETARY MAGNETIC FIELD

Recent investigations of the distributions of cutoff values at various sites and altitudes, and examinations of the penumbra in different situations, as well as development of more sophisticated techniques for relating particular penumbral features to specific trajectory forms, have brought a better understanding of the phenomenology of charged particle access to points within the geomagnetic field. The limited non-terrestrial work done to date (the examination of access into the main magnetic field of Jupiter, Cooke (1985)) confirms that the phenomenology pertains to other planetary fields, as expected. In the light of this current understanding it is possible to examine the main respects in which the earlier definitions, developed for a directional view of access in a field possessing axial symmetry, fail to translate to the rigidity view of cosmic ray access to points in the real, asymmetric, field.

Bound periodic orbits have especial significance. There is no doubt that they can exist in the real, asymmetric field - the existence of the terrestrial trapped radiation belts is a striking confirmation of this fact. Trajectory calculations suggest, too, that quasi-bound periodic orbits can be expected to exist in the real field of both Earth and Jupiter. It is necessary to investigate the significance of bound periodic orbits in the 'real' field, to ascertain whether or not orbits of the kind associated with the Stormer cone exist in this field, then to determine whether access to the point concerned from outside the field is forbidden at all lower rigidities. It is normally possible to infer, by calculation, that a direction evidently lies within the cone, by observing the existence of a continuum of quasi-periodic orbits over a finite range of initial parameters. The summary plot technique developed by Cooke and Bredesen (1981) in relation to access into the geomagnetic field represents one way of detecting such a continuum. Because of the departure of the real field from axial symmetry it could not, however, be assumed that entry into such orbits is unequivocally forbidden. (We exclude from our discussion the time variations of the real field which, of course, may allow entry into otherwise completely bound periodic orbits under certain conditions.)

In regard to the trajectory forms associated with the main cone, quasi-bound periodic orbits have particular significance. Although this type of trajectory is a singularity (as indeed it is in the dipole field, existing only for a single value of energy), it can be identified, because all trajectories within a finite range of the parameter space in which such an orbit is located show a characteristic doubly asymptotic form (Lemaitre and Vallarta, 1936a). Figure 1.2 shows a real field near-main-cone trajectory which has this form. It is possible to determine a value of main cone cutoff (or, more generally, to establish the position of the main cone in any parameter space) by ascertaining the trajectory which is characteristically asymptotic to the simplest type of periodic orbit. We shall refer to such main cutoffs, which are purely magnetically controlled, as being of type I, in contrast to type II cutoffs which are controlled by trajectory-planet intersections. Because the radius of curvature of these orbits is large relative to the scale dimensions of the field, the question of whether the orbits are truly bound, or merely possess quasi-bound properties over large trajectory path lengths, has proved difficult to resolve.

In order to illustrate important aspects of the phenomenology of charged particle approach to locations within a planetary magnetic field, typical characteristics of the terrestrial trajectory shown in figure 1.3 will be examined. For the purpose of this discussion the trajectory will be considered as possessing two portions, identified as A and B in the figure. In portion A, a positive particle enters from outside the field and penetrates downward whilst drifting from east to west around the Earth towards the longitude region of the arrival point. It is in this part of the trajectory that hemisphere to hemisphere oscillations, associated with the quasi-bound behavior, are to be found, particularly if the trajectory is a near-main-cone one (as it is in figure 1.3). The characteristic quasi-bound behavior is seen in a more exaggerated form in the trajectory of figure 1.2. Portion B of the trajectory of figure 1.3 describes the final motion of the particle towards the arrival point. Typically, if the arrival point is at other than very low latitudes the trajectory will loop one or more times within the local field. For practical purposes the boundary between portions A and B of the trajectory may be considered to

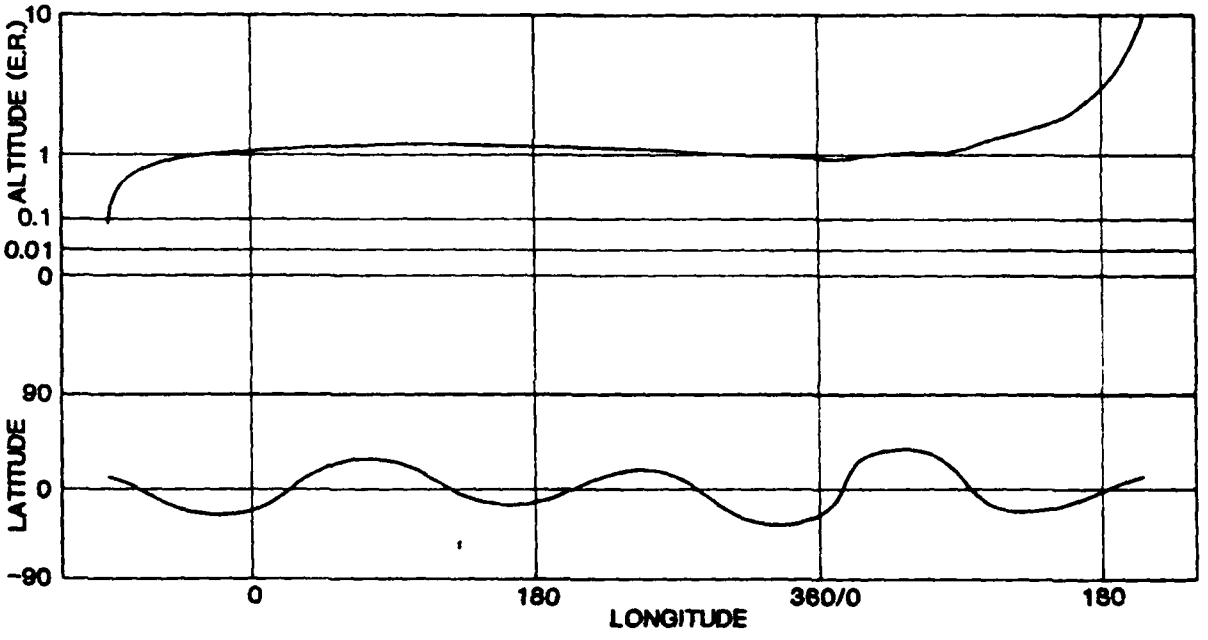

FIGURE 1.2

Typical "real field" doubly asymptotic trajectory which exists at rigidity values close to the main cone (trajectory starting point parameters: geographic latitude 10^{o} N, longitude 270^{o} E, zenith angle 7.9368^{o}, azimuth 270^{o}, rigidity 10.0 GV, 400 km geocentric altitude) calculated using the International Geomagnetic Field extrapolated forward to epoch 1980.0 (IAGA Division 1 Study Group, 1976). This trajectory is referred to as "doubly asymptotic" because it is twice asymptotic to the shell of essentially constant geomagnetic radius which contains the central quasi-bound section. One asymptote lies in the trajectory section close to its entry from outside the field, and the other lies close to the final Earth approach.

lie at the extreme latitudinal excursion before the equator is crossed for the last time as the particle moves towards the point of arrival. There is a direct correspondence between the location of these characteristic trajectory forms and the type of main cone produced. In particular, type I cutoffs are associated with quasi-bound periodic behavior in portion A of trajectories, whilst type II cutoffs are associated with earth tangency in trajectory loops which lie within portion B.

In general, trajectory-planet intersections which occur in portion A produce distinctly different structures (penumbral regions inaccessible to cosmic rays) than do those which occur in portion B. Consider the effect of a low point intersecting the planet within portion A. Such a low point can only occur for rigidities at or below the main cutoff, because only then can portion A possess a loop. Above the main cutoff rigidity value, the trajectory will pass once through the "shell" in which the bound periodic orbit would lie, without reversing its direction of motion relative to the shell. At the precise main cutoff rigidity, the orbit will lie totally within the shell. At rigidities even marginally below the main cutoff, the trajectory will possess reversals in the sense of motion relative to the shell, resulting in the formation of one or more loops along the trajectory.

The rigidity range over which any given loop will exist depends upon the path distance of the loop from the final point of arrival in the field. If any such loop intersects the surface of the planet then a penumbral forbidden band will be produced, whose width in rigidity will be at most equal to the rigidity range over which the intersecting loop exists. At large path distances, the loops and therefore any associated penumbral bands, can only exist for extremely narrow ranges of rigidity, whereas at short path distances from the arrival point the penumbral bands are relatively stable structures, existing over rigidity ranges of up to 1 GV or more.

In portion B of the trajectory, particles leave the quasi-bound section of the orbit and commence the helical motion associated with their approach to the final arrival point. These loops exist at all rigidities

and (λ_2,γ_2), then σ and γ are given by

$$\sigma = \arctan\left(\frac{\sin(\psi_2 - \psi_1)\cos\lambda_2}{\sin\lambda_1\cos\lambda_2 - \sin\lambda_1\cos\lambda_2\cos(\psi_2 - \psi_1)}\right)$$

$$\gamma = \arccos(\cos(\psi_2 - \psi_1)\cos\lambda_1\cos\lambda_2 + \sin\lambda_1\sin\lambda_2) \qquad \text{II}$$

Conversely, if the location of one point is known (λ_1,ψ_1, say), then it is possible to determine the latitude and longitude of a second whose position is defined in terms of a specified σ and γ, by means of

$$\text{latitude} = \arcsin(\cos\sigma\sin\gamma\cos\lambda_1 + \cos\gamma\sin\lambda_1)$$

$$\text{longitude} = \psi_1 + \arccos\left(\frac{\cos\gamma - \sin\lambda_1\sin\text{latitude}}{\cos\lambda_1\cos\text{latitude}}\right) \qquad \text{III}$$

3) The calculation of the magnetic zenith and azimuth uses the strategy of setting up a vector of known length (R") pointing in the direction of interest. The position of the tail of the vector, being the location of interest, is of course known in both geographic and magnetic coordinates (the latter determined by step 1), and similarly both geographic and offset dipole radius values pertaining to this point are known.

The geographic coordinates of the position of the head of the vector can be determined by using calculated σ and γ values, derived as follows (which values pertain to the projection of the vector onto a spherical surface).

$$\gamma = \arctan(R" \sin ze/(R + R" \cos ze))$$

$$\sigma = az \qquad \text{IV}$$

Having evaluated these angles, the geographic latitude and longitude of the vector head can be calculated using the relationships III. The offset

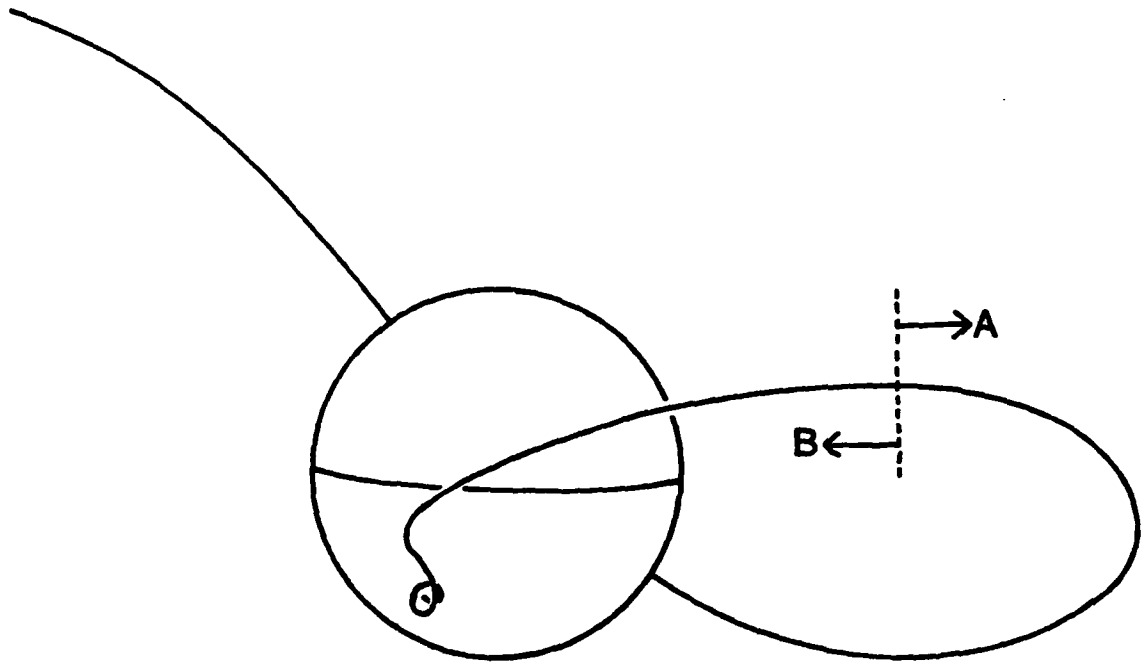

FIGURE 1.3

The trajectory within the geomagnetic field of a 5.65 GV cosmic ray particle en route to Williamstown, Australia (32.75° S, 151.80°, geographic), where it will arrive at 60° zenith angle and an azimuth of 150° east of geographic north. For the purposes of a general discussion of the effect of trajectory characteristics at points within the field, two portions of this typical trajectory are identified, and are labelled as A and B.

up to values significantly above the type I main cutoff, and, since they lie at short path lengths from the arrival point, are stable features of the trajectory. However, in reality, the planet's surface does prevent some of the trajectories from arriving in directions which might otherwise be allowed. The resulting solid angle of forbidden directions, at any given site, is referred to (by analogy with optics) as the planet's cosmic ray "shadow". The entire range of directions affected (made up of the shadows associated with intersections of each of the loops) is called the "shadow cone". The first order shadow cone, the most stable of these structures, is the range of directions associated with Earth intersections of the loop nearest the site; the second order shadow cone is that associated with the second loop, and so on. When the shadow cone extends above the type I main cone structure, the resulting structure is easily recognizable. Figure 1.4 illustrates an example of the terrestrial shadow cone structure as shown in the results of Cooke and Humble (1970) and Humble and Cooke (1975). In such situations it is the shadow cutoff structure which defines the main cone over the range of directions affected.

The terrestrial centered dipole field shadow cone described by the generators developed by Schremp (1938a,b), adopted by Vallarta (1938) and used in his subsequent work, was later found to be in strong disagreement with the experimental measurements of Winckler and Anderson (1954), and the later trajectory calculations of Schwartz (1959) and Kasper (1959). In addition, it should be noted that the distinctions between shadow and penumbral forbidden structures discussed by Kasper (1959, 1960), Schwartz (1959), and Vallarta (1961) are completely equivalent to that presented above. The earlier interpretations, however, are hard to follow because of the difficulty of perceiving all dimensions of the physical reality associated with the given characteristics of trajectories projected onto the meridian plane. Alpher (1950) converted the orthogonal projections developed by the earlier workers into convenient forms to enable their comparison with experimental data.

In addition to producing the shadow cone, trajectory loops within the local field also cause systematic structuring of the directional

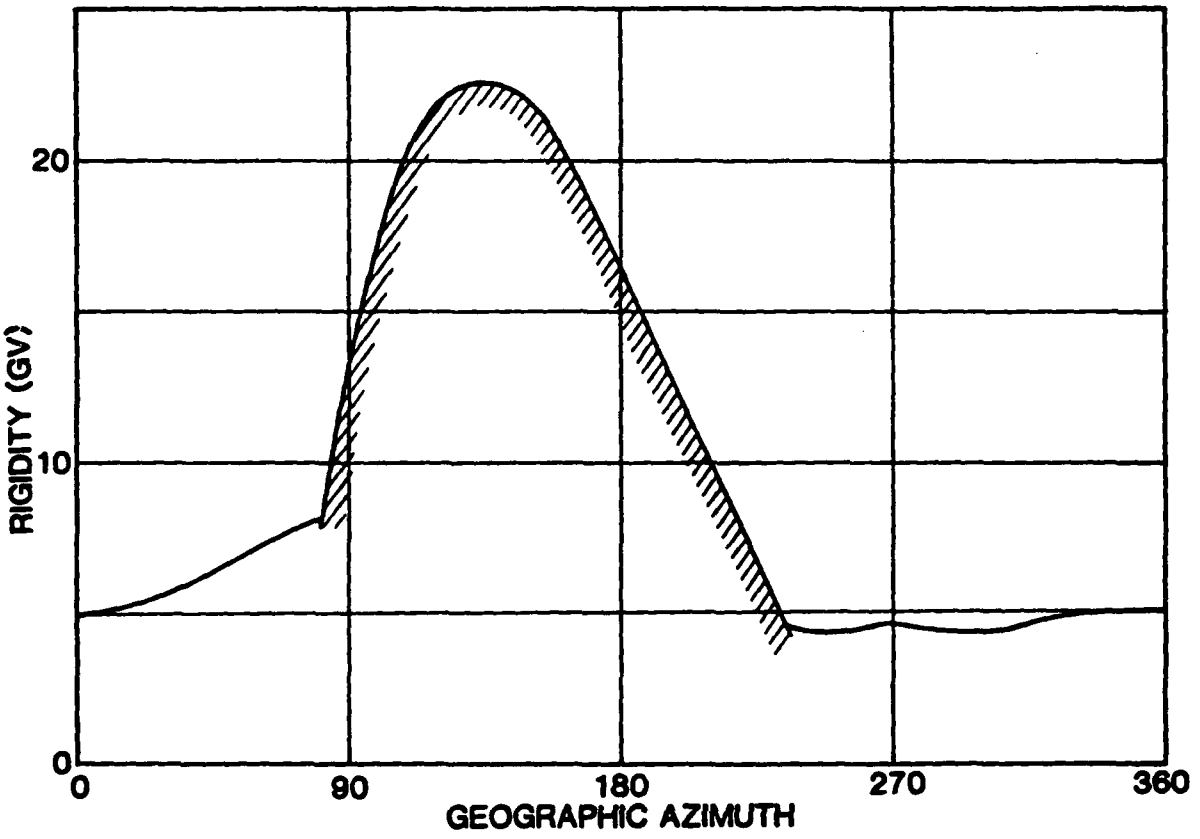

FIGURE 1.4

Variation of upper cutoff with geographic azimuth for a zenith angle of 80° at Brisbane, Australia (27.42° S, 153.08° E, geographic). The obtrusive structure between 80° and 230°, identified by the hatched lines, is "shadow cone" structure associated with short range earth-intersecting trajectories (after Cooke and Rumble, 1970).

distribution of type I cutoffs at non low-latitude sites. At any such site the main cutoff values are systematically diminished within a right circular cone, called the "loop cone" by Cooke and Humble (1970), the axis of which lies along the direction of the local field at the site. With increasing latitude, as each new loop forms in the local field, a new cone develops, and increases in size.

At the edge of each loop cone the main cutoff distribution displays "folding" - an abrupt change in cutoff value. Within the geomagnetic field cutoff changes of up to 40% have been found in association with the folding at the edge of the first order loop cone, the cone associated with trajectories having a single loop in their portion B. This effect, which is visible although not discussed in the work of Lemaitre and Vallarta, is particularly obvious in azimuthal scans of main cutoffs at affected location. The folded structure can be such that a curve of main cutoffs plotted for a range of azimuth angles at constant zenith, can be seen to turn back under itself, displaying an appreciable overhang. In directions where this effect occurs, three main cones exist simultaneously, one for each of three rigidities. This effect, which applies only over a limited range of directions, produces an exception to the otherwise general assertion that in any direction above the line-of-sight horizon the main cutoff defines a rigidity limit above which trajectories of all rigidities are allowed. In the case of folded structure, only the highest main cutoff value represents such a rigidity limit.

Examination of the form of individual trajectories reveals general patterns, such as path length, behavior at equator crossings, and the development of characteristic loop-like structures, which relate to distinct fiducial marks recognizable in observations of the cosmic ray rigidity spectrum at appropriate locations. For example, the initial development of loops in trajectories, as rigidity is reduced at the same site and arrival direction, signifies that the rigidity is approaching that of the main cone in that direction. Correspondingly, the "first discontinuity" (section 5) in the asymptotic longitude of allowed trajectories has been found to be an indicator of the approach, in rigidity space, of the main cutoff (Shea and Smart, 1971; Fluckiger et al., 1983).

the then-existing directional picture definitions in their determinations of cosmic ray cutoff rigidities. For example, the highest rigidity allowed/forbidden trajectory transition found in any given direction was labelled as the main cone cutoff (Shea et al., 1965). The main cone must, of necessity, lie at a rigidity greater than or equal to the rigidity value of the highest detected allowed/forbidden transition. The highest forbidden band can be extremely narrow and is therefore often missed in actual calculations performed ar discrete rigidity increments (Shea and Smart, 1975). Thus it is clear that the highest rigidity allowed/forbidden transition computed in a systematic survey at discrete rigidity intervals does not necessarily identify the true main cone.

Similarly, use of directional picture definitions in a rigidity based investigation led Shea et al. (1965) to identify the lowest rigidity allowed/forbidden transition found as the Stormer cone cut-off, and so this name came into use in presenting and discussing such results of trajectory calculations, even though it has since become clear that this association in most situations is probably invalid. Vallarta (1938) stated that even in a simple dipole field it may be that allowed trajectories do not lie adjacent to the Stormer cone.)

Not only has the question of the identification of the "true" main cone and Stormer cutoffs in the real field arisen in the computer-based studies, some additional complexities have also become apparent. For example, investigations by Humble et al. (1981) of the pattern of access to earth satellites have shown that an effectively reversed cutoff situation exists in directions below the optical (line of sight) horizon for particles approaching with relatively high rigidity. Particles of infinite rigidity are unable to reach a satellite from below horizontal directions, since their path is blocked by the presence of the planet. As the rigidity is steadily reduced, a value is eventually reached at which particles arriving from westerly (for the earth) directions are unable to reach the satellite, due to curvature of their path in the magnetic field. Humble et al. (1981) termed this cutoff the "allowed" cutoff, a name which they now believe to be undesirable. This cutoff is defined in section 1.5 as the "Horizon Limited Rigidity".

It is possible to utilize such characteristics to reduce the number of trajectory calculations required for cutoff determinations.

The form of the penumbra in the real geomagnetic field has also been mapped using the digital computer-based trajectory tracing technique (e.g. McCracken et al., 1962; Freon and McCracken, 1962; Shea et al., 1965; Cooke and Humble, 1979). Depending of the nature of the allowed/forbidden structure in a given direction the penumbral transmission for primary cosmic rays arriving in that direction at locations in the field can vary from zero to 100%.

Penumbral trajectories are almost invariably considerably more complex than are those lying within the allowed cone, and mapping by use of incrementally spaced parameters, generally rigidity, consequently requires large amounts of computer time. In a manner similar to that indicated previously in connection with main cones it is possible to identify trajectory characteristics peculiar to many penumbral bands. This systematic behavior of penumbral has enabled Cooke (1982) to develop the "trajectory parameterization" technique, by which individual penumbral structures may be traced by relating, in an automatic computer procedure, the structure to the trajectory feature responsible for its existence. (This technique also forms the basis of an automated method of locating the main cutoff to high precision.)

In relation to access into the earth's field the most stable penumbral band, that which is associated with the Earth intersection of a low point in the loop which lies at the last equatorial crossing in the quasi-bound periodic portion of the incoming orbit (normally the second-last equatorial crossing before the trajectory reaches the arrival point), has been called the "primary band" by Lund and Sorgen (1977). Because of the offset of the Earth's equivalent dipole, and the consequent positioning of trajectory loops relative to the Earth's surface, the primary band may or may not, depending upon the latitude and longitude of the site, be visible as an isolated forbidden band positioned above the remainder of the forbidden penumbral band structure.

A general indicator of the stability of the forbidden penumbral bands is the path length of the virtual trajectory (the path the trajectory would have followed had the planet not been present) from the last planet intersection to the location of interest. In the "reverse direction trajectory-tracing" sense this corresponds to the path length along the virtual trajectory from the origin of calculation to the first intersection. All relevant terrestrial cosmic ray studies, from both the directional and the rigidity viewpoints, support the attribution of large scale penumbral structure (wide penumbral bands, for example) to trajectory intersections with the Earth at relatively short path distances from the calculation origin, and that of fine penumbral structure to Earth intersections which occur at long virtual trajectory path lengths. Although the forbidden structures formed by the short range virtual trajectories are very stable, changes in the assumed field model have a very direct influence on the penumbral structure formed by long range trajectory path lengths.

The question arises as to the reality of fine penumbral structures in a planetary magnetic field. In the case of the earth it is clear that the atmosphere does not (contrary to the assumption made by most investigators) act as a simple barriers by which cosmic rays, having penetrated to a certain altitude, are cleanly removed from the incident cosmic ray flux. Clearly the total atmospheric depth traversed by the charged particle (which, in addition to altitude, depends directly on the trajectory curvature and configuration in the grazing section) will be a factor in determining whether a particle will survive a grazing incidence (see Lezniak et. al., 1975). Also, as pointed out by Petrou and Soutoul (1977), the atmospheric depth which can be traversed by a particle, without its loss, is a function of the identity of the particle. Thus it could well be that fine penumbral terrestrial structures are smeared out and essentially unobservable experimentally.

Time variations in a planetary magnetic field caused by the fluctuating pressure of the solar wind and by the rotation of the planet with respect to the solar wind direction are an additional effect which would lead to the smearing out of the fine structure.

In brief review, it can be stated that when trajectories calculated in a time-invariant, but otherwise realistic, model of the Earth's field are examined, all the analytically identified structures identified by the earlier workers in a simple axially symmetric field can be recognized. The limited calculations of trajectories in a higher order representation of the main field of Jupiter confirm that these same structures are found in that situation too.

There is good reason to introduce additional terminology in order to define useful quantities naturally associated with the standard sampling method of determining the real field cutoff values. These terms are presented in the following section, together with the "classical" terms, suitably qualified to allow their application in real field situations.

1.6 DEFINITIONS

The definitions referred to in the preceding sections are listed in table 1.1, and then discussed and illustrated later in the section. The terms, as listed, are subdivided into terms referring to the direction picture and the rigidity picture (see sections 1.5.1 and 1.5.2). The list is not exhaustive, but seeks to portray the most useful quantities in each situation.

1.6.1 Directional Definitions

The following terms are appropriate for use with the directional picture. Each definition is for charged particles of a single specified rigidity arriving at a particular point in the magnetic field.

ALLOWED CONE: The solid angle containing the directions of arrival of all trajectories which do not intersect the planet and which cannot possess sections asymptotic to bound periodic orbits (because the rigidity is too high to permit such sections to exist in the directions of arrival concerned).

TABLE 1.1 Summary of terms used in cutoff calculations. Quantities describing phenomena which are equivalent in the two pictures are listed on the same line.

DIRECTION PICTURE	RIGIDITY PICTURE
	Cutoff Rigidity
Allowed Cone	
Main Cone	Main Cutoff Rigidity
	First Discontinuity Rigidity
Shadow Cone	Shadow Cutoff Rigidity
Penumbra	Penumbra
Penumbral Band	Penumbral Band
	Primary Band
Stormer Cone	Stormer Cutoff Rigidity
Forbidden Cone	
	Upper Cutoff Rigidity
	Lower Cutoff Rigidity
	Horizon Limited Rigidity
	Effective Cutoff Rigidity
	Estimated Cutoff Rigidity

MAIN CONE: The boundary of the allowed cone. The main cone is constituted in part by trajectories which are asymptotic to the simplest bound periodic orbits and in part by trajectories which graze the surface of the planet. (In the case of the Earth the "surface" is generally taken to be the top of the effective atmosphere.)

FORBIDDEN CONE: The solid angle region within which all directions of arrival correspond to trajectories which, in the absence of the solid planet, would be permanently bound in the magnetic field. Access in these directions from outside the field is, therefore, impossible.

STORMER CONE: The boundary of the forbidden cone. In an axially symmetric field the surface forms a right circular cone.

SHADOW CONE: The solid angle containing all directions of particle arrival which are excluded due to short range planetary intersections of the approaching trajectories whilst loops within the local field line bundle are being traversed.

PENUMBRA: The solid angle region contained between the main cone and the Stormer cone. In general the penumbra contains a complex structure of allowed and forbidden bands of arrival directions.

PENUMBRAL BAND: A contiguous set of directions of arrival, within the penumbra, the members of which are either all allowed or all forbidden. Often, within any given forbidden band structure, it is possible to determine that a number of individual bands, each attributable to the intersection of the associated trajectories with the planet in a different low point, are overlapping to produce the entire forbidden band structure observed.

1.6.2 Rigidity Picture Definitions

The terms defined here are used in relation to particles arriving at a particular site within the planetary magnetic field from a specified direction.

CUTOFF RIGIDITY: The location of a transition, in rigidity space, from allowed to forbidden trajectories, as rigidity is decreased. Unless otherwise defined the value normally quoted, in representing the results of computer calculations is, for practical reasons, the rigidity of the allowed member of the appropriate juxtaposed allowed/forbidden pair of trajectories computed as part of a spaced series of traces. Sometimes the term is employed to refer to the location of a notional transition from one region to another, for example, at the Stormer cone, where an allowed trajectory may not perhaps exist at all.

MAIN CUTOFF RIGIDITY, R_M: The rigidity value at which the direction concerned is a generator of the main cone as defined in the "direction

picture". The associated trajectory is either one which is asymptotic to the simplest bound periodic orbit, or (owing to the presence of the solid planet) is one which is tangential to the planet's surface.

FIRST DISCONTINUITY RIGIDITY, R_1: The rigidity associated with the first discontinuity in asymptotic longitude as the trajectory calculations are performed for successively lower rigidities, starting with some value within the allowed cone. The value of R_1 is approximately equal to the main cone cutoff as defined above.

SHADOW CUTOFF RIGIDITY, R_{SH}: The rigidity value at which the edge of the shadow cone lies in the direction concerned.

PENUMBRA: The rigidity range lying between the main and the Stormer cutoff rigidities.

PENUMBRAL BAND: A continuous set of rigidity values, within the penumbra, all members of which have the same general access characteristics, either all allowed or all forbidden. Often, within any given forbidden band structure, it is possible to determine that a number of individual bands, each attributable to the intersection with the solid planet of the associated trajectories in a different low point, are overlapping to produce the entire forbidden band structure observed.

PRIMARY BAND: The stable forbidden penumbral band which as associated with the planetary intersection of a low point in the loop which lies at the last equatorial crossing before the trajectory (of its virtual extension in the assumed absence of the planet) takes on the characteristic guiding center motion down the local field line bundle.

STORMER CUTOFF RIGIDITY, R_S: The rigidity value for which the Stormer cone lies in the given direction. In a dipole field (and perhaps also in the real geomagnetic and other planetary fields) access for particles of all rigidity values lower than the Stormer cutoff rigidity is forbidden from outside the field. In a dipole approximation to the magnetic field, one form of the Stormer equation gives the Stormer cutoff rigidity, in GV, as:

$$R_S = \frac{M \cos^4\lambda}{r^2[1 + (1 - \cos^3\lambda \cos E \sin Z)^{1/2}]^2}$$

where M is the dipole moment, which, for the geomagnetic field, has a normalized value of 59.6 when r is expressed in units of earth radii, λ is the magnetic latitude, r is the distance from the dipole in earth radii, E is the azimuthal angle measured clockwise from the geomagnetic east direction (for positive particles), and Z is the angle from the local magnetic zenith direction.

UPPER CUTOFF RIGIDITY, R_U: The rigidity value of the highest detected allowed/forbidden transition among a set of computed trajectories. The upper cutoff rigidity can correspond to the main cutoff if and only if no trajectories asymptotic to bound periodic orbits lie at rigidities higher than this value. This can be identified from the nature of the trajectory associated with the main cutoff.

LOWER CUTOFF RIGIDITY, R_L: The lowest detected cutoff value (i.e. the rigidity value of the lowest allowed/forbidden transition observed in a set of computer calculations). If no penumbra exists, R_L will equal R_U.

HORIZON LIMITED RIGIDITY, R_H: The rigidity value of the most rigid allowed trajectory found in a set of computer calculations performed for a below horizon direction at a location above the surface of the planet.

EFFECTIVE CUTOFF RIGIDITY, R_C: The total effect of the penumbral structure in a given direction may usefully be represented, for many purposes, by the "effective cutoff rigidity" - a single numeric value which specifies the equivalent total accessible cosmic radiation within the penumbra in a specific direction. "Effective cutoffs" may either be linear averages of the allowed rigidity intervals in the penumbra (Shea et al., 1965), or functions weighted for the cosmic ray spectrum and/or detector response (Shea and Smart, 1970; Dorman et al., 1972). For a linear weighting this would have the form:

$$R_C = R_U - \sum_{R_L}^{R_U} \Delta R_i \text{ (allowed)}$$

where the trajectory calculations were performed at rigidity intervals R_i.

ESTIMATED CUTOFF RIGIDITY, R_{est}: A value obtained by using an empirically normalized equation to approximate the cosmic ray cutoff variation in the location of a particular point within a magnetic field in order to estimate a cutoff pertaining to the point. This value can be found by use of a variety of interpolation techniques, one of which is application of the Stormer equation given previously. Because the Stormer equation characterizes the spatial variation of the cutoff rigidity, with appropriate normalization it may be used to obtain useful estimates of the various cosmic ray cutoff rigidities, over intervals of latitude, longitude, zenith and azimuth, for example. In practice, estimates of the value of any cutoff can be obtained from adjacent calculated values to a reasonable accuracy by employing this method.

1.7 ILLUSTRATION OF DEFINITIONS

Not all the cutoffs defined in the previous section exist for every location and direction. Figure 1.5 shows typical cutoffs obtained, using trajectory calculations, for an arbitrarily selected location on the Earth (20° N, 270° E, altitude 400 km) at a zenith angle of 60°. Forbidden rigidities are shown in black, and allowed rigidities are indicated by white. The upper cutoff rigidity (R_U) and the lower cutoff rigidity (R_L) for each azimuth can readily be identified. In some directions, azimuth angles of 105° and 255° in this instance, R_U and R_L have the same value, within the 1% rigidity intervals used for these calculations. Note that R_U and R_L will be equal in any direction for which no allowed penumbral bands exist, a situation which is particularly common at low latitude locations.

Typical cosmic ray access patterns at zenith angles larger than that of the Earth horizon seen from a satellite are illustrated in figure 1.6,

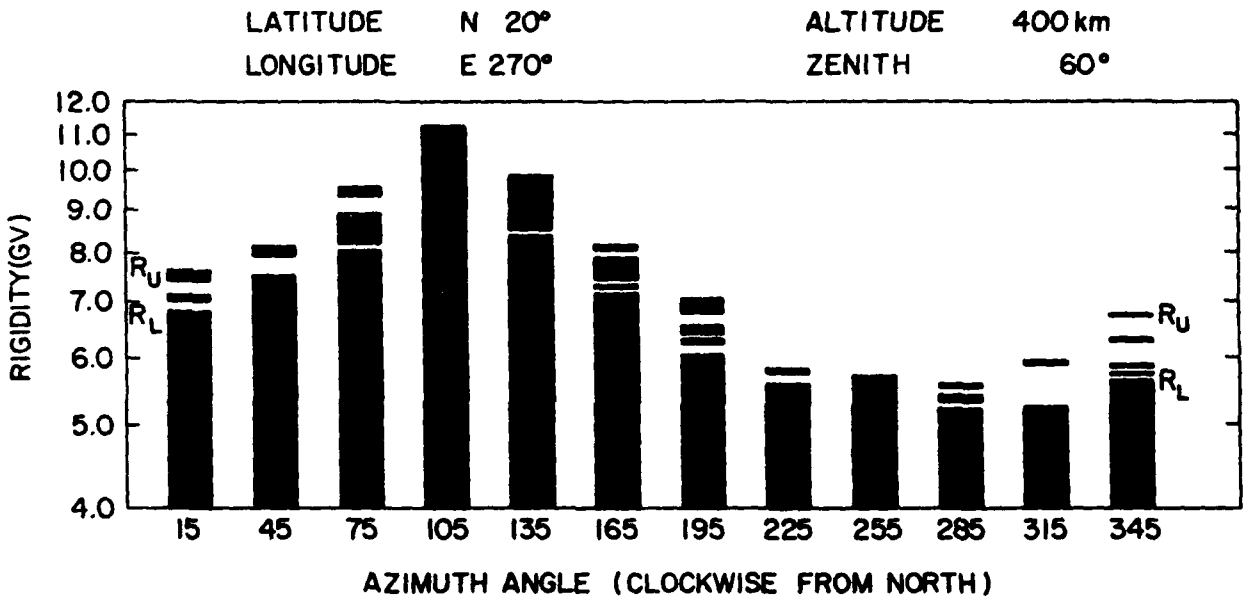

FIGURE 1.5

Illustration of cutoffs obtained at a particular location (20° N, 270° E, 400 km altitude) at a zenith angle of 60°. Trajectories at 1% rigidity spacing intervals were calculated every 30° in azimuth angle. Forbidden trajectories are illustrated by the dark areas, and allowed trajectories by white.

for the same location as in figure 1.5. The zenith angle of 120° is below the direction to the Earth's horizon (approximately 109° for a spacecraft at an altitude of 400 km). For this location and zenith angle all rigidities are forbidden in the north and easterly directions. However, for southerly and westerly directions a range of allowed rigidities exists within which cosmic ray particles may approach from angles below the satellite/Earth horizon without encountering the Earth. In such directions, of course, extremely rigid cosmic ray particle trajectories will intersect the Earth and the particles are therefore unable to reach the site. The highest rigidity that has access at any specified zenith angle below the spacecraft/Earth horizon is referred to as the horizon limited rigidity. These horizon limited rigidities are evident at azimuthal angles of 165° through 315° in figure 1.6.

Figure 1.7 illustrates penumbral structure encountered in the determination of the effective vertical cutoff, R_C, for three North American locations using linear weighting of penumbral bands. Note that there is an inherent assumption involved in determining the values of R_C, that the result of a trajectory calculation at a very specific rigidity typifies the result over a discrete rigidity interval. The allowed intervals in the penumbra are then summed (with appropriate weighting for detector response and spectrum as required) and subtracted from the calculated upper cutoff rigidity.

1.8 CONCLUDING REMARKS

It should be borne in mind that, because the definitions have deliberately been kept usefully general, the application of the terms may require more detailed qualification in some individual circumstances. For example, in below line-of-sight horizon directions at satellite altitudes it may be that there is not always access into the allowed cone for particles of any given rigidity, and so consequently there may not be a main cutoff in some cases. Nevertheless, particles within a limited rigidity range often can approach and have access in such below horizon directions (figure 1.5), and characteristic allowed/forbidden banded

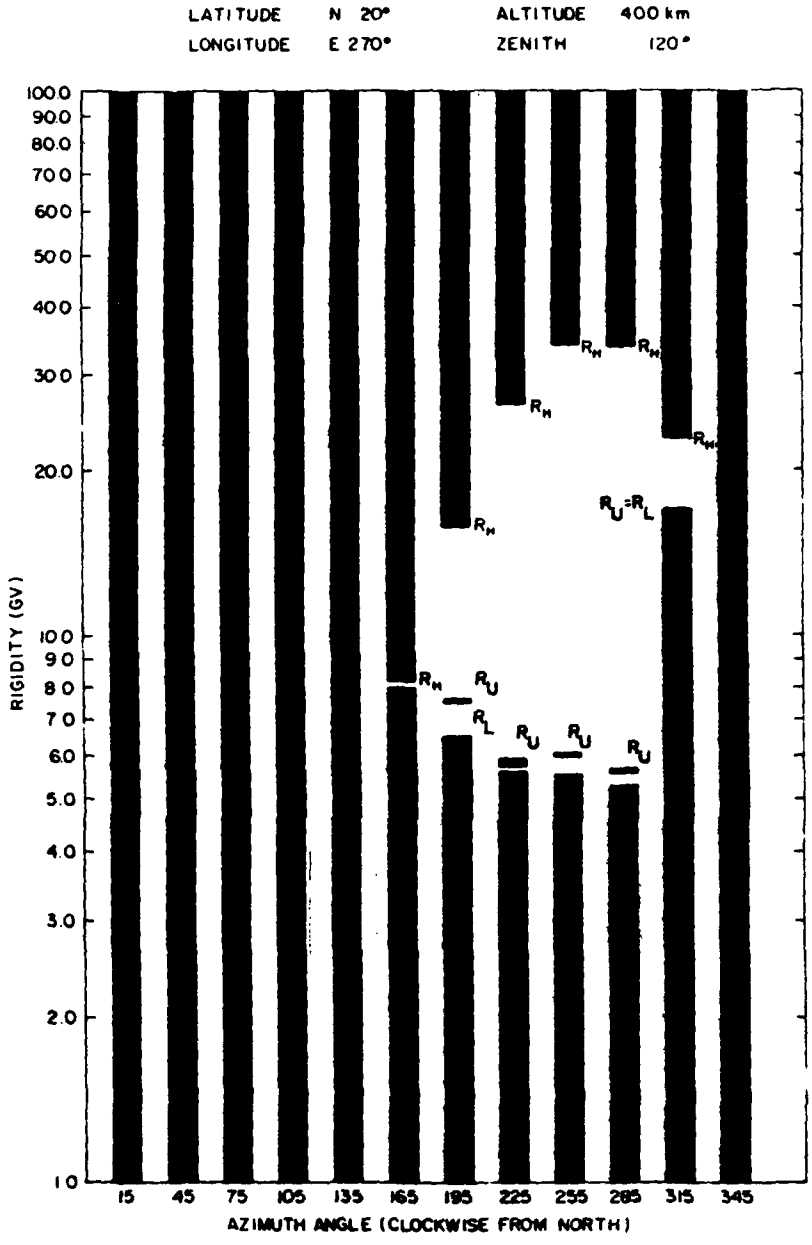

FIGURE 1.6

Illustration of "allowed" rigidities at a zenith angle below the direction of the local earth horizon for a satellite at 400 km altitude at a location 20° N, 270° E. Forbidden trajectories are indicated by black and allowed trajectories by white. The "horizon limited rigidities" are apparent as the high rigidity transition from allowed to forbidden trajectories.

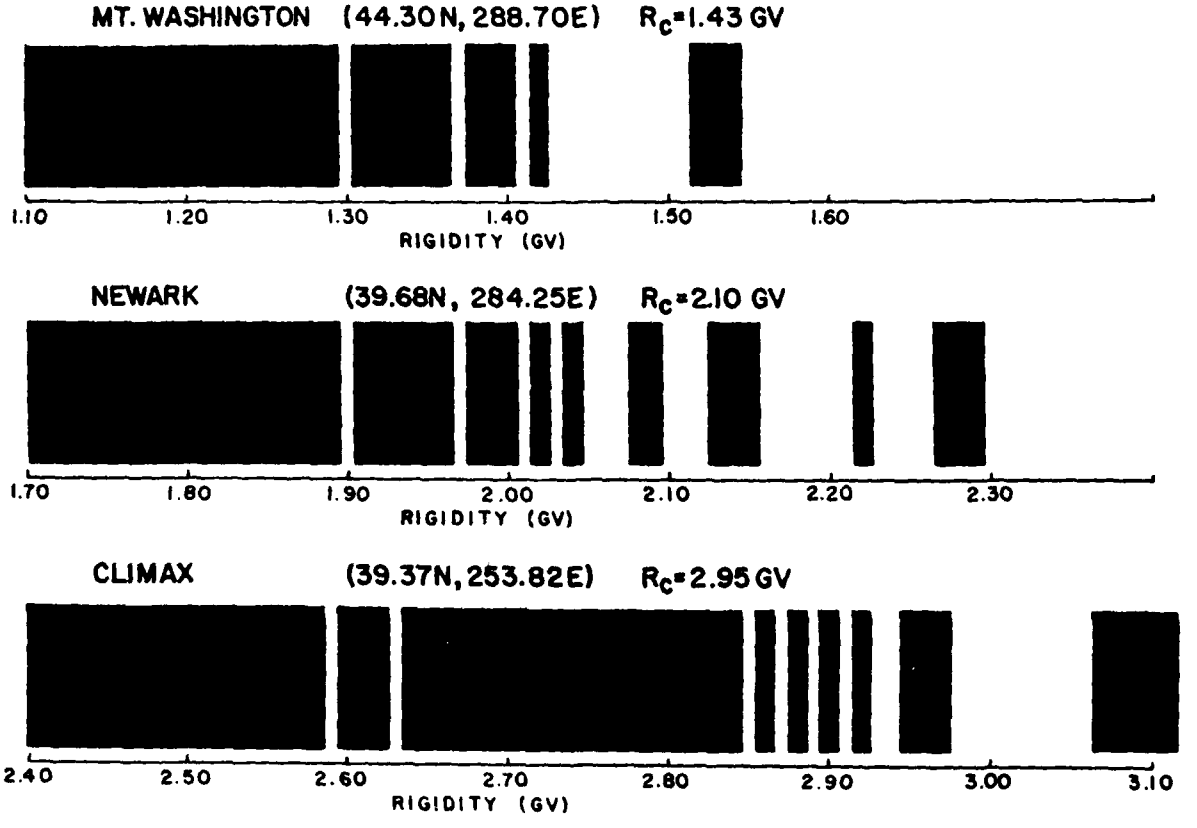

FIGURE 1.7

Illustration of the relationship between the penumbral structure and the effective vertical cutoff rigidity, R_C, for three North American cosmic ray stations. For these calculations the trajectories were vertically incident to the geoid at the station location, and were calculated at rigidity intervals of 0.01 GV using the International Geomagnetic Reference Field for 1980.0 (Peddie, 1982). Forbidden directions of arrival are illustrated by the dark areas and allowed by white.

penumbral structures clearly can exist in these situations. The question then arises as to what is the meaning of the term penumbra in these directions. With suitable qualification (i.e. of the rigidity or other range considered) the "penumbra" can be defined for any particular situation. For example, the "calculated penumbra" could be defined as the rigidity interval between the calculated upper cutoff rigidity and the calculated lowest cutoff rigidity.

Experimental cutoffs are becoming sufficiently precise to allow the resolution of the gross characteristics of the terrestrial cosmic ray penumbra (Lund and Sorgen, 1977; Byrnak et al., 1981; and Soutoul et al., 1981). For cutoff values derived from experimental measurements, definitions comparable to those discussed in the previous section can be used. In this situation, the terms "upper cutoff rigidity" and "lower cutoff rigidity" should be prefaced by an appropriate qualifier such as "measured" or "experimental".

There is no doubt that other physically meaningful quantities exist. It is believed, however, that the cutoff concepts described in this chapter presently have the greatest significance, and that the use of these definitions should alleviate most of the existing confusion, and satisfy the current requirements of investigators involved in cosmic ray access studies, both in relation to the Earth and the other planets possessing significant magnetospheres.

CHAPTER 2: USE OF THE STORMER EQUATION TO REPRESENT DIRECTIONAL CUTOFFS

2.1 INTRODUCTION

For many purposes it is useful to have a fast means of estimating directional cosmic ray cutoffs pertaining to any specified direction and location. The estimation of "real" directional cutoffs by computer is a lengthy process, expensive in computer time (even if the techniques described later in this report dramatically increase the efficiency of this process). The Stormer cutoff function (Stormer, 1930, 1955), which expresses the dependence of the Stormer cutoff on location and direction in a dipole approximation to the Earth's field, offers a means of determining cutoffs which is many orders of magnitude faster than any trajectory tracing method, but one which is sufficiently precise to produce useful estimates in non-critical applications - for the Earth's field and for any other planetary field which may be approximated by a dipole.

The fundamental imprecision in the Stormer expression in representing real field cutoffs, in particular due to failure to take into account higher order field harmonic terms, or the width and transparency of the penumbra, is normally exacerbated by the use of centered coordinates when invoking the expression. It is possible to appreciably improve the accuracy of the cutoff estimates by using "magnetic" coordinates (i.e. offset dipole latitude, longitude, zenith, and azimuth) when employing the expression, and in this way to take into account the offset and tilt of the equivalent dipole. By this means, inherently, the effect of ignoring the higher order field terms is minimized. Smart and Shea, 1977, have discussed the advantages of using offset dipole coordinates in conjunction with the Stormer expression, and the use of this expression for interpolating cosmic ray cutoffs over intervals within which precise calculated values do not exist.

A self contained system for transforming from geographic coordinates to offset dipole coordinates is described here. It has been used in the calculation of cutoff distribution functions for use in estimating detector

response to neutrinos of atmospheric origin. It has been necessary to take into account the effects of the magnetic cutoffs over the entire solid angle of acceptance of detectors at locations within the geomagnetic field.

2.1 STORMER EQUATION IMPLEMENTATION

The coordinate transformation has a number of stages, which are individually described in the following (this process is described as it applies to the Earth's field):

1) A coordinate conversion is used to determine the offset dipole latitude, longitude, and radius from the nominated geographic latitude and longitude, and geocentric altitude. This conversion takes into account the offset and inclination of the Earth's equivalent dipole for any required epoch, and assumes that the Earth is an oblate spheroid of eccentricity 0.00674. The angle conversion equations are as follows:

$$\text{offset dipole longitude } \phi = \arctan\left(\frac{R \sin\psi \cos\lambda - y \cos b}{C}\right)$$

$$\text{offset dipole latitude } \theta = \arctan(\cos\phi \tan\alpha) \qquad \text{I}$$

$$\text{offset dipole radius } R' = \frac{C}{\cos\theta \cos\phi}$$

where $\alpha = \arctan(F/G) + a$

$$C = \frac{G \cos\alpha}{\cos(\alpha - a)}$$

and $F = R \sin\lambda - x$

$$G = y \sin b + R \cos\lambda \cos(\psi - c)$$

λ and ψ are the geographic latitude and longitude respectively; R is the geographic radius at the specified location; x is the displacement of the

dipole from the center of the earth in a direction parallel with the geographic equatorial plane; a is the inclination of the dipole axis from a direction parallel to the geographic N-S axis; b is related to the angle between the zero magnetic longitude and the geographic longitudinal towards which the dipole is displaced; and c is the geographic longitudinal direction parallel to which the direction zero offset dipole longitude lies.

A procedure for establishing the position of the equivalent dipole with respect to the geocentric coordinate system at any epoch is presented by Smart and Shea, 1977. This procedure, which makes use of the low order terms in the spherical harmonic representation of the geomagnetic field, is discussed more fully by Roederer, 1972; and Akasofu and Chapman, 1975. The values of x, y, a, b, and c used in the presently reported coordinate transformation can thus be determined as required. The equivalent dipole position determination is included as a subroutine in the computer program which executes the Stormer cutoff evaluation.

2) The following steps rely on the use of a particular means of specifying the relative position of two points on the surface of a sphere. In particular, two angles are used, one (σ) defines the angle between the great circle connecting the two points and the meridian line intersecting one of them, and the other (γ) is the angle subtended at the center of the sphere by the two points (see figure 2.1).

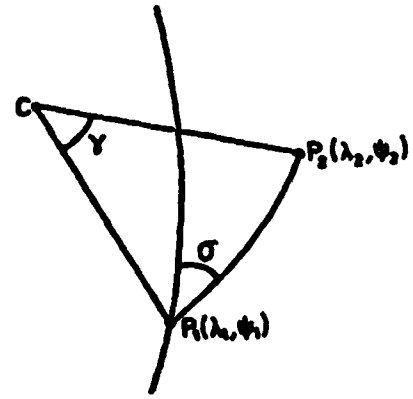

Figure 2.1 Diagram defining the angles σ and γ used to express the relative position of the two points P_1 and P_2 on a spherical surface. C is the center of the sphere.

If the two points are, as specified by latitude and longitude, (λ_1,γ_1)

dipole latitude and longitude, and the distance R* of the vector head from the dipole are then calculated using relationships I. Now, having the offset dipole coordinates of both ends of the vector, and angles and relating the two points (in the offset dipole frame of reference) can be calculated by means of the relationships II. The azimuth of the vector in the offset dipole frame of reference is simply the σ value, whilst the zenith angle is given by

$$ze = \arccos (R^* \cos \gamma - R')$$

where R' is the offset dipole radius of the vector tail (i,e, the distance of the vector tail from the offset dipole center).

2.3 CALCULATION OF STORMER CUTOFF VALUE:

By using the coordinate transformation procedure described, the position (latitude, longitude, and radius) of the site location relative to the offset dipole, and the zenith and azimuth pertaining to the direction of interest, may be calculated from the specified geographic coordinates and geocentric altitude. At each step during the derivation of these parameters tests are performed to ensure that calculated angle values lie in the correct quadrant, and appropriate corrections are made if they do not. Having thus determined the angles and distance relative to the equivalent dipole centered frame of reference the Stormer equation can be invoked with the greatest possible precision.

The appropriately normalized Stormer expression is as follows:

$$\text{cutoff} = \frac{59.4 \cos^4 \theta}{R'^2 \left(1 + \sqrt{1 - \cos^3 \theta \sin az \sin ze}\right)^2}$$

This expression takes in offset dipole latitude (θ), zenith (ze), azimuth (az - measured clockwise from magnetic north), and radial distance from the effective dipole center (R'); and produces cutoff rigidity values, in units of GV.

2.4 USE OF STORMER CUTOFFS IN THE DERIVATION OF GEOMAGNETIC CUTOFF DISTRIBUTION FUNCTIONS FOR USE IN ESTIMATING DETECTOR RESPONSE TO NEUTRINOS OF ATMOSPHERIC ORIGIN

A procedure has been developed, utilizing the Stormer cutoff expression for deriving functions which characterize the effect of geomagnetic cutoffs on the charged primary cosmic rays that give rise to neutrinos arriving in any given direction at specified points on or in the earth. These cutoff distribution functions, for use in atmospheric neutrino flux calculations, have been determined for eight nucleon decay experiment sites, using a technique which, in addition to employing the Stormer expression, assumes colinear motion of neutrino and parent primary.

Some large cosmic ray detectors, such as those used in nucleon decay research, have a finite response to neutrinos. It is necessary to be able to calculate the expected background flux of neutrinos incident upon such detectors on order to establish whether the angular distribution of certain classes of events has the characteristics of nucleon decay or of neutrino interactions, a distinction which has important physical and astrophysical implications.

The neutrinos produced in the atmosphere (muon and electron neutrinos associated with muon, pion and kaon decay) constitute a major part of the background. The rate of production of these neutrinos is related to the intensity of primary cosmic rays incident upon the atmosphere, which in turn depends on the primary cosmic ray spectrum, and, as discussed by Gaisser (1982), on the geomagnetic cutoffs pertaining in the given situation.

Let the differential intensity of neutrinos reaching a detector in the presence of the geomagnetic field be $A(R,\theta,\psi)$, where R is rigidity, and θ and ψ are the zenith and azimuth angles of neutrino arrival at the detector. If $B(R,\theta,\psi)$ is the intensity of neutrinos that would exist in the absence of the field, then the functions A and B can be related as follows:

$$A(R,\theta,\psi) = B(R,\theta,\psi)\ C(R,\theta,\psi) \qquad 2.1$$

where $C(R,\theta,\psi)$ expresses the effect of the geomagnetic cutoffs. This "cutoff distribution function" essentially describes, for a detector in a given location, the fraction of the total solid angle of the detector accessible to neutrinos that are descended from charged primaries of any given rigidity.

In deriving these functions, the cutoffs relating to points over the entire earth's surface have to be taken into account. (Because neutrinos can penetrate the earth, their production in the atmosphere on the distant side of the Earth, as well as in the local atmospheric mass, is significant.)

A computer based procedure has been developed for calculating the functions. It assumes that the detector has an isotropic directional response to neutrinos. The entire 4π steradian field of view is divided into a number of equal solid angle zones, where each zone, essentially an annulus, lies between defined upper and lower zenith angle limits. A separate function is determined for each of the zones. (In the present analysis eight $\pi/2$ steradian zones are employed, whose zenith angle limits are listed in Table 2.1.)

As a first step towards deriving the functions, each solid angle zone is divided into a large number of smaller elements of equal solid angle. The axial zenith and azimuth angles are computed for each element, and then these angles, together with the specified site position, are processed to determine the location and angle at which the "line-of-sight" vector intersects the assumed production level in the atmosphere (a height of 20 km above the earth, in the reported calculations).

A further set of transformations converts these angles into magnetic coordinates. In this work and inclined, offset, magnetic dipole approximating the 1980 magnetic field is assumed. The angle conversions and cutoff expressions from the preceding section are used to produce the directional cutoff values.

TABLE 2.1

Zenith angle extent of the eight solid angle zones for which cutoff distribution functions have been calculated at each site. (The zenith angle is expressed relative to the detector. Thus the first zone, extending from 0^{o} to 41.4^{o}, accepts neutrinos traveling downward, whilst zone 8, extending from 138.6^{o} to 180.0^{o}, accepts neutrinos traveling upwards.)

Zone	Zenith Angle Range (degrees)	Weighted Mean Zenith Angle (degrees)
1	0.0 - 41.4	27.7
2	41.4 - 60.0	51.1
3	60.0 - 75.0	67.9
4	75.5 - 90.0	82.8
5	90.0 - 104.5	97.2
6	104.5 - 120.0	112.1
7	120.0 - 138.6	128.9
8	138.6 - 180.0	152.3

These cutoff values do not take into account the non-dipole components of the Earth's field, penumbral effects, or the Earth's cosmic ray "shadow". For these reasons there are significant disparities between calculated real field cutoffs and the Stormer estimates. It is estimated, on the basis of direct comparative calculations, as well as by checks made with the use of the published real field cutoffs of Shea and Smart (1982), that the agreement is within about 40% in directions where the shadow effect is not present. At zenith angles greater than about 60^{o}, in directions where the shadow effect in present, discrepancies of the order of a factor of two can be encountered. Nevertheless it is felt that, in this first approach, the Stormer cutoff values constitute acceptable approximations to the real field cutoffs.

Having thus the means for quickly estimating the required directional

cutoffs, the summing of the effects of the cutoffs over all the solid angle elements within a zone is carried out by numerical integration, as follows:

$$C(R,\theta_n) = \sum_{\phi_i=0}^{2\pi} \sum_{\theta_j=\theta_1}^{\theta_2} \sum_{R=R_1}^{R_k} \frac{P_n(R)}{i \cdot j}$$

$$\text{where } P_n = \begin{matrix} 1 & R > \text{cutoff pertaining to direction } \theta,\phi \\ 0 & R < \text{ " } \quad \text{ " } \quad \text{ " } \quad \text{ " } \end{matrix}$$

with $R_c(\theta_i,\psi_j)$ the cutoff pertaining to the direction (θ_i,ψ_j). θ_n refers to the zenith angle range lying within the n^{th} zone (extending from θ_1 to θ_2). The function C is the same as that in equation 2.1, now integrated over all azimuths. If desired, limited ranges of the parameter ϕ can be introduced, in which case an azimuth dependence exists.

The cutoff distribution functions calculated for the sites listed in Table 2.2 are presented in Figures 2.1-8. The zenith angle and latitude dependence of the functions are well displayed in these figures, which are arranged in order of decreasing magnetic latitude.

It is believed that these functions have basically the correct form, in spite of the simplified approach to the calculations. It is worth noting that any step to improve the precision of the functions, either by introducing real field cutoffs, or by taking into account the transverse momentum in the primary cosmic ray interactions, would require an amount of computer time greater by many orders of magnitude. That the neutrino event rates observed by the particle detectors are extremely low, in any case, argues for the simpler approach employed at this time.

The effect of the simplifying assumptions on the functions may be anticipated. Note, for example, that for zones 1 through 5, the median value of the functions lie at a rigidity value corresponding to the vertical Stormer cutoff value. This fact suggests that, as a first order correction to take into account the disparity between the Stormer and real field cutoffs, these curves could be displaced to positions for which the median value of the functions lie at the real field vertical effective cutoff pertaining to each individual site.

If a more realistic, three dimensional, neutrino production model were to be utilized, a "smearing" of the functions would be expected, which would probably result in less well defined zenith angle dependence. On the other hand, the effect of the Earth's shadow, and of secondary particle deflection over large atmospheric path lengths, could be expected to cause the functions applying to near horizontal directions to extend to rigidity values appreciably greater than the curves indicate.

Gaisser et al., 1983, have recently used the cutoff distribution functions (as computed in a form relating to upwards and downward directed detector response cones of various half angles) in calculating the flux of atmospheric neutrinos. They have shown that the geomagnetic effect has a very significant effect on the expected up-down ratios of neutrinos of the two flavors, and hence on the interpretation of the experimental data from the large detectors.

TABLE 2.2

Locations for which cutoff distribution functions have been calculated. A single calculation has been carried out for the two tunnel sites on the French/Italian border because the two experiment locations are sufficiently close spaced to possess essentially the same cutoff distribution functions.

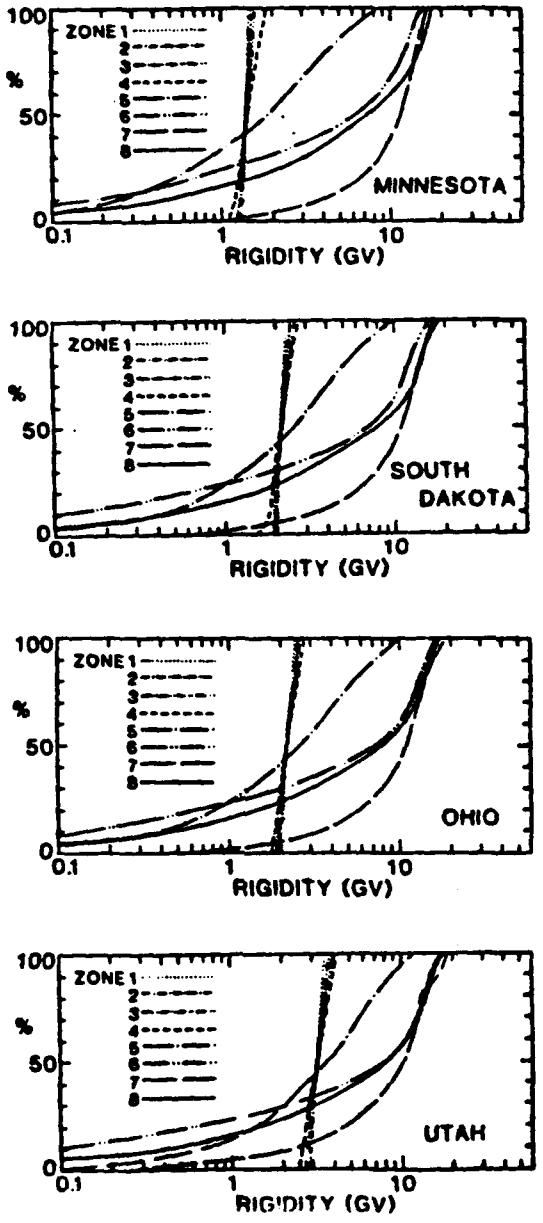

FIGURES 2.2-2.5 (in descending order)

Integral cutoff distribution functions for the locations shown in table 2.2. For each location a set of curves is presented, each member of which corresponds to a different solid angle zone and represents the percentage of the total solid angle of the zone accessible to neutrinos that are descended from charged primaries of any given rigidity. The zenith-angle extent of each zone is identified in table 2.1.

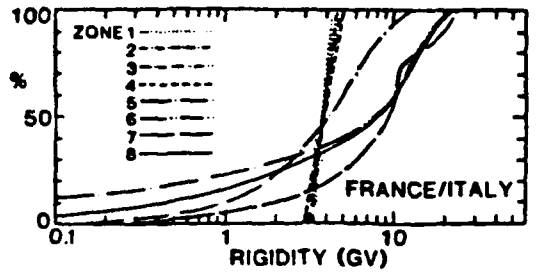

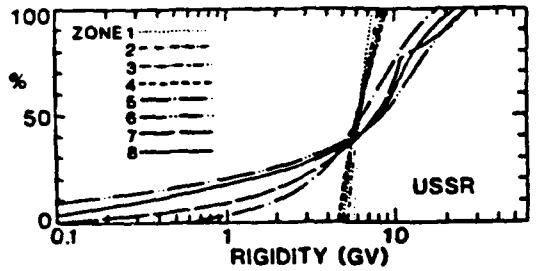

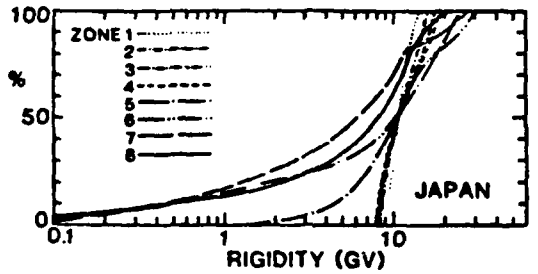

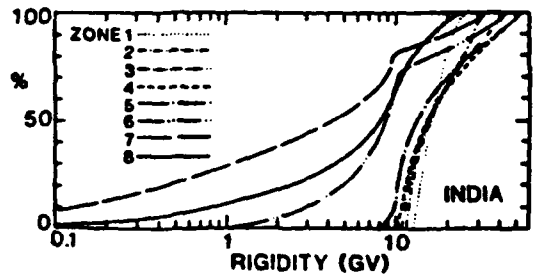

FIGURES 2.6-2.9 (in descending order)

See caption for preceding figures.

CHAPTER 3: THE EFFECT OF MAGNETIC CUTOFFS ON THE FLUX OF CHARGED PRIMARY COSMIC RAYS WITHIN THE MAIN FIELD OF JUPITER

3.1 INTRODUCTION

With the prospect of the Galileo spacecraft soon to be placed in orbit around Jupiter, there is a direct interest in estimating the charged particle fluxes in the orbital environment. Although Stormer cutoffs could have been used to approximate cutoff values (as done for Jupiter's magnetosphere by Cooke, 1974) a higher precision was desired at the present time. In the present investigation, therefore, "real" main cutoff values were derived using visual inspection of trajectories plotter by computer. In particular, trajectories were presented on a video screen for a range of rigidity values, corresponding to particular locations and directions of arrival in Jupiter's field. The form of the trajectory corresponding to each set of conditions was inspected as the rigidity value progressively refined until the simplest possible quasi-bound periodic orbit was found to be associated with the approach trajectory. The rigidity value thus found corresponds to the main cutoff value (this association of the simplest quasi-periodic orbit with the main cone is discussed further in chapter 6, in relation to the geomagnetic field).

Techniques described in the preceding chapter have been applied to calculate the effect of the magnetic cutoffs on the primaries within the magnetic field of Jupiter, expressed by means of cutoff distribution functions (CDF's). Cutoff distribution functions have been derived for primary cosmic rays having access to a 4.5 Jupiter radius satellite orbit, for longitudes over the latitude range +20 to -20°. These functions represent the fraction of the total 4π steradian solid angle which is accessible to charged primaries of any given rigidity.

3.2 DISCUSSION

Let the differential intensity of charged primaries reaching a given

point, in the presence of Jupiter's field be $A(R,\lambda,\phi,r)$ (where R is rigidity, λ and ϕ are the latitude and longitude, and r is the radial position of the point in the field). If $B(R,\lambda,\phi,r)$ is the intensity of charged primaries that would exist in the absence of the field, then the functions A and B can be related as follows:

$$A(R,\lambda,\phi,r) = B(R,\lambda,\phi,r)\ C(R,\lambda,\phi,r)$$

where $C(R,\lambda,\phi,r)$, the cutoff distribution function, expresses the effect of the magnetic cutoffs. It defines, for a given location, the fraction of the total solid angle accessible to charged primaries of any given rigidity.

The computer-based procedure described in chapter 2, there employed for calculations in the geomagnetic field, is used to calculate these functions, using a pre-calculated set of main cutoff values. These cutoffs, which were calculated for a spaced set of zenith and azimuth angles pertaining to a grid of latitude and longitude values, specify, for any given direction and location, the lower limit of full accessibility of primaries from outside the field. As briefly discussed earlier, this lower limit, the "main cutoff" (see chapter 1), was identified, in each case, by locating the rigidity value for which the simplest bound periodic orbit was able to exist. The O_4 mathematical representation of Jupiter's main field (Acuna and Ness, 1976) was used in making the cutoff calculations. During these computations it was observed that relatively few allowed trajectories were encountered at rigidities below the main cutoff, tending to validate the use of the main cutoff to represent the lower limit of accessibility. At 4.5 Jupiter radii, to which the cutoff values pertain, the effect of the

FIGURE 3.1

General form of the cutoff distribution function. The rigidity values R_L, R_M, and R_U, used to characterize functions of this kind, are shown.

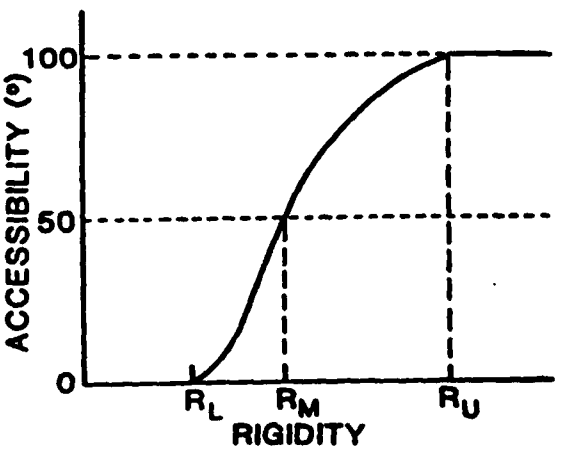

"shadow" of the solid planet is restricted to a very small (~1%) effect at very high rigidities.

In detail, the derivation of the CDF's for any location involves summation of the effects of the cutoffs over many small solid angle elements, using cutoff values interpolated from the stored set. Because charged particle access varies from location to location, the resulting CDF is different for each different location. The representation of the large number of individual functions pertaining to a wide range of latitude and longitude values is clearly impractical here, so an alternate graphical representation has been employed, which uses three contour plots to show the variation in the value of each of three parameters which are here used to characterize the function. Figure 3.1 shows the typical form of a CDF. R_L, R_M, and R_U are three rigidity values which respectively represent the lower limit, the rigidity at which the function has value 50%, and the upper rigidity limit of the function.

3.3 RESULTS:

Figures 3.2A, 3.2B, and 3.2C show contour plots of the values of R_L, R_M, and R_U, respectively, for all longitudes over the latitude range +20 to -20^o. At any desired location the values of the three parameters can be deduced, and used to construct the appropriate CDF. The contour plots pertain to a 4,5 Jupiter radius shell. Approximate functions for other radius values may be deduced by invoking an inverse square law of variation of rigidity value.

Finally, the flux at any given location can be deduced by folding the appropriate CDF with the primary spectrum. If it is desired that energy be used rather than rigidity as the spectral variable, then at the rigidity values involved the conversion is simple. Proton energy is almost exactly numerically equal to rigidity; alpha nucleon energy is numerically equal to half the rigidity value.

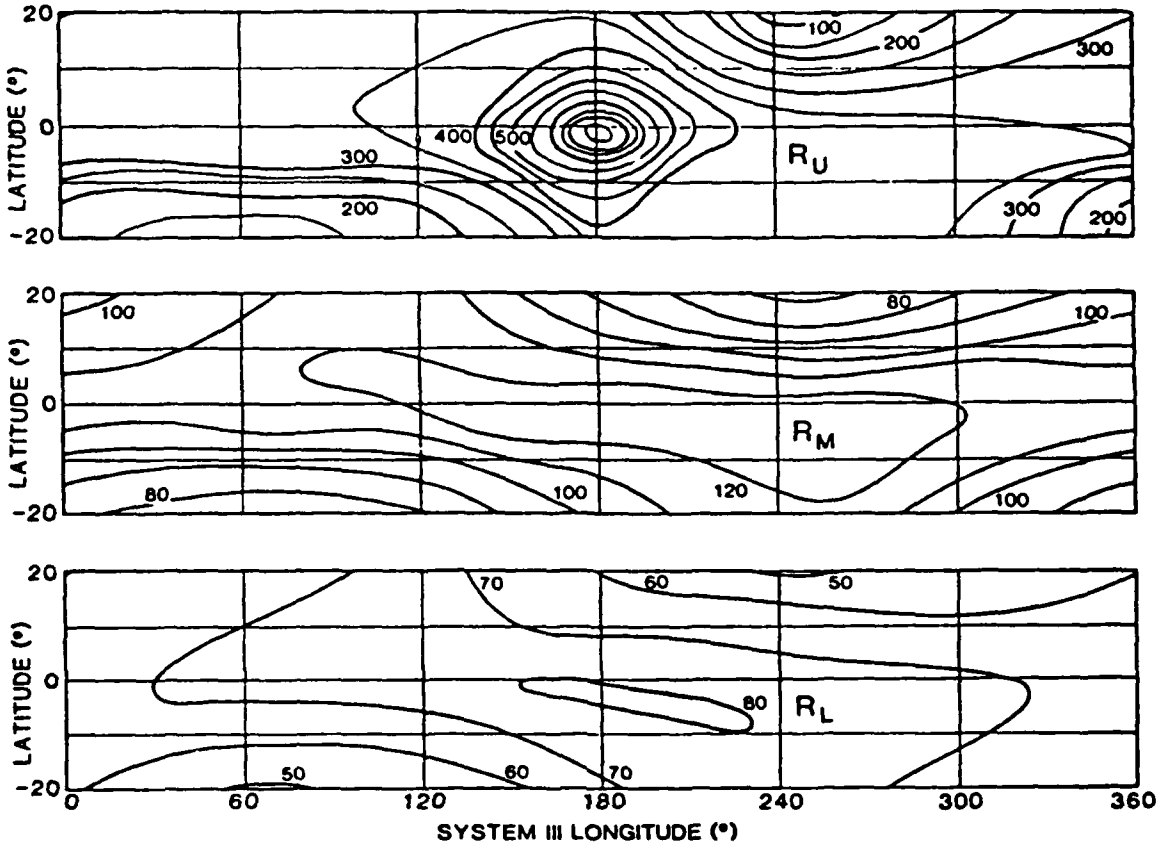

FIGURE 3.2A (top panel)

Contour map of the value of the parameter R_U, one of the three rigidity values used to characterize the cutoff distribution functions.

FIGURE 3.2B (central panel)

Contour map of the value of R_M.

FIGURE 3.2C (lowest panel)

Contour map of the value of R_L.

CHAPTER 4: TRAJECTORY PARAMETERIZATION

4.1 INTRODUCTION

Prior to the development of the techniques presented in this report the study of cosmic ray access into planetary magnetospheres (mainly that of the Earth) had been carried out by methods which could broadly be divided into two types. The earlier, analytic or quasi-analytic approaches (including the work of Stormer, 1930; Lemaitre and Vallarta, 1936a,b; for example) were limited to consideration of field models which possessed axial symmetry. These approaches, whilst significantly limited in the extent to which they could represent the real geomagnetic field, nevertheless yielded very valuable insights into the phenomenology of cosmic ray access to points within the field.

The later work, utilizing the speed and power of the digital computer, involved direct testing of access by systematic tracing of trajectories at close spaced rigidities for the range of final directions at the point of interest within the magnetosphere. This technique is capable of producing cutoffs to as high a precision as required (limited only by the accuracy of the modelling of the field, atmosphere etc.), but is not capable of giving any insight into the phenomenology of cosmic ray access, and has proved to be a very inefficient means of mapping cutoffs. In practice, trajectories have to be traced for every possible angle, position and rigidity in any location, in order to build up a picture of cosmic ray access in the given situation.

The research summarized in this report has involved developing techniques for numerically characterizing trajectories in order to allow a computer to relate trajectories over any continuum of rigidity, angle, and position, for example. This technique, referred to as "Trajectory Parameterization", allows full insight into the relationship between trajectory characteristics, such as local points of maximum and minimum altitude, equator crossings, and so on, and the types of access regions summarized in the Chapter 1.

The development of the techniques passed through a number of different phases, before reaching the fully developed form finally achieved. This chapter reviews this process of development.

4.2 RELATION BETWEEN TRAJECTORY CHARACTERISTICS AND PENUMBRAL FEATURES

The iterative digital computer-based technique determines, by direct testing, the ability of particles of any particular rigidity to arrive at a given site in a given direction. A "negative" trajectory trace is carried out, with the computation starting at the site, in the direction of interest. Failure of the trajectory, as calculated in the reverse direction, to travel successfully to the outer boundary of the geomagnetic field indicates that a cosmic ray particle would be unable to arrive at the site under the given conditions.

For any particular direction at a given site there is generally a complex intermingling of escaping (in the negative time sense), non-escaping (including those which intersect the surface of the planet) trajectories, which gives rise to a complicated pattern of allowed and forbidden rigidity values (i.e. the penumbra). The complexity arises out of the characteristic trajectory deflection produced by the Lorentz force which affects the charged particle as it moves through the magnetic field. Calculations show that particles destined to arrive at any given site on the Earth with rigidity values within the penumbra typically travel from east to west towards the site, and swing back and forth across the magnetic equator. In the longitude range in the proximity of the arrival site the trajectories become tied to the local field line bundle, tending to loop within this bundle in the final stages of their flight towards the site.

Figure 4.1 shows a trajectory in which this behavior is very clearly displayed. The trajectory (as traced "negatively" - i.e away from the point of arrival) moves from west to east, and swings repeatedly from one side of the geomagnetic equator to the other, with the altitude changing continuously. If, in one of the low points, the surface of the Earth is encountered, cosmic ray access via that trajectory would not be allowed.

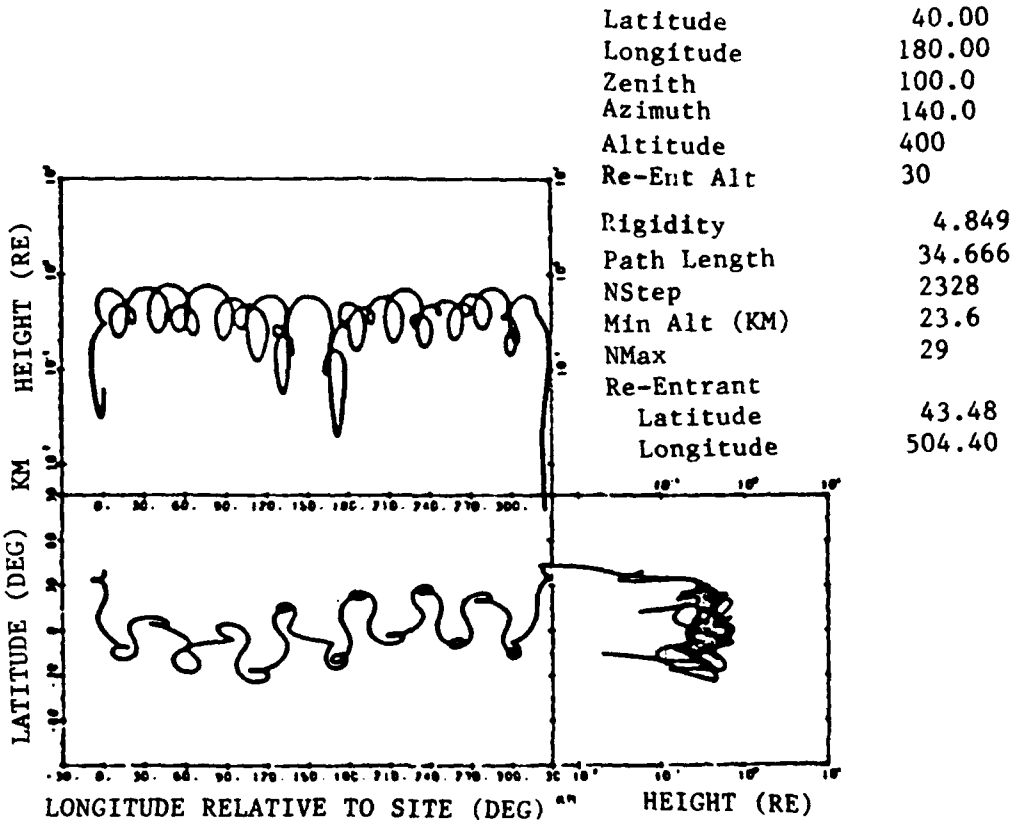

FIGURE 4.1

A trajectory displaying marked quasi-bound periodic orbit behavior. Note that the plots use geographic latitude and longitude scales. The position of the cosmic ray equator may clearly be seen from examination of the distortion of the gross trajectory form in the latitude vs. longitude plot.

The intersections demonstrably responsible for the failure of particles to enter along a particular trajectory may in principle be classified according to the section of the trajectory in which they occur. Consider such trajectories as being followed in the "negative" direction - traced outward away from the site. The trajectories are seen to pass through loops and other contortions which take the "particle" alternately towards and away from the planet. If, in one of the approaching sections, the planet's surface (i.e. the top of the atmosphere, in the case of the Earth) is intersected, then that particular trajectory will be forbidden to particles of the given rigidity from outside the magnetic field.

The point along the trajectory at which reentry occurs characterizes the allowed/forbidden structure of the penumbra in the physical location/direction/rigidity space of the particle. Very clearly defined regions of this space may be distinguished. First of all, we will consider those produced by intersection with the planet of the particle trajectories within the local field line bundle. The traditional shadow cone forbidden region is due to intersection of trajectories in the immediate locality of the site in question before even a single loop is performed. Other shadow cone regions are associated with the intersection of the second, third, or etc. loop with the surface of the planet.

Intersection of these loops with the surface of the planet occurs in the general vicinity of the site. Because of the short path traversed by the computational "particle" in traveling from the site to the point of intersection of the loops with the surface of the planet, and because the paths are restricted to relatively low altitudes, the penumbral structures so produced are relatively stable and field independent.

On the other hand, if the negative "particle" travels successfully through the local field, negotiating the loops (if present) without intersecting the planet's surface, then its motion takes on a more broadly identifiable character. Such trajectories are seen to travel back and forth between the northern and southern magnetic hemispheres, while moving from west to east. This portion of the trajectories will be referred to as the periodic orbit part. The trajectory may possess zero, one, or more

loops in each section (we define a section as any individual part of a trajectory lying to one side or other of the magnetic equator), depending on the nature of the particular trajectory. Within the loops the charged particle is able to approach the planet most closely, and the trajectory may intersect the planet's surface at one of these points. Although trajectories in the immediate physical location/direction/rigidity space will also be affected, the fact that the path between the site and the reentry point is relatively long means that the forbidden space tends to be of restricted extent, and to be parameter and field sensitive.

Because of the greatly increased number of near approach points in long multiple section trajectories, and the greater trajectory path lengths involved, the penumbral structure so produced is very much more finely structured, complex and field sensitive than the shadow cone structures. Nevertheless, it is in principle possible to classify the penumbral structure detail according to the section of the trajectory in which the reentry has occurred, and to explore the sensitivity of the structure to the field and parameter changes. Systematic labelling of the trajectory structures would open the way for investigating the nature of the penumbra, and the other allowed/forbidden structures (as reviewed in Chapter 1).

As a first step towards implementing such a scheme for use in an automated computer-based system, trajectories were characterized in terms of the number of loops performed in each of the trajectory sections. A standard trajectory tracing program was modified to allow the appropriate detection and counting of trajectory loops.

What is a loop? A loop is considered to have been executed when the curvature vector associated with the trajectory has rotated through 360^{o}. Figure 4.2 shows a reentrant trajectory within the geomagnetic field which contains six loops, three very obvious ones (seen clearly in the altitude vs. longitude plot), and three others - one near the site, one more just before the first crossing of the geomagnetic equator, and another in the last section of the trajectory, in its passage towards the surface of the earth. In practice loops such as these are detected automatically by computer during the trajectory trace. The number of loops in each section

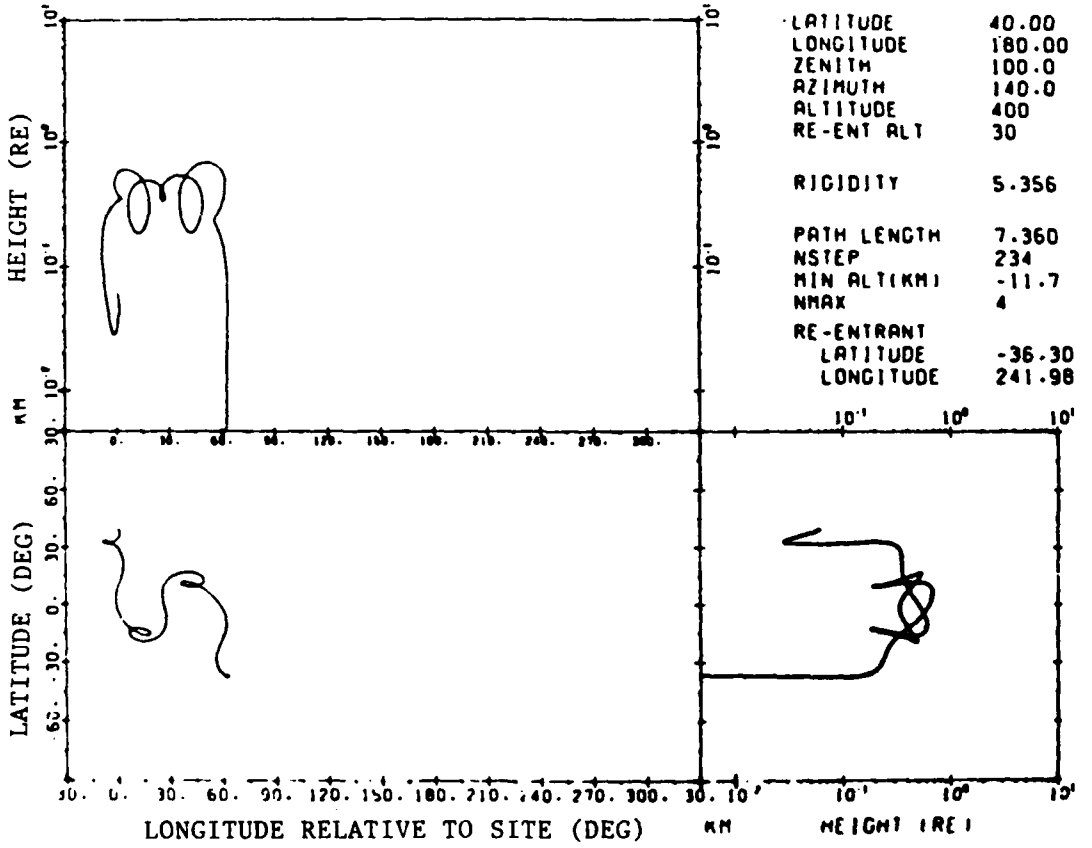

FIGURE 4.2

A sample trajectory, showing six loops (categorized by computer as a 2211 reentrant trajectory).

is counted as the trace proceeds, and is stored for printing at the end of the calculation. The order of the loop numbers as they are listed (in figure 4.3, for example) is such that the first number refers to the section closest to the site.

Figure 4.3 shows a plot based on the trajectory loop numbers. This plot represents a section of the terrestrial penumbra for an azimuth range of 129-145° geographic for the given situation (100° zenith angle, 400 km altitude, 40° latitude, 180° longitude, field model IGRF 1975.0 modified to Epoch 1980.0). Trajectory loop numbers are presented for 1% rigidity intervals in the range 10.025 to 4.054 GV. This situation was investigated as part of another study, and is not represented as having any particular significance to this present discussion. Although the particular structure (including the "overhung" shadow cone, made up of unlooped reentrant trajectories) is in detail characteristic only of the given site and conditions, the applicability of the category scheme to a complex situation such as this is well illustrated.

Inspection of the listed categories shows that there exists a well-ordered structure of penumbral bands, even in the continuum of forbidden trajectories below the few allowed trajectories in the region of 8-9 GV. Bands have been shaded to emphasize the band structure. Calculated loop numbers for intermediate azimuths (not shown) have been used to help resolve the complexity in some areas. At the 1% rigidity interval utilized here the wider bands attributable to short and medium range reentrant trajectories (involving trajectories having up to approximately 3 equatorial crossings) show clearly. With decreasing rigidity an orderly succession of bands appears, produced by trajectories possessing greater and greater number of loops. At any point the low order bands due to short range earth intersections overlie the higher order bands resulting from intersections further along the trajectories. An apparent continuum of forbidden trajectories may in fact consist of many overlapping bands (where the latter may be infinitesimally narrow). Calculations carried out for progressively finer rigidity intervals (and for finer azimuth spacing) tend to reveal progressively greater detail in the high order penumbral band structure.

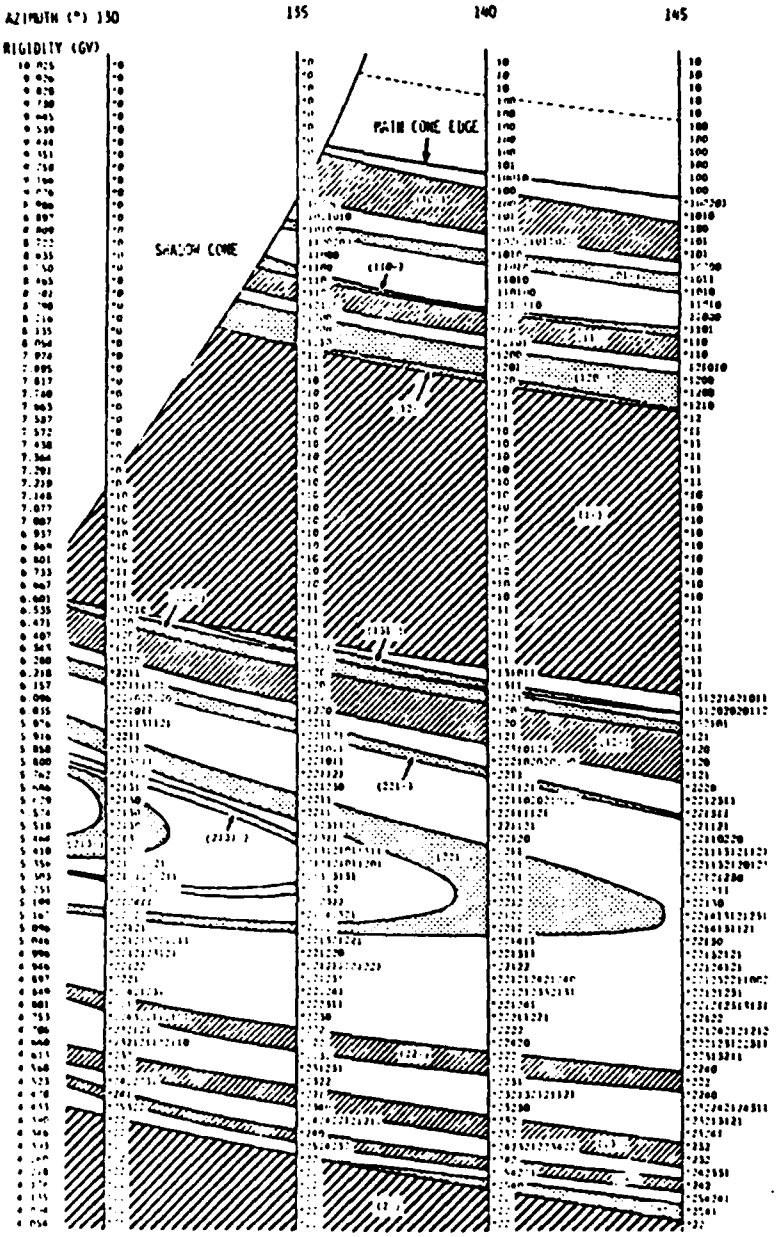

FIGURE 4.3

Listed computer derived loop numbers (truncated to a maximum of 12 digits) for a sample penumbral region at 100° zenith angle (the location etc., is defined the text). Clearly distinguished penumbral bands are numerically identified and shaded (heaviest shading: 1 trajectory equator crossing, lightest: 4 crossings). The asterisks identify reentrant orbits. Unshaded areas in the penumbra may contain either forbidden bands or allowed trajectories.

This technique revealed some very interesting insights into some particular aspects of the main cone and penumbra.

a) In the calculated penumbra it is the forbidden bands, not the allowed bands, that are defined. An allowed band can only exist when no obscuring forbidden bands lie at the rigidity in question (analogous to looking at a distant view between the trunks of a forest of trees - one sees the view when there are no trunks in the way; it only takes one trunk to obscure the view, no matter how many gaps there are also in the line-of-sight).

b) Penumbral structure produced by earth intersections in sections close to the site are much wider and more stable than those resulting from longer range reentrant trajectories.

c) The offset of the basic geomagnetic dipole manifests itself in differences in the degree of overlapping and mixing of penumbral bands at different points on the Earth's surface.

d) Higher order penumbral bands (those possessing several sections) have greater sensitivity to geomagnetic field perturbations and to changes in field model parameters than do those of lower order, and so are relatively unstable.

There is a very high degree of order in the penumbra which is usefully displayed in diagrams of the type that figure 4.3 represents. This kind of plot has to be prepared by inspection of the arrays of loop numbers, a very inefficient process. Another kind of plot can better be used to show the penumbral order - one involving a plot of trajectory feature positions, which is prepared completely by computer.

4.3 SUMMARY PLOT REPRESENTATION OF THE PENUMBRA

The "Summary Plot" representation is more efficient, and a somewhat more refined way of representing trajectory access information.

Trajectories are effectively summarized in terms of plots of the positions of the trajectory "cardinal points". These cardinal points are loops, low points and magnetic equator crossing points. These points change position (both path length and altitude) in a systematic manner with changing rigidity. The cardinal point positions may be plotted to produce the so-called summary plot, in which for each of the types of cardinal points the point positions are presented for a range of values of rigidity (or for a range of whatever parameter is of particular interest). These plots are prepared on a printer, using printed characters positioned on a page so that their position is related to the path length along the trajectory, as traced in the "negative time" direction, away from the final arrival point). The character used to represent each point represents useful information about the point; for example, altitude in the case of low points, and "loop development" in the case of the loop position plot.

Figure 4.4 shows a typical summary plot set (this is a direct reproduction of a microfiche, as reproduced from Cooke et al., 1981). Cooke and Bredesen, 1981, presented another set of summary plots which, like these reveal a very highly ordered structure. In figure 4.4 the penumbral forbidden bands are clearly shown as points where the low points intersect the reference height corresponding to what is deemed to be the grazing height in the atmosphere. The penumbral bands are directly displayed on the plot which shows the position of the intersection points. Note that the edge of the Stormer cone is displayed clearly in this plot, as the boundary below which all trajectories display bound periodic behavior. After the onset of this behavior, the trajectories are completely bound, and cannot escape the field (and therefore cosmic rays outside the field with the particular rigidities are unable to gain access to the particular point and direction involved).

The technique is employed of continuing the trajectory traces beyond these intersection points so that structures may be traced from one side to the other of the range of rigidity in which a forbidden band lies. It should be clearly understood, however, that the intersection trajectories do not represent "real" trajectories, but are merely a useful aid to the tracing of continuous structures.

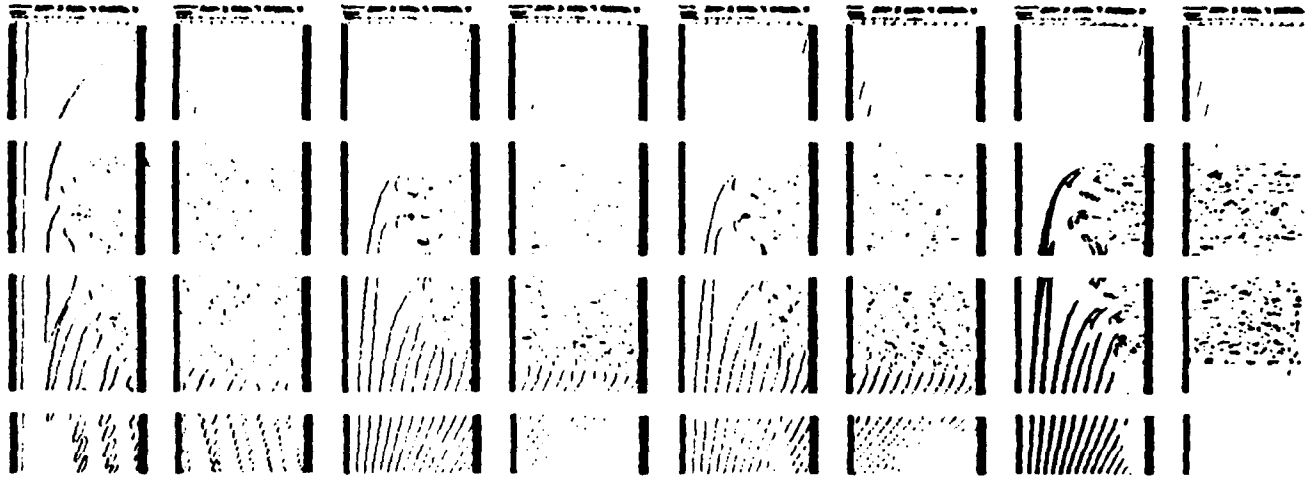

FIGURE 4.4

Summary plot set of Cooke and Bredesen, 1981, representing positions of equatorial crossings, loops, low points, and earth/atmosphere intersections (paired columns from left to right), for a range of rigidity values from 15.00 GV down to 5.00 GV in 0.05 GV increments. These calculations were carried out for vertical incidence at the location with geographic latitude -10° and longitude 270°, and 400 km altitude; for magnetic field IGRF 1975.0 updated to 1980.0. The paired diagrams show detail for trajectory path lengths of 0-12 and 12-24 earth radii. The distinct change in behavior of the longer trajectory sections, which occurs at 7.20 GV, is interpreted as being produced by transit of the Stormer cone edge.

The scale of the trajectory cardinal point structures and the penumbral structures varies over a wide range - those a short range trajectory sections may exist for many GV, while at long trajectory ranges the structures may exist only fleetingly and may be represented by only a single point on a summary plot, if seen at all. Nevertheless, when examined at appropriately fine rigidity intervals they show the same characteristic forms as the larger scale, short range, structures.

4.4 AUTOMATED TRAJECTORY PARAMETERIZATION

As a final stage in the use of trajectory parameters to aid in the exploration of cosmic ray access to points within the geomagnetic field, strategies have been developed and incorporated into computer programs that locate the trajectory cardinal points and then correlate the position of these points with change in any of the parameters involved in the computations, in order to map the features associated with the cardinal points with any required range of parameter value. The new approach, while utilizing the speed, efficiency and "real" geomagnetic field modeling capabilities of the digital computer, yields an analytical insight equivalent to the earlier and elegant approaches of Stormer and Lemaitre and Vallarta. The technique is applicable to cosmic ray access into any planetary magnetosphere, although the discussion here is presented in terms of the situation in the geomagnetic field, in relation to which the technique was developed.

Like the basic digital computer iterative penumbral mapping procedure out of which it has grown (Shea et al., 1965), the parameterization approach involves the tracing of trajectories in the reverse, "negative time", direction, out away from the point in the magnetic field for which the penumbra is to be studied. Similarly, the input parameters required for the trajectory traces include those identifying the location and direction of interest at the site - latitude, longitude, altitude, zenith and azimuth - and other parameters such as particle rigidity, grazing altitude (altitude above the Earth's surface at which a trajectory is deemed to graze the atmosphere), magnetic field parameters, and time.

Whereas the standard penumbral mapping technique involves a systematic testing of whether individual trajectories are allowed or forbidden for sets of discrete parameter values (typically for varying rigidity), the "parameterization" approach takes advantage of the fact that trajectories possess a continuity of form over variation in any parameter in the set to efficiently trace particular penumbral features, or to elucidate their characteristics.

Although the trajectory configuration may in some situations alter exceedingly rapidly with variation of a given parameter, the changes in form take place in a continuous manner. The trajectory "cardinal points" are found to change position in a quite systematic manner with changes in any parameter. Figure 4.5, an enlarged section of one of the trajectory summary plots of Cooke and Bredesen, 1981, illustrates this clearly.

As recognized by Lemaitre and Vallarta (1936a), the generators of penumbral structures (i.e., the trajectories defining the edge of the allowed regions, lying at the transition from allowed to forbidden regions) are allowed trajectories that graze the planet (Earth's atmosphere) at some point along their length.

Assume that the parameters belonging to a transition trajectory in a given situation have been established - the trajectory has been traced and found to graze the planet at a low point associated with one of the loops along the trajectory. Varying the value of any one parameter over a small interval will tend to alter the low point altitude so that the trajectory, initially grazing, is now clearly allowed or forbidden (depending on whether the low point rises or falls). Normally it is possible to vary the value of one of the other parameters in order to again make the same trajectory low point graze the surface even though, of course, the overall trajectory form will have changed slightly with the matched change in the two parameters.

This operation of matching the change in two parameters in order to maintain trajectory grazing is the key to the parameterization technique. A family of techniques can be implemented through the suitable use of this

FIGURE 4.5

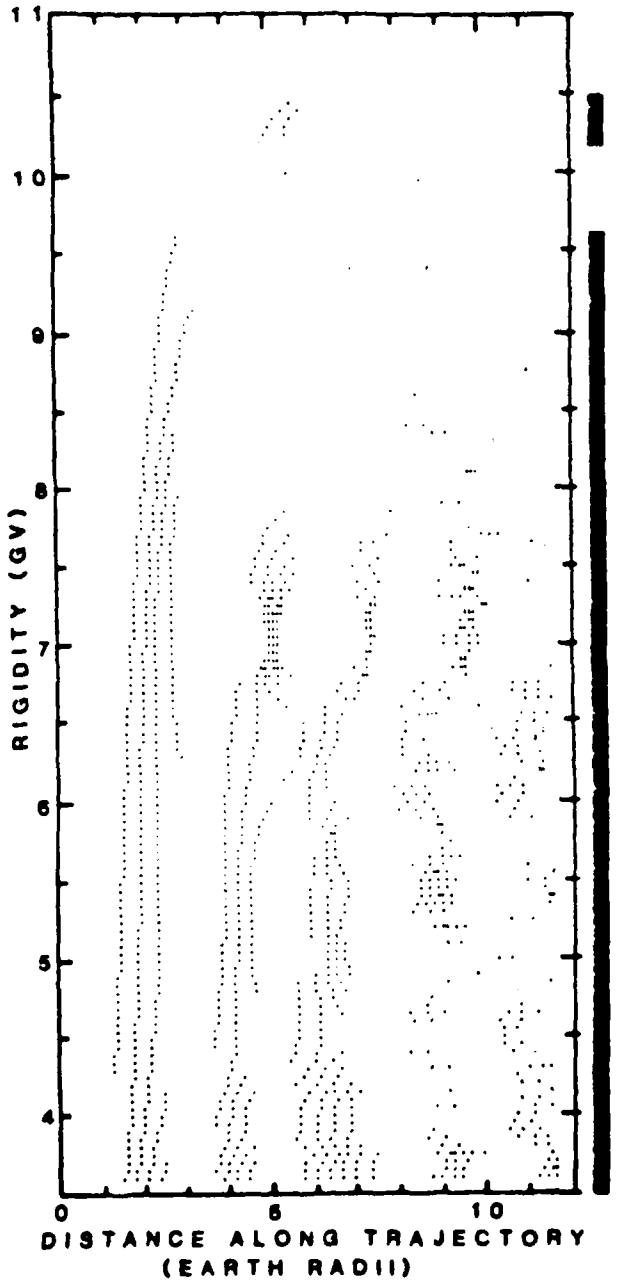

Section of one of the summary plots diagrams of Cooke and Bredesen (1981), showing the position of low points along trajectories as a function of rigidity over the range 3.5 to 11.0 GV, for trajectories arriving with vertical incidence at the site and under the conditions for which the plot of figure 4.4 was made. In this summary plot each line of print shows the positions of low points along the trajectory pertaining to the rigidity indicated by the vertical scale. The numbers represent the height of each of the low points above the Earth's surface, in tenths of Earth radii, for points above the atmosphere. Low points calculated to occur within the atmosphere or Earth are denoted by a large dot (the summary plot technique involves continuing the calculations on beyond an Earth or atmosphere intersection). On the right of the diagram may be seen the equivalent conventional representation of the allowed and forbidden penumbral structures that exist in this situation.

basic step - mapping, determination of the stability of penumbral structures, "migration" of structures over ranges of parameters (in order to establish, for example, change in a structure along the path of a satellite in orbit), to name a few of the techniques that have already been implemented in the computer program developed for use in the study of the penumbra.

The parameterization approach depends critically on the ability of the computer program to reliably identify particular cardinal points and to follow these in the presence of continued change in trajectory configuration, even though the trajectories are generally complex and possess a changing number of low points and loops. The key to the automatic tracking of trajectory cardinal points is the use of position and "development" parameters. In practice the position of the given cardinal feature (normally a low point) along a trajectory, as measured from the trajectory starting point, is monitored, and the observed changes in position are related to the change in the variable input parameter. Interpolation or extrapolation is then employed to calculate where the feature would be expected to lie under the modified set of conditions. That a certain feature lies close to the anticipated position is, however, not a sufficient condition for unambiguous identification of the trajectory features of particular interest. The "development parameter", related to the degree of development of each feature (and in part related to the trajectory curvature at the point), is computed for each feature along a trajectory. This parameter, while varying relatively slowly with change in the input parameter, differs significantly from feature to feature, and so can be used as an identification label to aid recognition of particular features. The application and use of both the position and development parameters has been found sufficient to allow the computer program to "recognize" features, and to monitor their role in contributing to penumbral structures.

Because the iterative trajectory trace procedure is inherently a noncontinuous process, and because the traces are carried out for discrete values of the parameters used to define the situation of interest, it has been of prime importance to develop high precision interpolation and

extrapolation techniques to allow the estimation of the required values of the variables from the sets of discrete parameter values available. In addition to the use of such techniques in the prediction of the position and development parameter values, as mentioned in the preceding, the techniques are critically important to the accurate and efficient determination of the location of band edges in any parameter space (including cutoff values), and in the procedures employed in the automatic mapping of penumbral structures.

The computer program can operate in a number of different modes, each designed to carry out one of the well defined tasks involved in the various aspects of examining and mapping the penumbra. Although the selection and definition of the individual program task modes is under interactive control, the execution of each task is performed completely automatically by the computer. The more important of the program modes of operation are described in the following sections.

4.4.1 MAPPING: The mapping facility traces the edges of the penumbral bands by means of a continued cycle of operations in which two parameters (zenith and azimuth, or latitude and longitude, for example) are continuously varied while the matching condition is continuously applied. This procedure is essentially a starting point calculation in the two parameter space, in which the locus is traced of paired values of parameters for which grazing occurs at the low point of interest.

The domain over which the locus (or "sheet", as Lemaitre and Vallarta termed it) contains the allowed-forbidden transition trajectories is normally limited because of the intruding effects of other trajectory minima. Generally some low point other than the one initially considered, will move downward with continued change in the variable parameters, and at some place on the locus this second low point will lie at the grazing height. Beyond this the newly significant low point will cause the trajectory to be forbidden so that now the further "virtual" extension of the locus will no longer define the allowed-forbidden transition (although it is useful, for some purposes, to map such virtual penumbral band edges).

The transition will now, for some finite domain within the two parameter space, be defined by a locus associated with grazing by the second loop. The whole penumbral structure in any situation is constituted of sets of such intersecting sheets.

A predictor-corrector system allows the program to "feel" its way along any given sheet, adjusting the size of its steps and the direction followed according to its predictive success in the preceding steps. In the computer program the option may be taken of tracing the system of sheets, automatically transferring from one sheet to another at the points of intersection. Alternatively, the entire extent of a sheet, including its virtual extensions, may be traced.

Figure 4.6 shows a typical example of the kind of mapping that can be carried out. This example shows the zenith-azimuth position of the various major penumbral structures for the specified conditions, for rigidity values of 7.7, 14.0, 30.0 and ∞ GV. Many fine bands co-exist here too, lying predominantly close to and parallel to those bands mapped. The characteristics of the major structures in the diagram are broadly similar to those found by Lemaitre and Vallarta (for example, see figure 7 of Lemaitre and Vallarta, 1936b). The characteristic distortion of the structures in the north-east is produced by "folding" associated with the loop cone effect of Cooke and Humble (1970). The 7.7 GV figure displays some very significant features, in particular the isolated forbidden "island", which form as the penumbral bands associated with the higher rigidity structures separate from the major underlying penumbral edge with diminishing rigidity.

Figure 4.7 shows a map of the boundary of the shadow cone for 30 GV particles, as traced by computer, using the trajectory parameterization technique (refer to Chapter 1 for definition of "shadow cone"). In brief - it is the shadow of the planet (in this case the Earth) for particles of the given rigidity. It is interesting to note that the shape of the shadow is not a simple circle or oval as might intuitively be expected, it instead exhibits a cusp at its highest zenith angle excursion. This occurs because of the development of an intermediate loop (i.e. between the "horizon" and

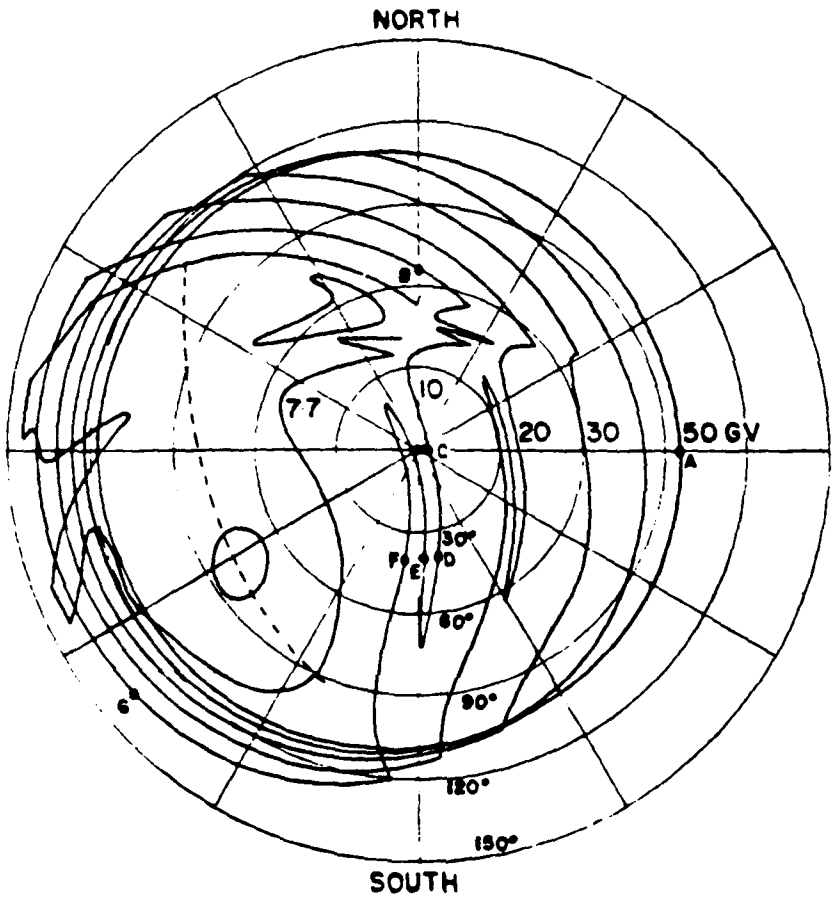

FIGURE 4.6

Penumbral structure for 50,30,20,14,10 and 7.7 GV at the point in the geomagnetic field with geographic latitude 10° N and longitude 270°, and altitude 400 km. The magnetic field model used was IGRF updated to 1980.0. The letters used to identify portions of the structures for which Band Stability Factors have been calculated (the results are presented in table 4.2). The reference circles lie 30° apart in zenith, and the radial lines 30° in azimuth.

the arrival site) at some particular azimuth. With further changing azimuth this loop develops to the point where it intersects the surface of the Earth, upon which it then defines part of the original bounding line.

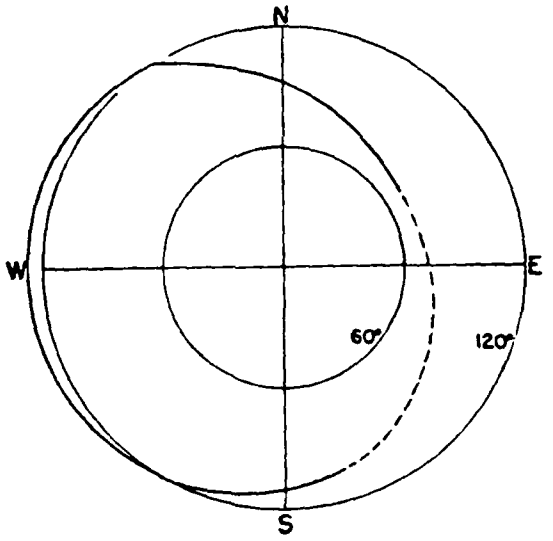

FIGURE 4.7 Simple shadow cone calculated for 30 GV charged cosmic ray particles approaching a site with geographic coordinates: Latitude 10°, longitude 270° (other calculation parameters are the same as used for the plots in figure 4.6).

4.4.2 MIGRATION: The operation of migrating a penumbral structure is essentially similar to mapping. In this case the objective is to track the position of a given penumbral band edge as it moves in response to change in any of the input parameters, rather than to completely ascertain the form of the penumbral structure in the domain of interest. Changes in band edge position occurring in response to changes in a number of parameters can be established by migrating the band edge either one parameter at a time or alternatively by simultaneous stepped proportional change in all parameters.

Table 4.1 shows an example of multiple parameter migration. In this example, the band edge which exists for the conditions shown in step 1 is to be traced, and the longitude at which the band will lie at for the new situation listed in step 7, determined. During this migration each of the parameters other than longitude is being changed proportionally. Longitude value is, in this case, being allowed to "float" - an appropriate value being determined for each of the steps.

In single parameter migration, one parameter is being changed while

the other, nominated, parameter is allowed to float. In practice, for the case of single parameter migration, it has proved convenient to use zenith angle as the dependent (or floating) parameter, so that the position of the band edge is followed in zenith angle as each parameter is varied.

TABLE 4.1

Example of multiple parameter "migration". The penumbral band edge which lies at the location given in step 1 is traced to find at what longitude it would lie for the parameter values listed in step 7 (note that the longitude value, initially defined, is allowed to "float", in order to find what new value of longitude would place the same band edge in the new location and direction. Angles are expressed in degrees.

STEP	LATITUDE	LONGITUDE	ZENITH	AZIMUTH	RIGIDITY	ALTITUDE
1	7.5	270.0	0.0	0.0	10.0	400.0
2	7.7	(268.5)	0.4	24.1	10.1	395.6
3	8.8	(266.1)	1.4	76.3	10.3	386.1
4	8.7	(262.4)	2.4	131.3	10.5	376.1
5	9.2	(255.8)	3.4	186.3	10.7	366.1
6	9.7	(247.3)	4.4	241.3	10.9	356.1
7	10.0	(243.1)	5.0	275.0	11.0	350.0

4.4.3 PENUMBRAL BAND STABILITY: The stability of any given portion of a penumbral band edge can very simply be expressed in terms of the "Band Shift Factor", BSF = $\delta R/\delta P$, and determined by computer as BSF = $(\delta R/\delta P_i)_{\delta P_i \to 0}$ where δR is the change in rigidity R required to maintain grazing in the low point responsible for the penumbral feature, for a change δP_i in the i^{th} parameter P_i. The BSF, being the measure of the rate at which the band edge shifts with variation in the independent parameter, is essentially a factor describing the stability of the structure. The independent parameters used to establish the BSFs could be extended to include quantitative measures of individual internal or external field

sources, internal calculation parameters, or any other "real" or artificial parameter involved in the calculations. The computer program has been set up to produce, on demand, a full set of BSFs pertaining to a nominated band edge, for the basic set of input parameters.

TABLE 4.2

Values of Band Shift Factor, a measure of penumbral band edge stability, for the structures indicated alphabetically in figure 4.6.

		Band shift factor value for different structures at identified locations								
Independent Parameter	Absolute Value of Parameter	A	B	C	D	E	F	G	H	Unit
Latitude	10°	2.6772	0.3131	0.0818	0.0319	0.0107	0.0044	0.4668	-0.0079	GV/°
Longitude	270°	-0.1510	0.1993	-0.0018	-0.0608	-0.0518	-0.0529	-0.0507	-0.0002	GV/°
Geocentric alt.	400 km	-0.0395	-0.0096	-0.0033	-0.0009	-0.0029	-0.0031	0.0095	-0.0523	GV/km
Grazing height	30 km	0.0247	0.0069	0.0004	0.0033	-0.0001	0.0001	-0.0542	-0.0001	GV/km
Zenith angle	various*	-0.4212	-0.3299	-0.2235	-0.2827	-0.2119	-0.2290	0.0038	-0.0814	GV/°
Azimuth angle	various* *see fig.1	-0.2932	-0.0006	-0.0663	-0.1231	-0.0837	-0.0816	-0.0128	-0.0263	GV/°

The dependence of the change in penumbral band edge position in any parameter P_1 for change in any other parameter P_2 can be obtained by suitable combination of the BSF's, viz.

$$\frac{\partial P_1}{\partial P_2} = \frac{\partial R}{\partial P_2} \times \frac{\partial P_1}{\partial R}$$

Similarly, the stability of the entire penumbral band can be expressed by suitable combination of BSFs to form the Band Growth Factor (BGF):

$$BGF = \frac{(\partial R_U/\partial P - \partial R_L/\partial P)}{R_U - R_L} \times 100 \quad \%$$

per unit change in the independent parameter P, where R_U and R_L are the rigidities defining the upper and lower edges of the penumbral band. The BGF is a measure of the percentage rate of change in width of a penumbral band with change in any given parameter for a given set of conditions.

Table 4.2 presents calculated values of the Band Shift Factors pertaining to eight points on the penumbral structures presented in figure 4.6, where the points are labeled alphabetically. Note the tendency for the stability to be greater for larger scale, short range, structures, and for higher rigidities (a high BSF implies high stability).

4.5 CONCLUSIONS

The trajectory parameterization technique offers a very powerful means of determining the characteristics of the penumbra in any particular situation. Use of the technique has revealed some very interesting, and some unexpected, information about the penumbra. For example, the penumbral "islands" displayed in figure 4.6 were not known to exist previously. Use of the migration and stability techniques show these islands to have interesting properties, in particular, a great sensitivity to rigidity and field model (for example, the 7.7 GV penumbral island, centered at 76° zenith angle and 279° azimuth in figure 4.6, disappears when the rigidity is reduced by 0.085 GV, and does not exist at 7.7 GV when the mapping is carried out using the IGRF 1975 geomagnetic field).

In the following chapters the parameterization technique is used to investigate other aspects of the penumbra within the geomagnetic field. These techniques would apply equally well to the magnetic field of Jupiter, for example, but to date have not yet been applied to fields other than that of the Earth.

CHAPTER 5: THE HIGH ZENITH ANGLE LIMITS OF COSMIC RAY ACCESS TO AN EARTH SATELLITE

5.1 INTRODUCTION

A knowledge is often required of the highest zenith angle for which a charged particle of given rigidity has access to an earth satellite lying in a particular orbital configuration.

Because of the complexities of the trajectories by which below-line-of sight access to a satellite occurs it has proven difficult to determine systematically whether absolute limits exist beyond which access is forbidden. The general approach to this problem has been to directly test for access by carrying out a large volume of trajectory traces. This method, however, is not completely satisfactory because the absence of detected access beyond a given angle does not constitute a satisfactory proof that access could not occur (either via undetected allowed trajectories that exist under the geomagnetic field conditions simulated, or under even slight perturbations away from these conditions).

A technique has been developed, based on the trajectory parameterization technique, which allows a very much more definitive insight into the problem of establishing the high zenith angle limits.

5.2 DISCUSSION

The new method involves the examination of the form of trajectories along which particles approach a satellite, and consideration of whether these orbits can or cannot provide access for charged particles entering from outside the geomagnetic field. (In line with ordinary trajectory tracing practice the traces are carried out in the reverse, negative-time, direction - out away from the satellite.)

Before discussing the technique further it is appropriate to briefly review the question of access to a point in an axially symmetric

representation of the geomagnetic field (more fully discussed in Chapter 1). In a simple, axially symmetric field, three types of solid angle region may be distinguished relative to any point in the field - the "main allowed" cone, the "Stormer" cone, and the penumbra.

For the purpose of the work reported here it has proven practical and useful to distinguish four different kinds of solid angle regions relative to a given point in the "real" field. These are the regions within which:

1) access is forbidden because of short range intersection with the Earth (as detected in the outward trajectory trace). These trajectories correspond to the short range "shadow" orbits of Lemaitre and Vallarta.

2) access from outside the geomagnetic field either does, or possibly could, occur along aperiodic or unstable quasi-periodic orbits.

3) entry would only be by aperiodic of quasi-periodic orbits that intersect the surface of the earth.

4) approach could occur via quasi-periodic orbits that have no detected intersection with the atmosphere. Such trajectories can extend for very large distances in the field without any detected field escape or earth intersection. It is impractical (or even sometimes impossible) to trace these to some definite end, so the traces are terminated at a nominated path length. Thus the matter of access via such trajectories remains unresolved (the question of the precision of very long trajectory traces necessarily enters here, but will not be discussed).

Figures 5.1 through 5.4 illustrate trajectories associated with the four kinds of region. In the trajectory parameterization technique used in this study it is important to continue the trajectory traces on beyond the first intersection with the surface of the Earth. This is an artifact necessary to the operation of the technique (and in the identification of trajectory form), and is not held to represent any kind of reality. Thus, in figures 5.1 and 5.3, the trajectories are seen to pass through the surface of the solid Earth (shown by a dashed line).

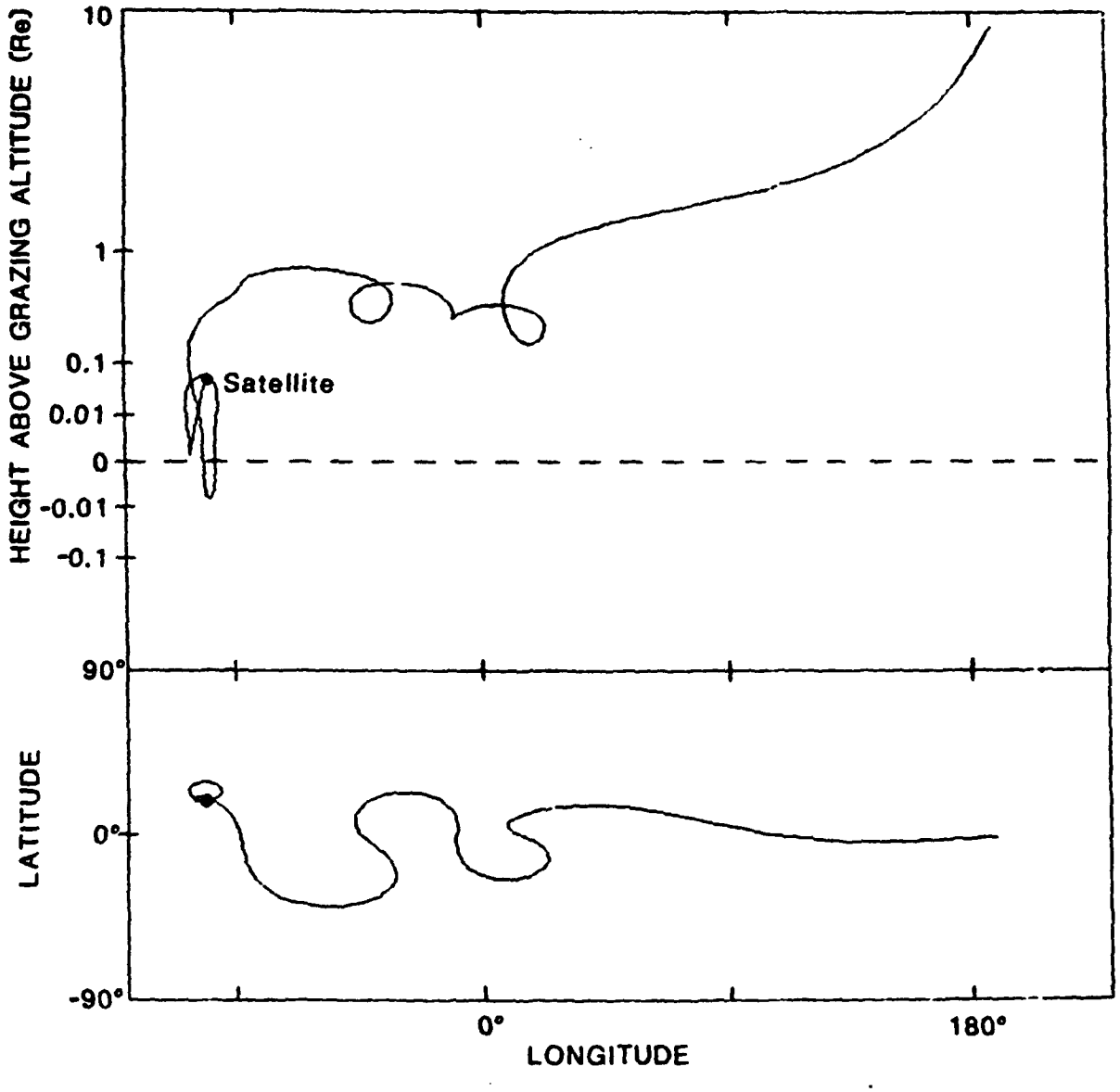

FIGURE 5.1

Trajectory (type (1)) displaying short range "shadow" intersection with the atmosphere. The trajectory, which was continued on past the intersection, indicated that escape from the field (or entry from outside the field) would otherwise have been possible.
[Trajectory arrival point parameters: latitude = 17.5° N, longitude = 260° E, zenith = 145°, azimuth = 270°, rigidity = 7.5 GV, Altitude = 400 km, grazing height = 30 km; geomagnetic field IGRF80].

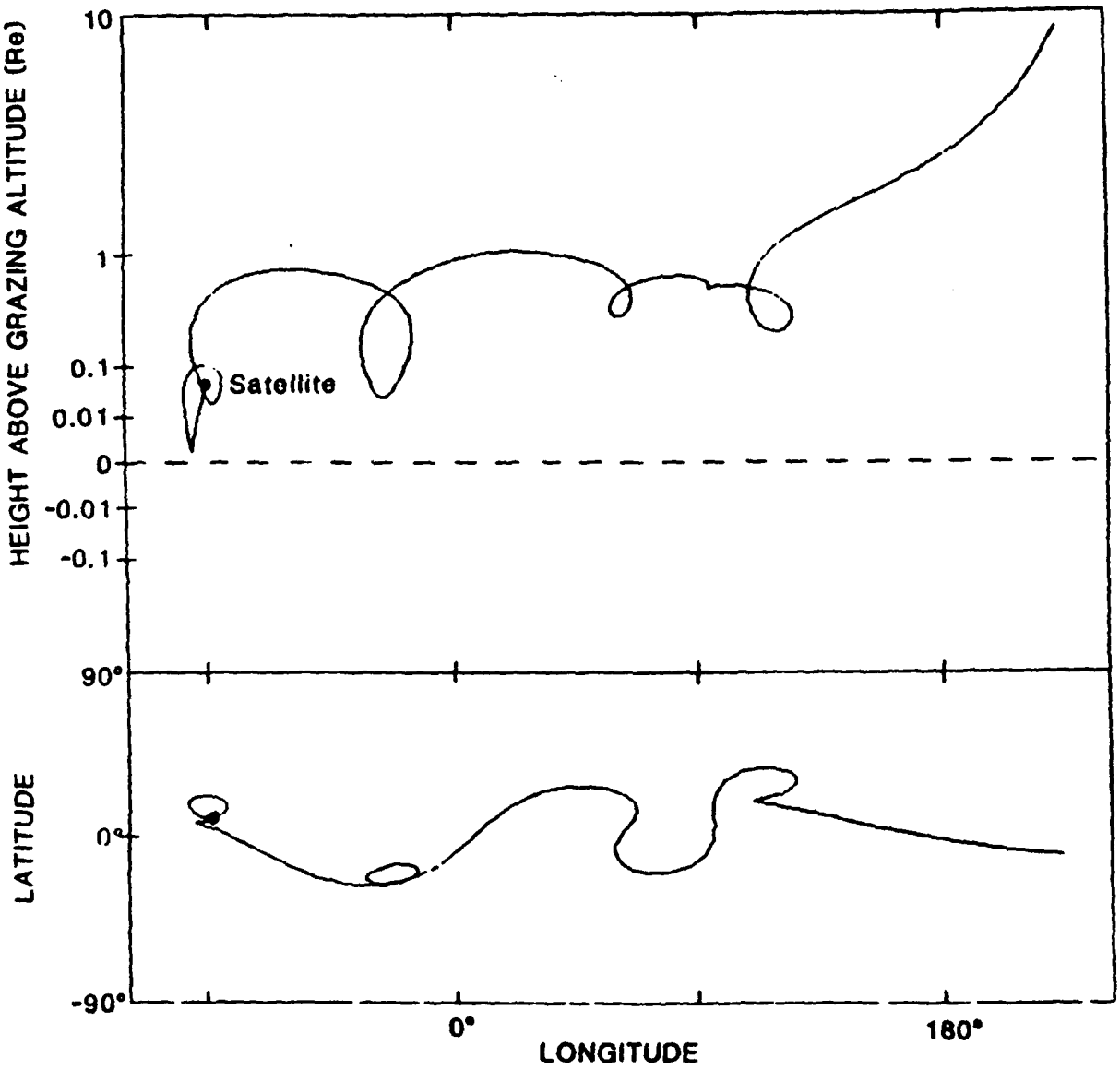

FIGURE 5.2

Trajectory of type (2) - along which the point in the field is accessible via aperiodic orbit.
[Trajectory parameters: latitude = 10°, longitude = 270°, zenith = 144.5°, azimuth = 278°, rigidity = 7.7, altitude = 400 km, grazing height = 30 km; geomagnetic field IGRF80].

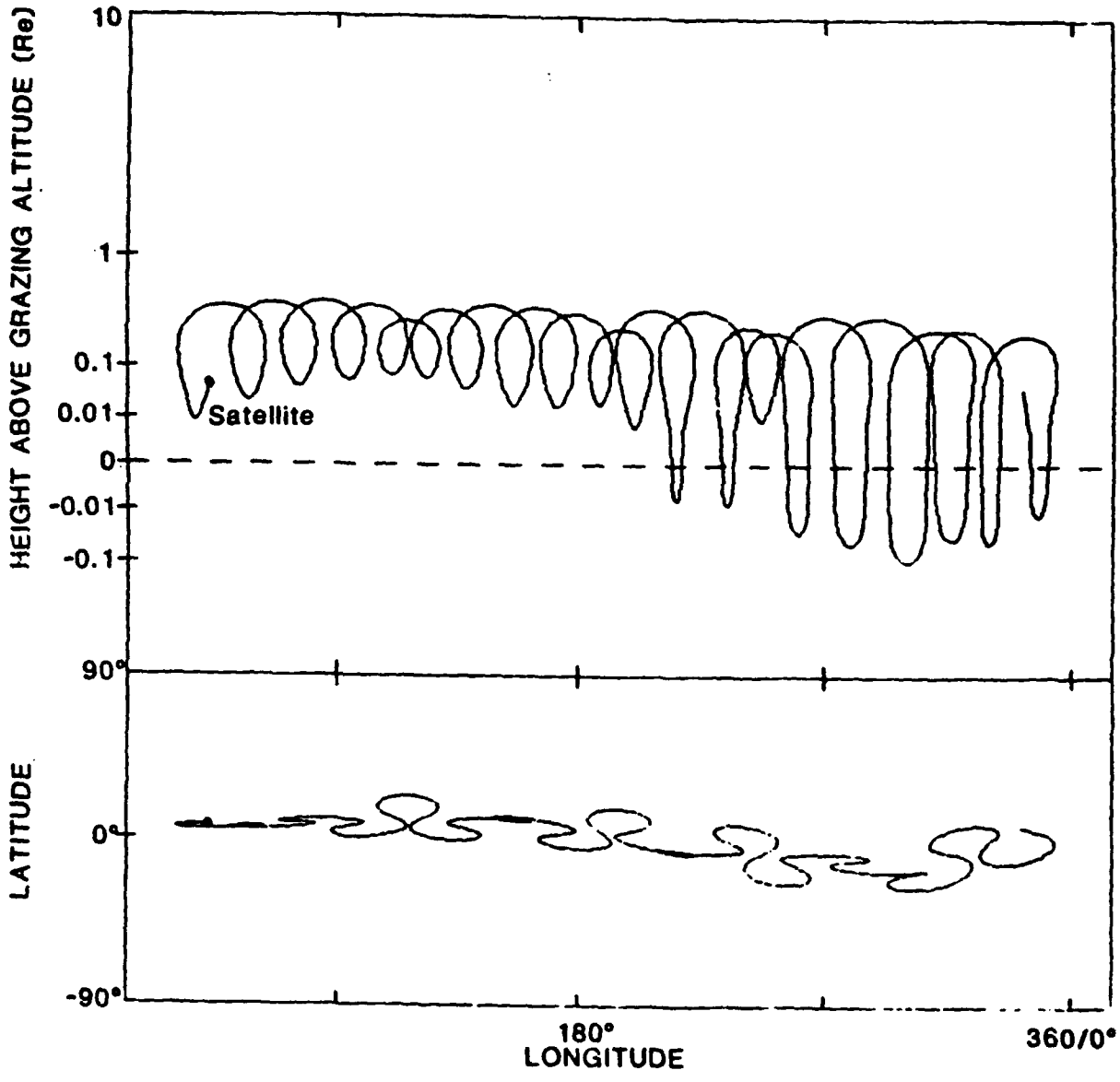

FIGURE 5.3

Type (3) trajectory - showing regular quasi-bound periodic form, intersecting the atmosphere.
[Trajectory parameters: latitude = 7.5° N, longitude = 45°, zenith = 145°, azimuth = 270°, rigidity = 7.5 GV, altitude = 400 km, grazing height = 30 km; geomagnetic field IGRF80].

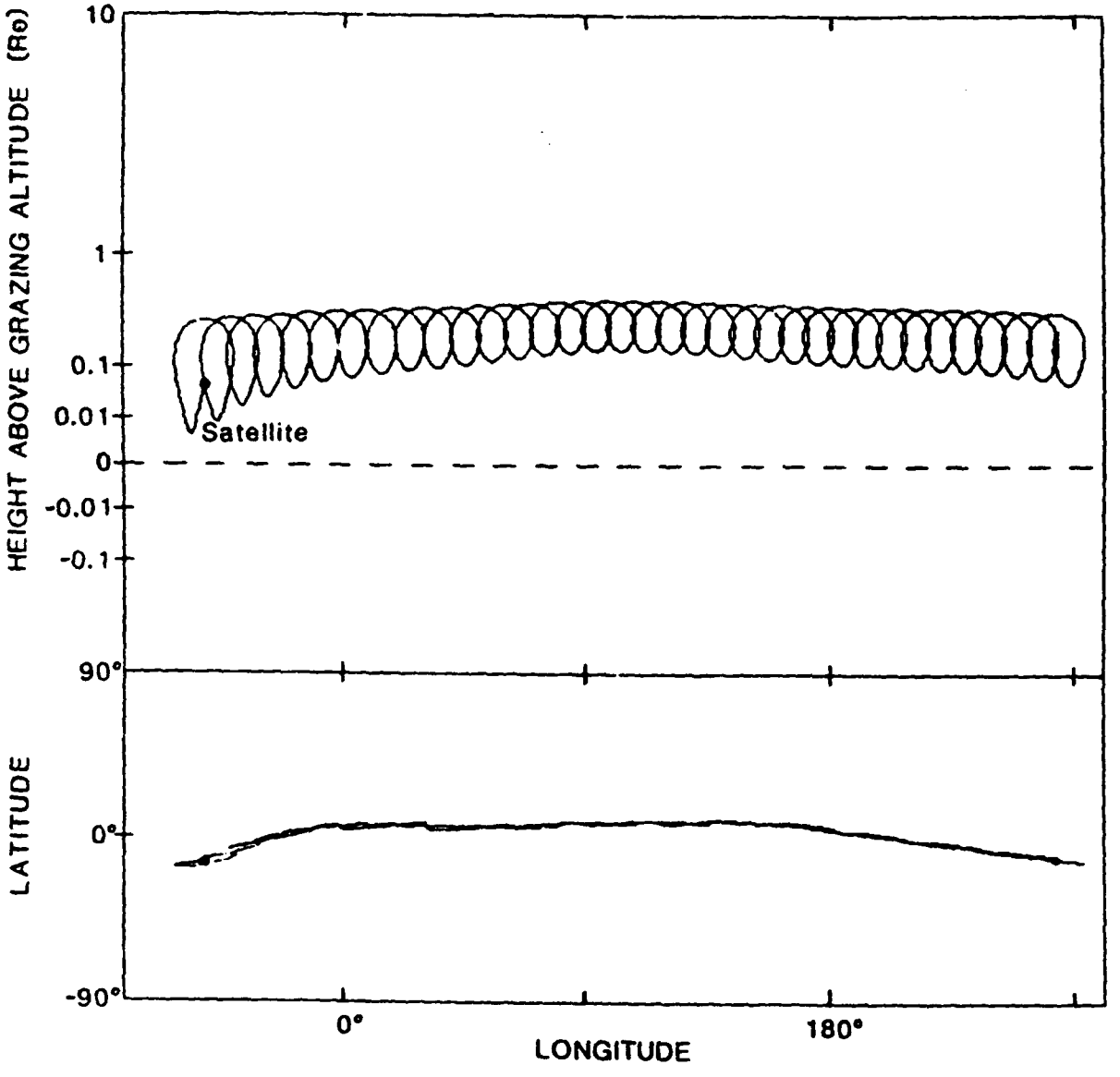

FIGURE 5.4

Trajectory of type (4) - bound periodic form with no detected intersection with the atmosphere (in this case there was no intersection as the trajectory was found to stay clear of the atmosphere at all longitudes).
[Trajectory parameters: latitude = 13.5° S, longitude = 310, zenith = 270°, azimuth = 5°, rigidity = 4, altitude = 400, grazing altitude = 30; geomagnetic field IGRF80].

Preliminary investigations have been carried out to elucidate the form and properties of the regions containing the trajectories of the four kinds. As a first step in this study, the regions containing trajectories of type (4) are mapped, either in zenith-azimuth, or in latitude-longitude, space. An example of zenith-azimuth mapping, as given by Cooke, 1982, is reproduced in part as figure 5.5. The high zenith angle limits are set by the structure visible in the west at ~145° zenith angle. This boundary is formed by short range shadow orbits.

When mapped in latitude and longitude the regions typically have the form shown in figure 5.6. At the given zenith and azimuth (150° and 270° respectively) access by positively charged 7 GeV particles to a satellite in a 400 km geocentric orbit is explicitly forbidden at all points on the Earth's surface shown by the hatching. The boundary of the central region (within which access is not explicitly forbidden as a result of 1st and 2nd loop Earth intersections) is in part formed by the edge of the region associated with 1st loop intersections, and in part by the edge of the region associated with the 2nd loop intersections. As rigidity varies the region defined by the first order shadow orbits changes shape as shown in figure 5.7. The 2nd order shadow limits are more stable, and change very little over this rigidity range. A change in zenith typically produces the shift shown in Figure 5.8, and change in azimuth the shift to the positions shown in figure 5.9 and 5.10.

The Band Shift Factor (see Chapter 4) can be used to quantitatively express the stability of these structures (see Table 5.1). It is interesting to note the relatively great stability of the central second order structure, which lies along the geomagnetic equator.

By examination of the form and position of the shadow orbit defined regions it is possible to discount the possibility of high zenith angle entry at azimuths well away from the west, and to rigidities less than a given value (which value depends on the zenith angle considered, e.g. entry is forbidden for rigidity > 9 GV at zenith angle of 150°).

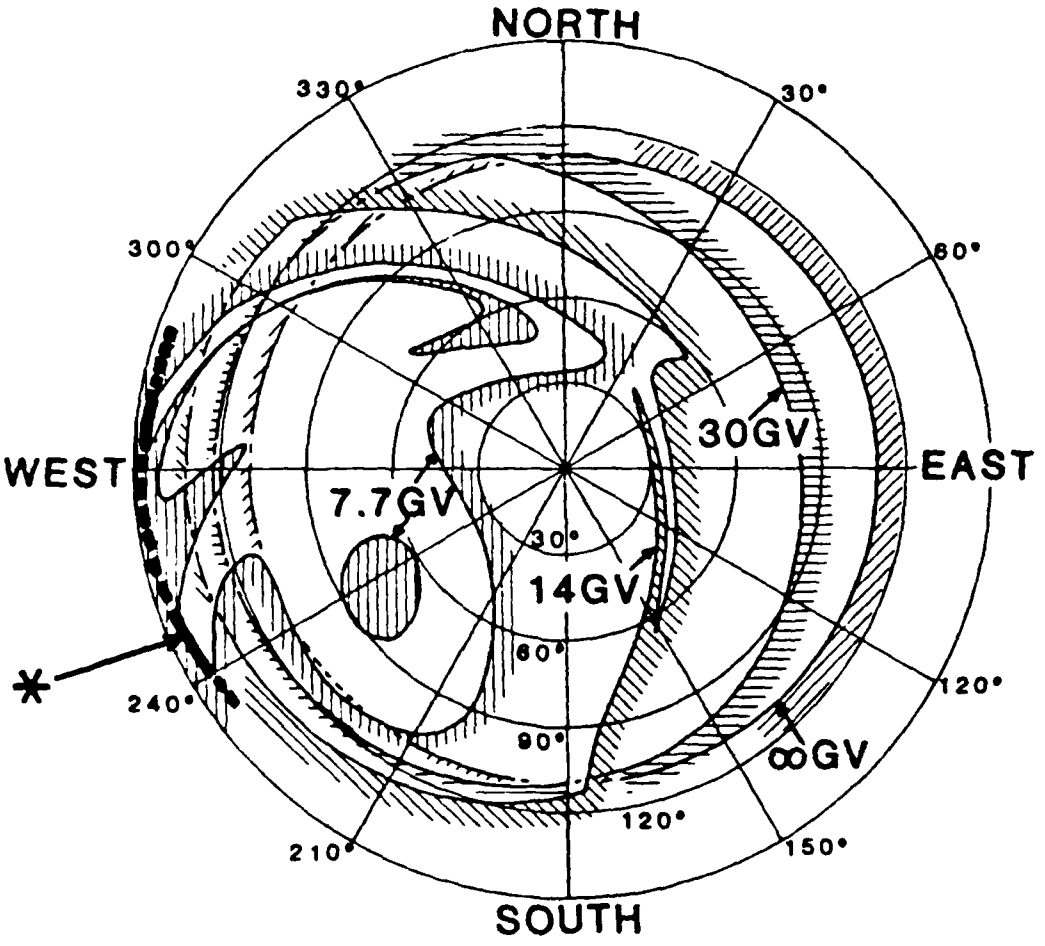

FIGURE 5.5

Position of allowed and forbidden structures mapped in zenith and azimuth space for the indicated rigidity values, at the point 10^{o} N latitude, 270 E longitude (IGRF80 field). The shadow structure limiting the high zenith angle entry in the west, for the 7.7 GV rigidity value, is indicated by an asterisk.

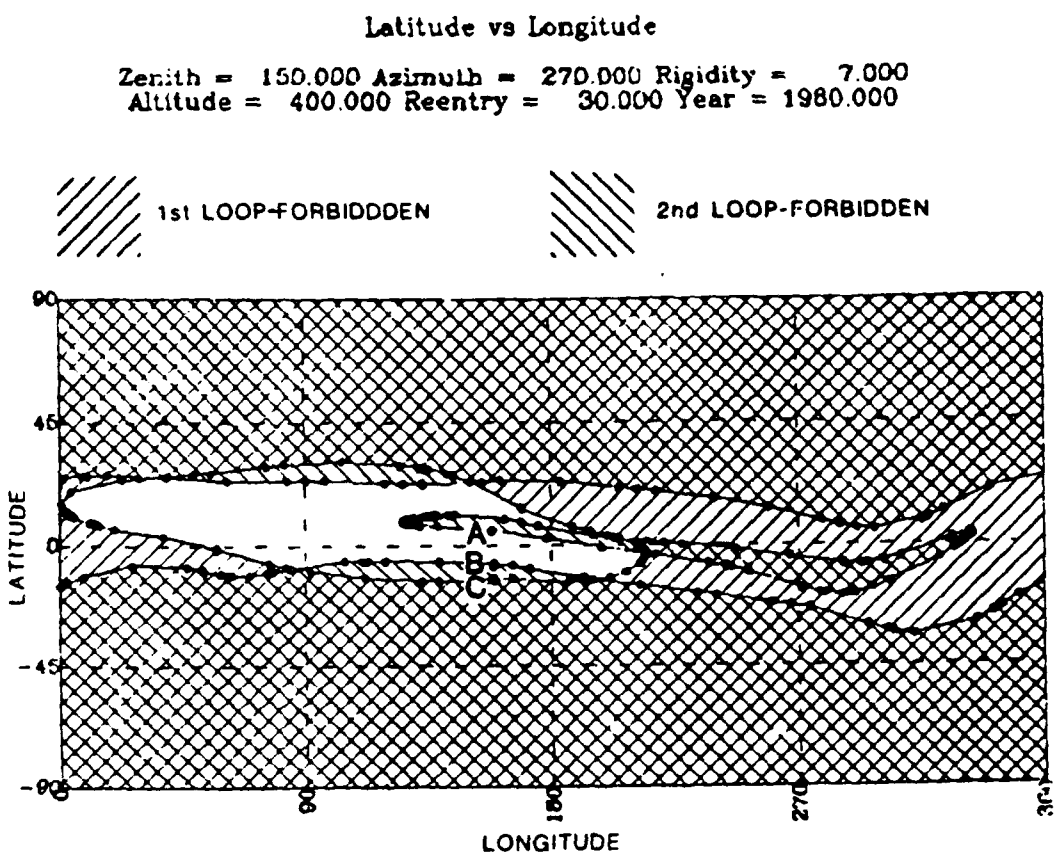

FIGURE 5.6

Latitude-longitude map showing zones of access under the indicated conditions. The Band Shift Factors have been calculated for points A, B, and C, and are presented in Table 5.1. The shaded region is inaccessible due to intersection of 1st and/or 2nd loops with the atmosphere.

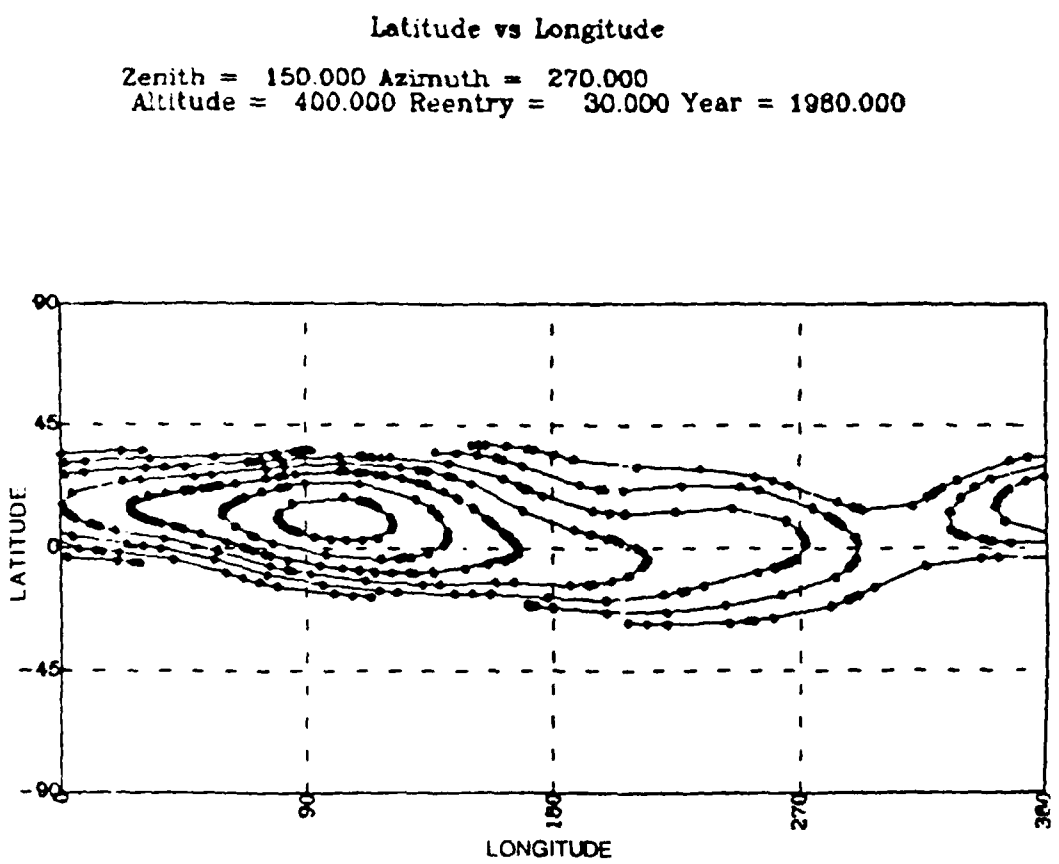

FIGURE 5.7

Position of the first order shadow edge for 8.5, 8.0, 7.5, 6.5, 6.0, and 5.5 GV (8.5 GV is the innermost, smallest, region), under the stated conditions.

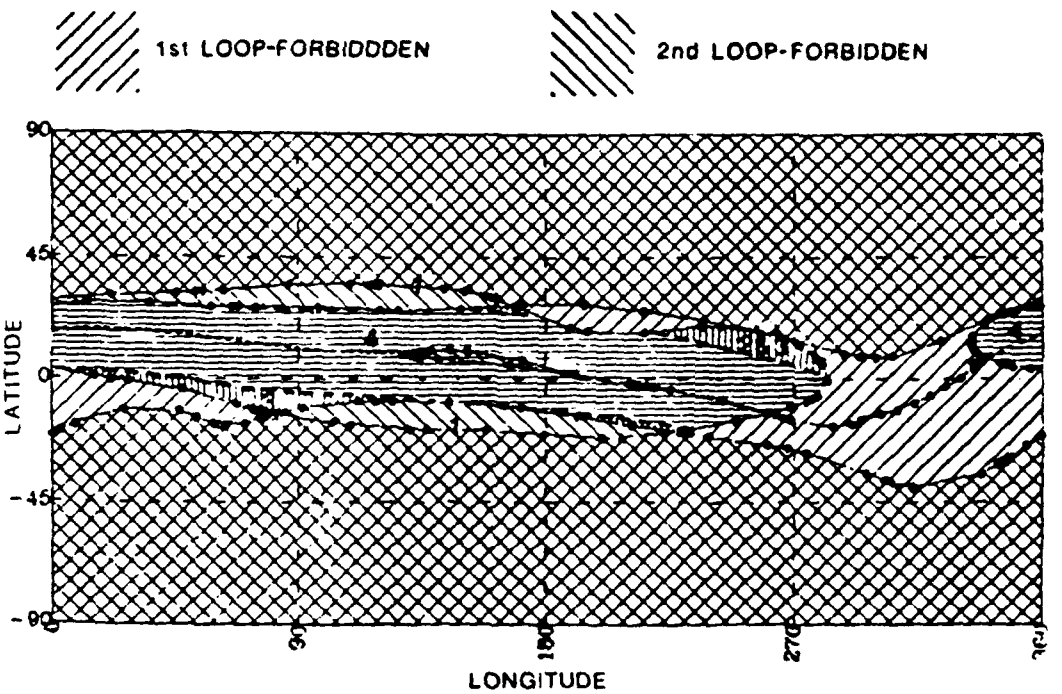

FIGURE 5.8

Latitude-longitude map for the conditions noted, showing categorized zones of access (this figure corresponds to the same set of conditions under which figure 5.6 was produced, except that it pertains to 145° zenith rather than the 150° zenith of Figure 5.6).

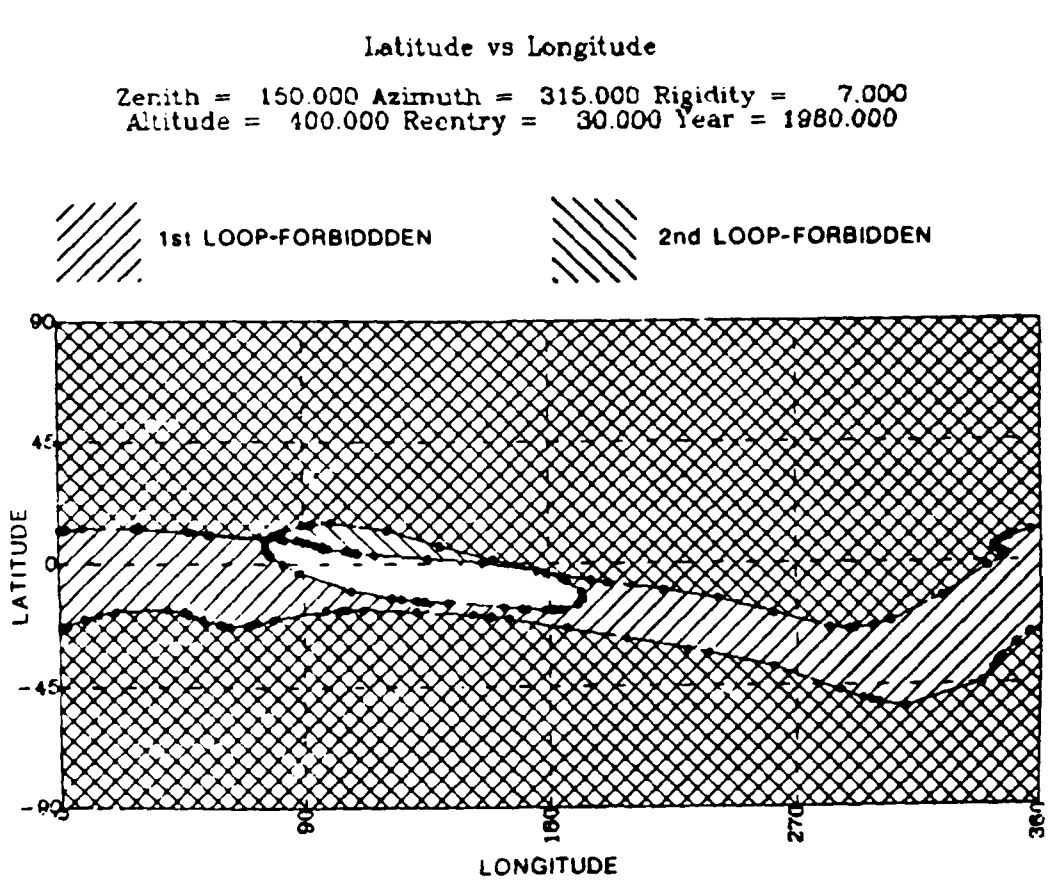

FIGURE 5.9

Latitude-longitude map drawn for same conditions as for Figure 6, except that the azimuth is now 225°, rather than 270° east of north.

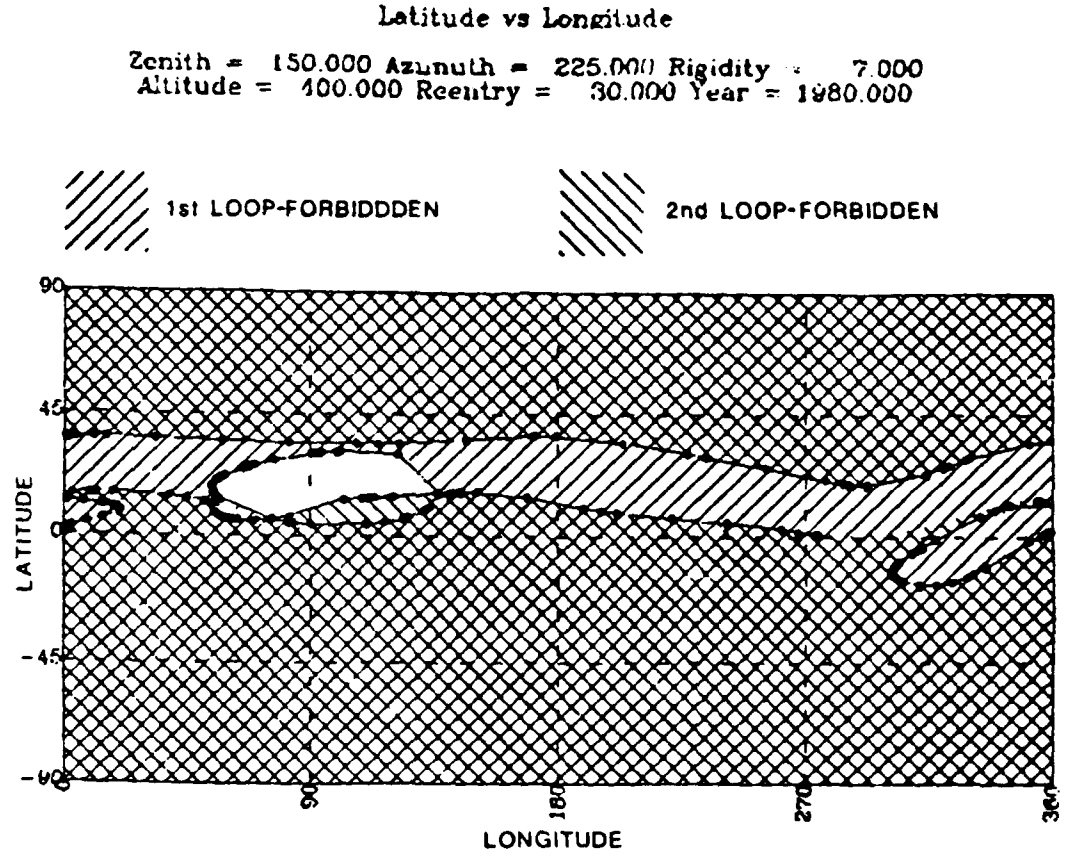

FIGURE 5.10

Latitude-longitude map drawn for the same conditions as for figure 5.6, except that the azimuth is now 315°, rather than 270° east of north.

TABLE 5.1

Band Stability Factor $\delta R/\delta P$, where R is rigidity, and P is the parameter in question, for the points A, B, and C in Figure 5.6. Large BSF values are associated with relatively stable structures.

POINT	LAT	LON	ZE	AZ	ALT	GRAZ
A	-0.595	-0.043	-0.174	-0.054	0.015	-0.018
B	-0.750	-0.030	0.236	-0.247	-0.014	0.013
C	0.109	-0.004	-0.245	0.032	0.019	-0.023

Within the central region exist fine allowed-forbidden structures associated with 3rd, 4th, and so on, loop intersections. The mapping of these structures has been found impractical because of the large amount of computer time required. In any case the detailed form of the structures depend significantly on the choice of geomagnetic field model used in the calculations (whereas the structures associated with 1st and 2nd loop intersections are relatively stable). It is therefore necessary to use some other means of determining what access is possible into this region.

Examination of the form of the trajectories associated with approach to points within the central region allows the question of access from points outside the geomagnetic field to be pursued, and permits general conclusions to be drawn about whether access is possible or impossible in given situations. This examination has been done by means of sets of trajectory traces applying to directions spaced in latitude and longitude (typically at 5^{o} intervals in latitude, and 30^{o} in longitude). The trajectories are displayed on a video terminal and visually categorized into types 2,3, or 4. Generally type 3 and 4 orbits are readily distinguished, although there is a less distinct difference between type 3 and type 2 orbits. The question arises of when short range quasi-periodicity turns into a regular periodicity. Not withstanding this point, meaningful boundaries can be established. Figure 5.8 shows the location of the boundaries for this set of conditions.

In general it is found that trajectories originating close to the geomagnetic equator show the most simple and regular periodicity (see figures 5.3 and 5.4). Further away to either side the trajectories become more complex in their periodic form, and further away again degenerate into unstable quasi-periodic or aperiodic forms (see figure 5.2), along which access may occur from outside the field (the short range shadow structures tend to be responsible for preventing access along what otherwise may be allowed trajectories). It is possible to anticipate whether trajectories of type 2 occur before the shadow edges close off access, and it is therefore found unnecessary to actually locate an allowed trajectory in order to anticipate possible access via trajectories of this type.

The offset of the earth's dipole gives rise to a strong longitudinal asymmetry in the form of the regions (see figure 5.7, for example). There is a strong tendency for type 4 trajectories to be normally associated with access to points at longitudes close to 300^{o}, whereas type 3 predominate over the rest of the longitude range. Because the 1st order shadow patterns are mainly (for the conditions of interest) centered within the range 90-180^{o} longitude, these regions can be regarded as being populated largely by type 3 trajectories, with type 2 orbits (if they occur at all in a given situation) lying at points removed from the geomagnetic equator.

In general, as rigidity decreases, the size of the mapped regions increase. At the same time, however, the trajectory configurations evolve into a much more tightly bound periodic form, of types 3 and 4. Particles could conceivably populate such trajectories - possibly primary cosmic rays under time varying conditions, or splash albedo particles, for example.

5.3 CONCLUSION

In extending this preliminary investigation it will be necessary to make an examination of the zenith, azimuth, rigidity, and altitude dependence of the mapped regions. In this way a more complete picture could be drawn up of the zenith angle limits of access - limits to the regions containing trajectories associated with access of the kinds possible and impossible, probable and improbable.

CHAPTER 6: THE MAIN CONE IN THE REAL MAGNETIC FIELD

6.1 INTRODUCTION

The "main cone" is the boundary of the fully unconditionally allowed cone within which cosmic rays of a given rigidity approach a point within a planetary magnetic field. It is constituted in part by trajectories which are asymptotic to the simplest bound periodic orbits, and in part by trajectories which graze the surface of the planet. In this chapter the phenomenology of the former of these two types of trajectories is discussed, and a technique is described by which main cone cutoffs may be calculated by computer to very high precision.

Lemaitre and Vallarta investigated the properties of the main cone as it applies to a simple dipole representation of the Earth's magnetic field. The currently reported research has shown that a corresponding true main cone also exists at locations in the real geomagnetic field. The form of the main cone in the real field is very similar to that found by Lemaitre and Vallarta to occur in the simple dipole field representation.

The facility of determining the main cone structure in the real field is valuable, because often a knowledge is required of the rigidity limit above which unconditional cosmic ray entry could be expected to exist in specific situations under real field conditions. The normal unmodified iterative trajectory trace method of penumbral mapping, relying as it does on the detection of forbidden trajectories, cannot yield a reliable estimate of this upper rigidity limit.

6.2 DISCUSSION

Figure 6.1 shows a typical main cone trajectory, which displays characteristic regular equator crossings. Note that the trajectory, like others of its kind, lies essentially within a constant altitude shell, disposed at an essentially constant distance from the Earth's equivalent dipole. The dependence of the position of the shell, as determined from

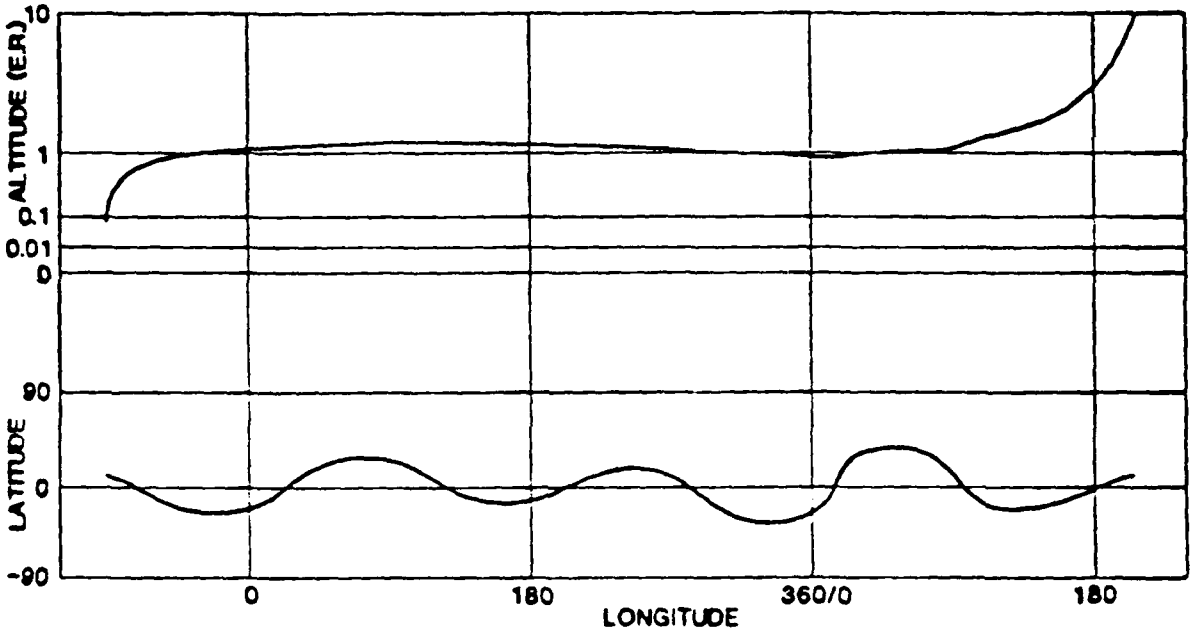

FIGURE 6.1

Typical "real" field asymptotic quasi-bound periodic orbit, which lies very close to the main cone edge (trajectory starting point parameters: geographic latitude 10^{o} N, longitude 270^{o} E, zenith angle 7.9368^{o}, azimuth 270^{o}, rigidity 10 GV, 400 km geocentric altitude; IGRF80 field representation). The position of the trajectory is plotted as a function of geographic latitude and longitude, and geocentric altitude.

trajectories calculated to exist in a real field representation, on rigidity corresponds closely to the Stormer radius for the given rigidity (the radius at which a charges particle traces a circular orbit about the Earth's equivalent dipole). Figure 5.2 shows the dependence of the position of the shell as a function of rigidity, both as found to exist in a real field representation, and as predicted by the Stormer relation

$$\text{radius} = \sqrt{(59.6/\text{rigidity})} \quad \text{for the Earth's field}$$

It is useful to appreciate that main cone cutoff values of more than about 60 GV cannot exist in the real field because the shell containing the bound periodic orbit would have to lie within the solid Earth. Neither could main cone cutoff values below about 0.3 GV be found in the real field because, in this case, the shell containing the bound periodic orbit would have to lie at a radius of more than 10 Earth radii from the Earth's equivalent dipole - which would place the shell outside the magnetospheric boundary on the "upwind" (i.e. solar wind) side of the field.

Trajectories, for specific rigidity values, traced in the "negative time" direction, from the point of interest in the field outward through the magnetosphere, cut through the shells corresponding to lower rigidity values with a positive slope. In particular, at the point along the trajectory where the magnetic equator is crossed, the slope of the trajectory at those points is positive. On the other hand, it is found that the slopes at the corresponding equator crossings associated with rigidity values lower than the main cone cutoff are normally negative.

The present method of determining precise main cone cutoff values utilizes this fact, and the computer program which evaluates the cutoffs locates the equator crossings and determines their slopes. Because, however, trajectories pertaining to rigidities well removed (mainly higher) from the main cone cutoff may have few of no equator crossings, it is necessary first to derive an initial estimate of the main cone cutoff before refining it by use of the equator crossing slopes.

To this end the Stormer equation is invoked. The resulting rigidity

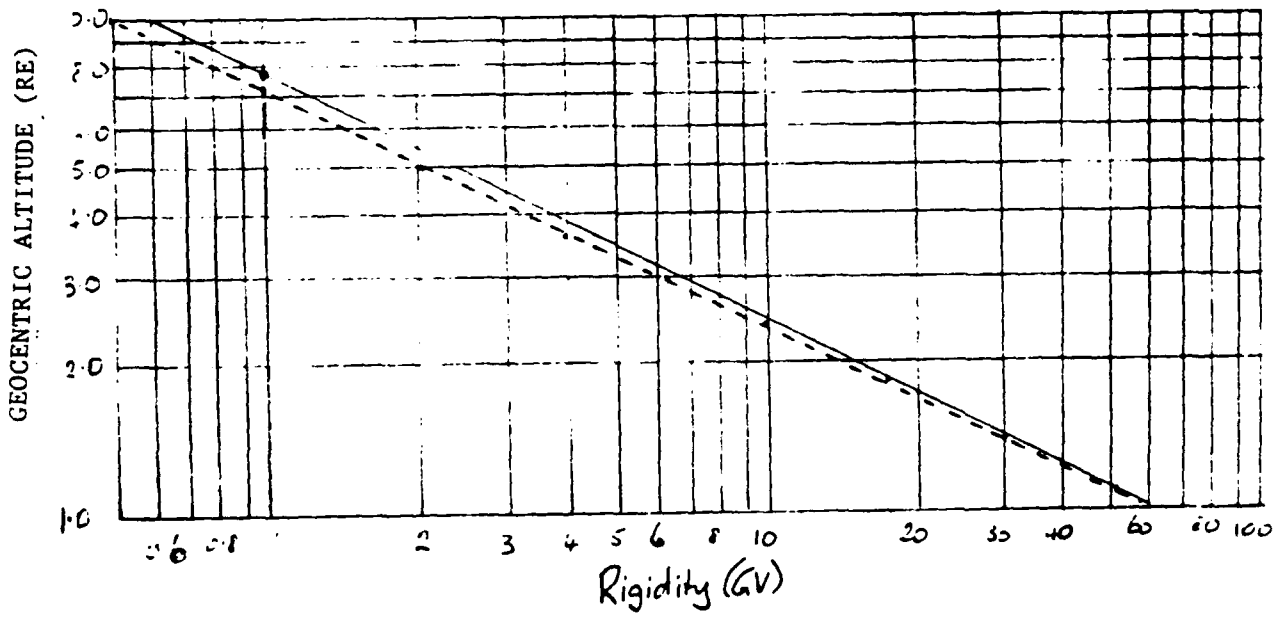

FIGURE 6.2

Altitude of shell which contains real field bound periodic orbit as a function of rigidity (dashed line). The altitude predicted from the Stormer relation is also plotted, as a solid line.

trajectories calculated to exist in a real field representation, on rigidity corresponds closely to the Stormer radius for the given rigidity (the radius at which a charges particle traces a circular orbit about the Earth's equivalent dipole). Figure 6.2 shows the dependence of the position of the shell as a function of rigidity, both as found to exist in a real field representation, and as predicted by the Stormer relation

$$\text{radius} = \sqrt{(59.6/\text{rigidity})} \quad \text{for the Earth's field}$$

It is useful to appreciate that main cone cutoff values of more than about 60 GV cannot exist in the real field because the shell containing the bound periodic orbit would have to lie within the solid Earth. Neither could main cone cutoff values below about 0.5 GV be found in the real field because, in this case, the shell containing the bound periodic orbit would have to lie at a radius of more than 10 Earth radii from the Earth's equivalent dipole - which would place the shell outside the magnetospheric boundary on the "upwind" (i.e. solar wind) side of the field.

Trajectories, for specific rigidity values, traced in the "negative time" direction, from the point of interest in the field outward through the magnetosphere, cut through the shells corresponding to lower rigidity values with a positive slope. In particular, at the point along the trajectory where the magnetic equator is crossed, the slope of the trajectory at those points is positive. On the other hand, it is found that the slopes at the corresponding equator crossings associated with rigidity values lower than the main cone cutoff are normally negative.

The present method of determining precise main cone cutoff values utilizes this fact, and the computer program which evaluates the cutoffs locates the equator crossings and determines their slopes. Because, however, trajectories pertaining to rigidities well removed (mainly higher) from the main cone cutoff may have few of no equator crossings, it is necessary first to derive an initial estimate of the main cone cutoff before refining it by use of the equator crossing slopes.

To this end the Stormer equation is invoked. The resulting rigidity

value is a very rough estimate - to within only about 40%. This estimate is still not good enough to start the cutoff refining procedures, so in order to improve the estimate, two trajectories are traced which, although only a small incremental rigidity value apart, are clearly above the actual main cone cutoff value (the chosen rigidity values are, in fact, related to the Stormer estimate multiplied by 1.5). The values of the slope of these trajectories as they pass through the shell altitude at which a bound periodic orbit could exist at their particular rigidity values are then used to produce a more precise estimate of the main cone cutoff value. These estimates are accurate to within about 5% - quite accurate enough to start the cutoff value refining process.

A pair of trajectories are traced for this rigidity value plus and minus a small rigidity increment. This pair of trajectories are found generally to contain three or more equator crossings. The values of the slopes of the third equator crossings are noted, and the dependence of the slope on rigidity is deduced. The value of the rigidity for which the slope would be zero is then computed.

A new incremental pair of trajectories are traced for this new rigidity value (the increment is decreased by approximately an order of magnitude each time a new incremental pair of trajectories is used) and the slope at the fourth equator crossing used to produce a new, refined, estimate of the main cone cutoff. Successive incremental pairs of trajectories are traced and the position of successive equator crossings used to progressively adjust the rigidity value.

This series of rigidity estimates asymptotically approaches the "true" main cone value. It is possible, in most situations, to trace main cone edge trajectories for many equator crossings after the refining process has operated for a few cycles of operation - ten crossings is generally possible. The precision achieved in the main cone cutoff estimate is correspondingly great, if in the limit, unreal, due to limitations on the precision of modeling the geomagnetic field. For most purposes it has been found sufficient to aim for a precision of 0.001 GV, which involves tracing between ten and twenty trajectories for between 5 and 7 equator crossings

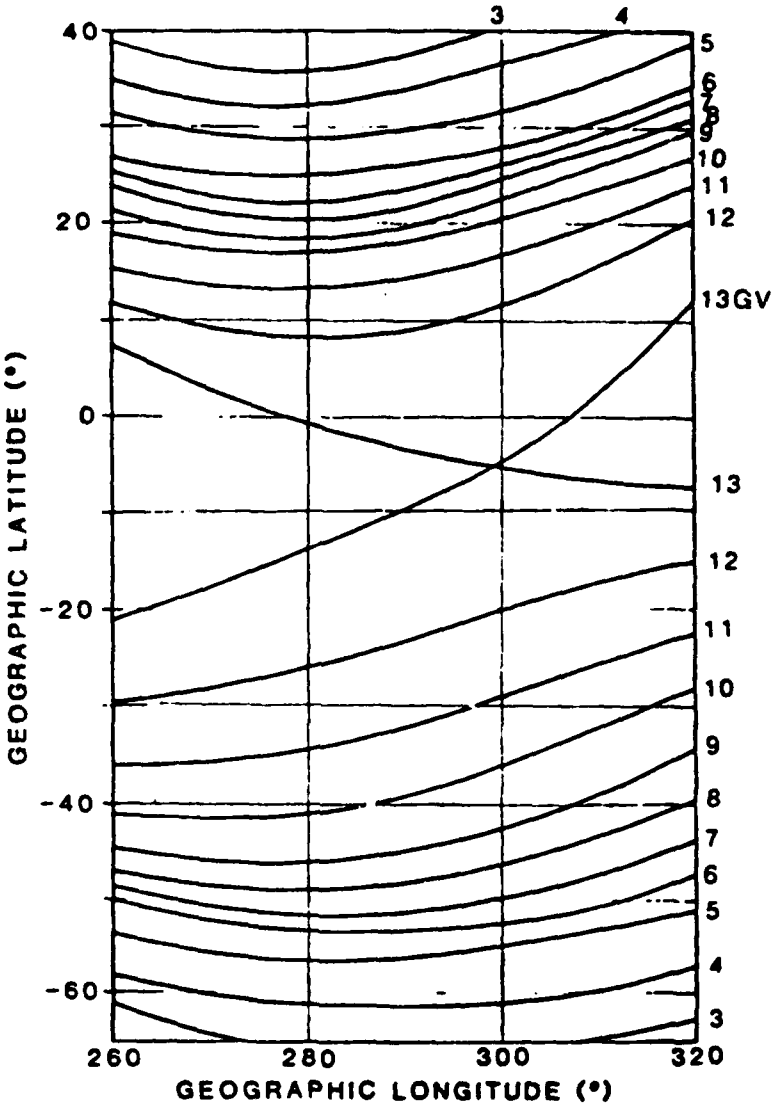

FIGURE 6.3

Contours of mail cutoff rigidity as a function of geographic latitude and longitude at 1 GV intervals in both hemispheres.

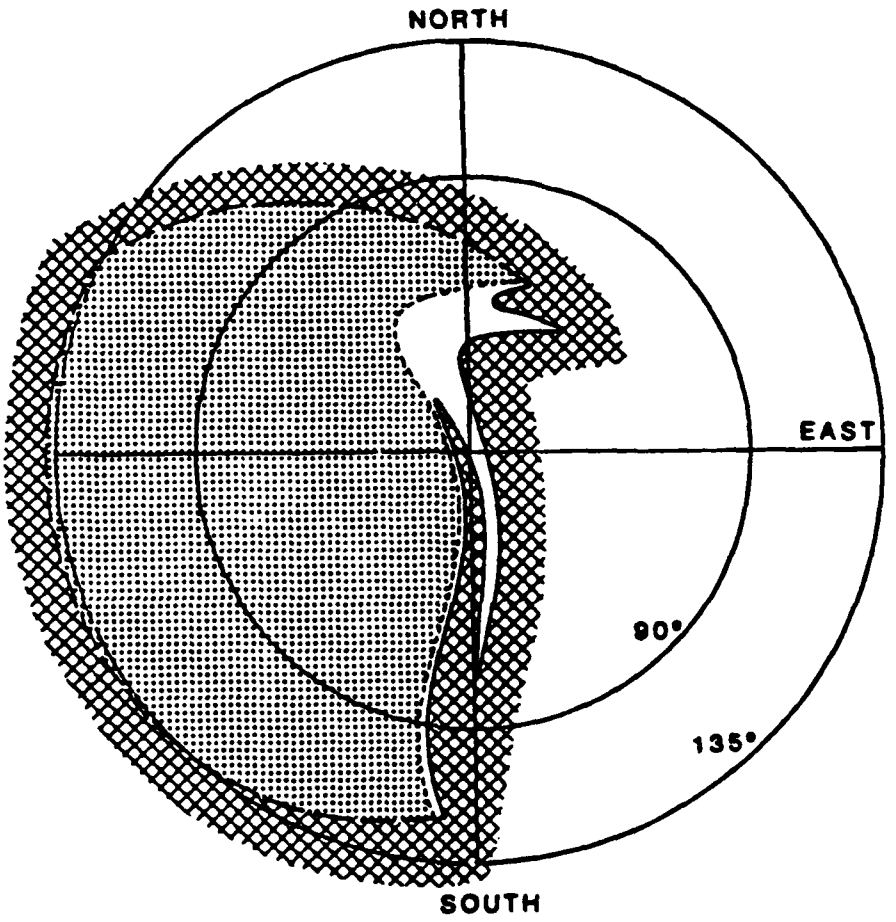

FIGURE 6.4

Penumbral information for 10 GV rigidity at the location specified in the figure 1 caption. The dotted region is the main allowed cone, the cross hatched region is forbidden due to the shadow cone and penumbral bands, and the unshaded region between is the undefined penumbra.

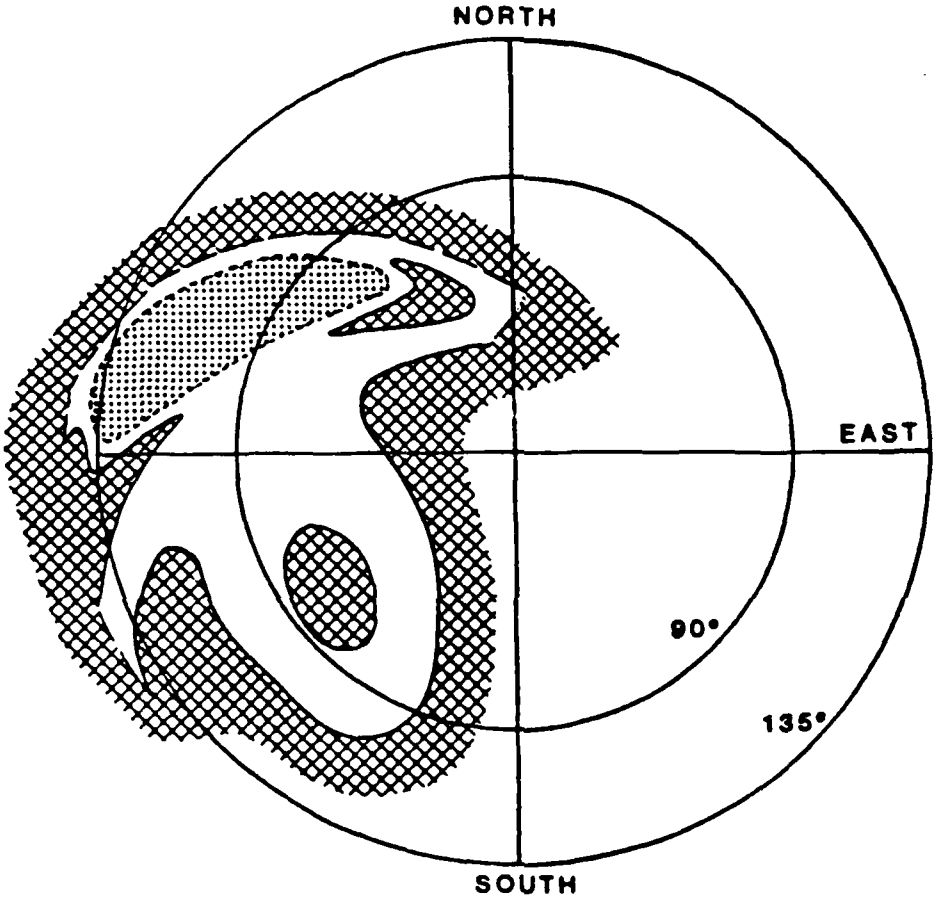

FIGURE 6.5

As for figure 6.4, for 7.7 GV.

case in penumbral trajectories, but only to the particular equator crossing targeted at the given stage in the computation procedure.

Table 6.1 presents a list of rigidity values which were produced in an actual main cutoff determination, which shows how the values very quickly asymptote to the final high precision value.

TABLE 6.1

A typical list of rigidity values associated with a main cone cutoff determination, showing the progressive refinement of the estimates, as successive equator crossings are examined. In this case the precision required of the final cutoff value was 0.001 GV.

EQUATOR CROSSING	RIGIDITY
-	14.527 (initial Stormer-based estimate)
-	10.424 (refined 1st estimate)
2	9.924243
3	9.931371
4	9.927419
5	9.927419
6	9.925816
7	9.925418
	9.925425 (final main cutoff value)

It should be noted that the procedure is unaffected by the form of the trajectory in the area of the starting point. Loops in the magnetic field line bundle in this region, via which entry into the asymptotic trajectory must be made, are responsible, as discussed by Cooke and Humble (1970), for the detailed "folded" structure in the form of the main cone. Nevertheless, the main cone edge may be located regardless of the complexity of this part of the orbit and for any arrival direction at the site of interest.

The trajectory parameterization method of deriving the main cone cutoff values is completely automatic, requiring only initial insertion of parameters specifying the location and direction of interest in the magnetic field. Examples of the results obtainable by the method are given in figures 6.4 and 6.5.

The results of this method agree with the main cutoffs derived by Shea and Smart using a procedure that enables them to detect the main cutoff while the standard iterative penumbral mapping is proceeding. Their method essentially relies on the same phenomenology as the parameterization method.

CHAPTER 7: CONCLUSIONS

7.1 USE OF THE "TRAJECTORY PARAMETERIZATION" PENUMBRAL MAPPING TECHNIQUE

A range of techniques are now available to allow the detailed mapping of cosmic ray access to locations within planetary magnetospheres. Computer programs embodying these techniques have been developed that trace the main cutoff value in any direction, trace penumbral band structure over zenith-azimuth space, or longitude-latitude space, and establish the stability of these in any direction. The assembly of these directional cutoffs into integrated cutoff distributed functions is also now a routine operation. The development of a further technique was commenced but not completed - a system by which very finely detailed penumbral structure in any direction may be automatically mapped, as a function of rigidity.

This cutoff rigidity mapping technique utilizes the trajectory parameterization approach to locate regimes of rigidity within which trajectory approach is forbidden due to some particular planet (or atmosphere) intersection. By examining the details of the trajectory at the point where it makes the intersection it is possible to efficiently establish the rigidity width of the resulting penumbral band, whether it be fine or wide. By automating strategies by which this examination is made, the program very rapidly determines the position and width of the penumbral bands, obviating the process of tracing trajectories at very fine rigidity intervals that previously had been necessary to map the penumbra in any direction. In the new technique, when a wide penumbral band is responsible for the failure of trajectories, it is necessary only to calculate a few trajectories, widely spaced in rigidity, in order to determine the band position and width. On the other hand, narrow bands are reliably detected and their details established to an equivalent precision.

7.2 POSSIBLE USE OF MAPPED PENUMBRAL DETAIL TO ESTABLISH WHETHER COSMIC RAY OBSERVATIONS COULD BE USED TO CHECK AND IMPROVE THE CURRENT MATHEMATICAL MODELS OF THE GEOMAGNETIC FIELD

Some of the penumbral features explored exhibited a very sensitive dependence on the geomagnetic field model. For example, the penumbral "islands" discussed in Chapter 4 show such a sensitive dependence. The possibility of using these structures to experimentally determine the appropriateness of any given mathematical model of the Earth's field, for example, exists. In principal if a detector could be used to observe primary cosmic rays arriving at a site in the direction of the axis of symmetry about which the islands are disposed, the spectral characteristics of the observed flux ought to reflect the characteristics of the islands - the rigidity at which, for example, the penumbral island finally disappears with reducing rigidity ought to be visible as a discontinuity in the spectrum of the cosmic ray flux. Because this rigidity value is very directly dependent on the field modeling, a comparison could be made between the cosmic ray flux in the actual situation and that predicted.

Figure 7.1 shows how the "islands" and the surrounding major penumbral structure change form with rigidity. The penumbral transmission in the axial direction of the islands would have the form, as a function of rigidity, shown in figure 7.2. Such a spectral signature should be detectable. Another phenomenon which could be observable, too, in principle, is the gradient associated with the structure in the north-west, which is a constant position over a range of rigidity.

A major difficulty arises, however, in that it would be necessary to locate the detector in fixed locations at relatively low satellite altitudes in order to accumulate the required net detector observations. The alternative to this impossible requirement would be to carry out a very long term experiment, and to correlate the events observed at different locations with the penumbral structure at the site where the event was registered, and by shifting the relative rigidity scales and effectively superimposing events, accumulate a sufficiently great normalized event total to check the form of the calculated spectra, and thus the field model.

Ground level observations are unsuitable for two reasons. First, the flux within the atmosphere would consist of secondary particles, and so the

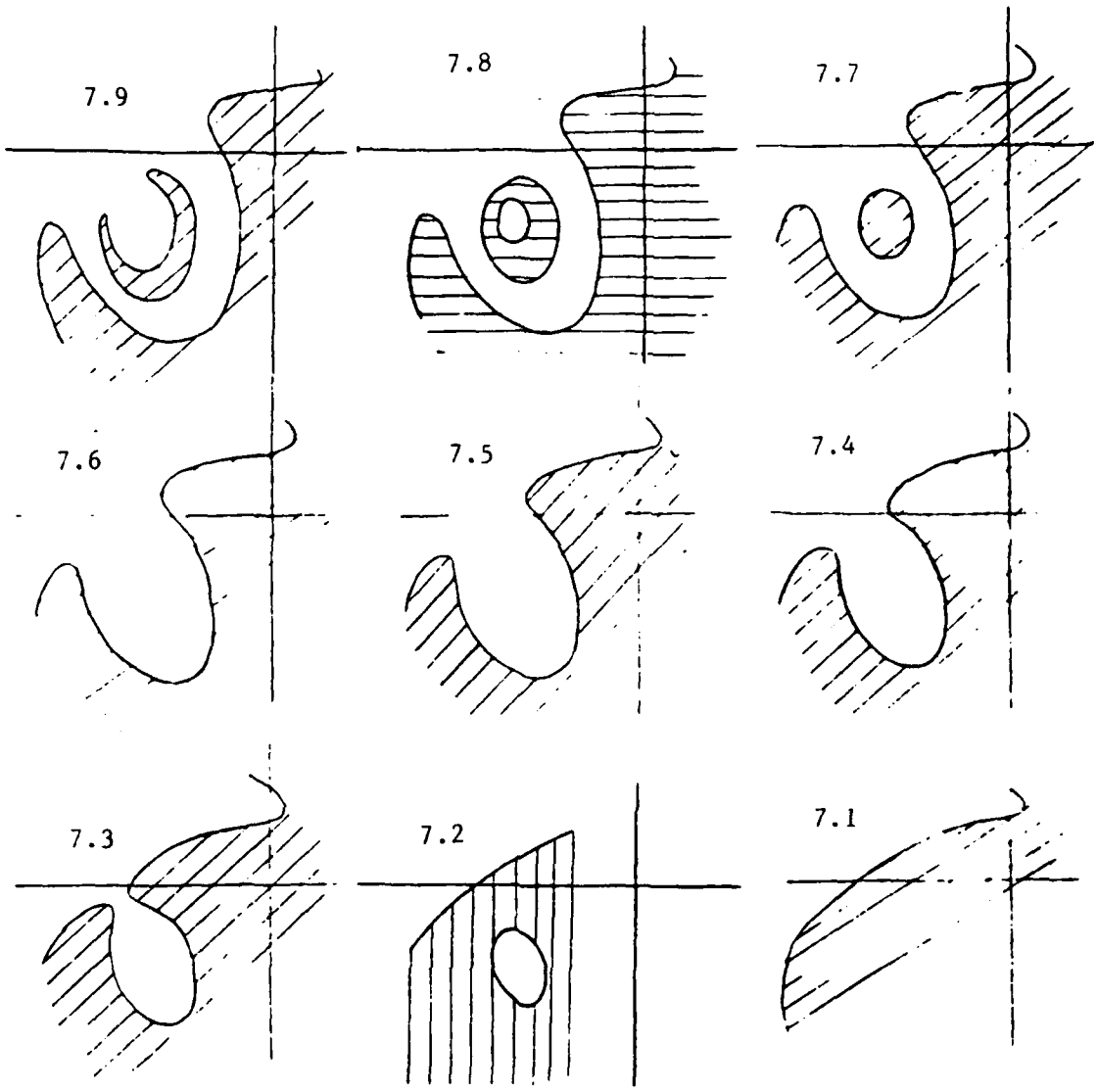

FIGURE 7.1

Variation of the size and shape of the penumbral islands and surrounding major penumbral structure with changing rigidity. The rigidity values range from 7.1 to 7.9 Gv in 0.1 GV steps. The parameters relating to these plots are the same as for figure 5.5 (10° N latitude, 270° E longitude, 400 km altitude; IGRF80 field). These are zenith-azimuth plots of the same form as figure 5.5, and may usefully be compared with that plot.

rigidity spectrum of the primaries would not be directly observable. In any case, the penumbral islands lie at high zenith angles, and would be below the horizon at ground level.

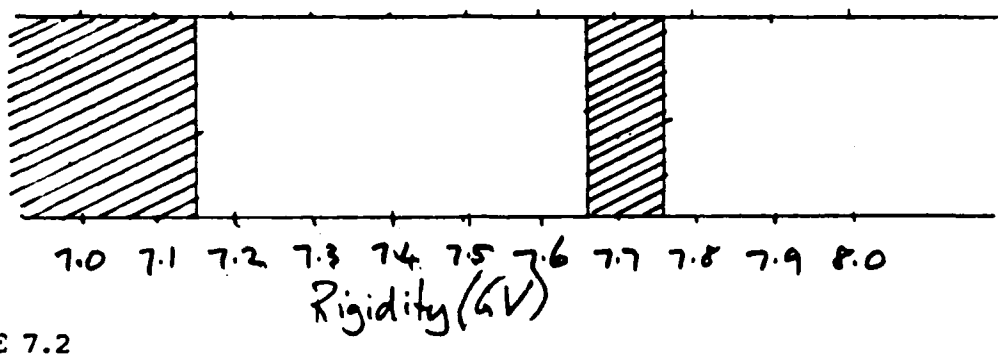

FIGURE 7.2

Penumbral transmission in the axial direction (28° zenith, 235° azimuth) of the penumbral islands in figure 7.1, as a function of rigidity (hatching represents forbidden trajectories).

An alternative is to use an experiment on board a geosynchronous satellite to correlate the existing cosmic ray fluxes with those predicted using particular field models. In order to pursue this possibility further, the parameterization technique was used to map the penumbral structure as it would exist at the orbit of a stationary satellite. Figure 7.3 presents the penumbral maps. These, calculated for a range of rigidity values, show essentially the shadow of the Earth at the given rigidities. A great degree of sensitivity does exist in some of these structures. In particular, at the rigidity where the high rigidity, essentially line-of-sight pattern bifurcates into two forbidden regions (corresponding to the Earth's shadow as seen by particles approaching from both directions along the local field line bundle) the pattern displays great sensitivity to change in the calculational parameters. An experiment on board a satellite in a stationary orbit could be used to monitor the cosmic ray fluxes in this direction, and to correlate the directional intensities with field model and time (a time dependence due to the magnetospheric compression would be expected).

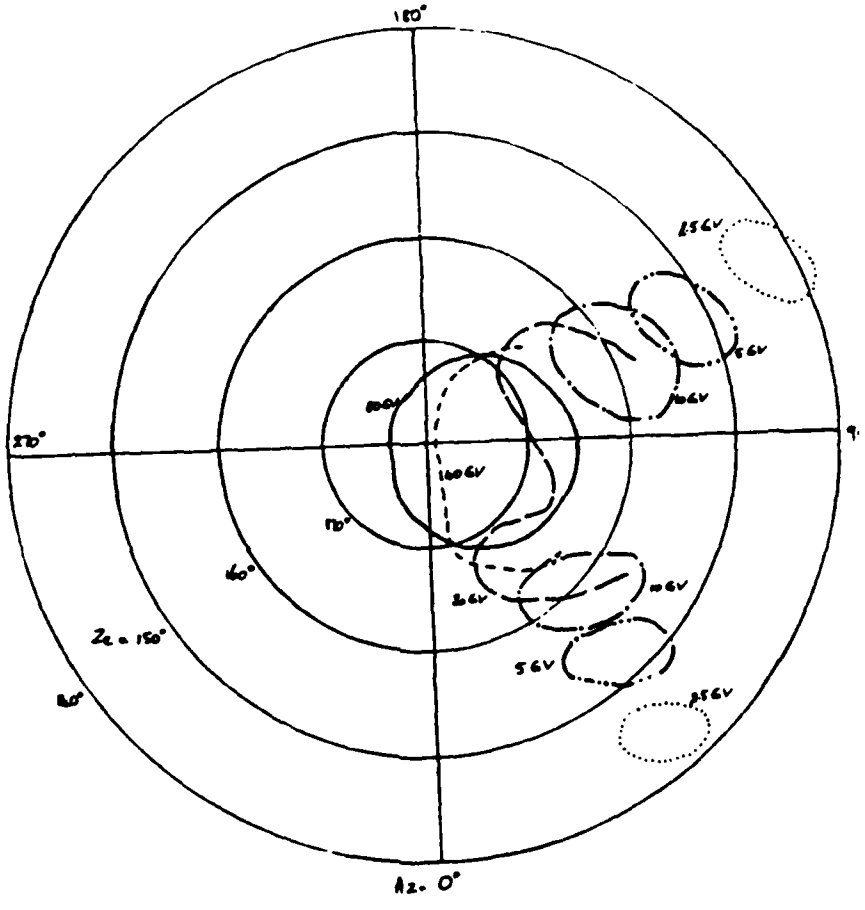

FIGURE 7.3

Penumbral structures for a range of rigidity values, as appropriate to a geosynchronous satellite lying at latitude 0^{o}, longitude 0^{o}.

REFERENCES

Acuna, M.H., and N.F. Ness, J. Geophys. Res., 81, 2917, 1976

Akasofu, S., and S. Chapman, Solar-Terrestrial Physics , Chapter 2, Oxford University Press, London, 1972

Alpher, R.A., J. Geophys. Res., 55,437, 1950

Bouckaert, L., Ann. de la Soc. Sci. de Bruxelles, A54, 174, 1934

Brunberg, E. A., Tellus, 5, 135, 1953

Brunberg, E. A., and A. Dattner, Tellus, 5, 269, 1953

Byrnak, B., N. Lund, I.L. Rasmussen, B. Peters, T. Risbo, M. Rotenberg, N.J. Westergaard, and N. Petrou, 17th ICRC, Conf. Papers, 2, 8, 1981

Cooke, D.J., U.S. Air Force Geophysics Laboratory Report No. AFGL-TR-83-0102, 1983 ADA130079

Cooke, D.J., U.S. Air Force Geophysics Laboratory Report No. AFGL-TR-83-0103, 1983 ADA130216

Cooke, D.J., Phys. Rev. Letters 51, 320, 1983

Cooke, D.J., 17th ICRC, Conf. Papers, 4, 255, 1981

Cooke, D.J., Geophys. Res. Lett., 9, 591, 1982

Cooke, D.J., 17th ICRC, Conf. Papers, 4, 263, 1981

Cooke, D.J., and J.E. Humble, J. Geophys. Res., 75, 5961, 1970

Cooke, D.J., Proc. Astron. Soc. Aust. 2,296,1974

Cooke, D.J., and J.E. Humble, 16th ICRC, Conf. Papers, 12, 243, 1979

Cooke, D.J., and S.C. Bredesen, 17th ICRC, Conf. Papers,

Dorman, L.I., R.T.Gushchina, M.A. Shea, and D.F. Smart, Nauka, Moscow, 1972

Fluckiger, E.O., D.F. Smart, and M.A. Shea, J. Geoph. Res., 88, 6961, 1983

Freon, A., and K.G. McCracken, J. Geophys. Res., 67, 888, 1962

Gaisser, T.K., T. Stanev, S.A. Bludman, and H. Lee, Phys. Rev. Lett. 51, 223, 1983

Gaisser, T.K., in Science Underground - 1982, edited by M.M. Nieto et al., AIP conf. Proc. No. 96 (Amer. Inst. of Phys., New York, 1983)

Gall, R., 17th ICRC, Conf. Papers, 13, 239, 1981

Humble, J.E., and D.J. Cooke, 14th ICRC, Conf Papers, 1341, 1975

Humble, J.E., D.F. Smart, and M.A. Shea, 17th ICRC, Conf. Pap, 10,270, 1981

Hutner, R.A., Phys. Rev., 55, 15, 1939a

Hutner, R.A., Phys. Rev., 55, 614, 1939b

IAGA Division 1 Study Group, J. Geophys. Res., 81, 5163, 1976

Kasper, J.E., Suppl. Nuovo Cimento, 11, 1, 1959

Kasper, J.E., J. Geophys. Res., 65, 39, 1960

Lemaitre, G., and M.S. Vallarta, Phys. Rev. 49, 719, 1936a

Lemaitre, G., and M.S. Vallarta, Phys. Rev., 50,493, 1936b

Lemaitre, G., M.S. Vallarta, and L. Bouckert, Phys. Rev., 47, 434, 1935

Lezniak, J.A., D.F. Smart, and M.A. Shea, 14th ICRC, Conf. Papers, 4, 1315, 1975

Lund, N., and A. Sorgen, 15th ICRC, Conf. Papers, 11, 292, 1977

McCracken, K.G., U.R. Rao, B.C. Fowler, M.A. Shea, and D.F. Smart, IQSY Instruction Manual No. 10, 1965

McCracken, K.G., U.R. Rao, B.C. Fowler, M.A. Shea, and D.F. Smart, Annals of the IQSY, 1, 198, 1968

McCracken, K.G., MIT Tech. Report, 77, NYQ-2670, 1962

Malmfors, K.G., Ark. for Matematik, Astronomi och Fysik, 32A, 8, 1, 1946

Obayashi, T., and Y. Hakura, J. Atmos. Terrestr. Phys., 18, 101,1960

Peddie, N.W., J. Geophys. Geoelectr., 34, 309, 1982

Petrou, N., and A. Soutoul, 15th ICRC, Conf. Papers, 11, 273, 1977

Quenby, J.J., and W.R. Webber, Phil. Mag.(eight series) 4, 90, 1959

Roederer, J.G., Rev. Geophys. & Space Phys. 10,599, 1972

Schremp, E.J., Phys. Rev., 54, 153, 1938a.

Schremp, E.J., Phys. Rev., 54, 158, 1938b

Schwartz. Suppl., Nuovo Cimento, 11, 27, 1959

Shea, M.A., and D.F. Smart, Acta Physica, 29, Suppl 2, 533, 1970

Shea, M.A., and D.F. Smart, 12th ICRC, Conf. Papers, 3, 854, 1971

Shea, M.A., and D.F. Smart, J. Geophys. Res.,80, 1202, 1975

Shea, M.A., and D.F. Smart,

Shea M.A., D.F. Smart, and J.R. McCall, Can. J. Phys., 46, S1098, 1968

Shea, M.A., D.F. Smart, and K.G. McCracken, J. Geophys. Res., 70, 4117, 1965

Smart, D.F., and M.A. Shea, U.S. Air Force Geophysics Laboratory Report No. AFGL-TR-82-0320, 1982. ADA126266

Soutoul, A., J.J. Engelmann, P. Goret, E. Juliusson, L. Koch-Miramond, P. Masse, N. Petrou, Y. Rio, and T. Ribo, 17th ICRC, Conf. Papers, 9, 105, 1981

Stormer, C., Zeits. fur Astrophys., 1, 237, 1930

Stormer, C., The Polar Aurora, Oxford Univ. Press, London, 1955

Treiman, S.B., Phys. Rev., 89, 130, 1953

Vallarta, M.S., An Outline of the Theory of the Allowed Cone of Cosmic Radiation, Univ. of Toronto Studies, Appl. Math. Series No. 3, Univ. Toronto Press, Toronto, 1938

Vallarta, M.S., Handbuch der Physik, XLVI/I, 88, 1961

Vallarta, M.S., 12th ICRC, Conf. Papers, Invited Papers, 474, 1971

Winkler, J.R., and K. Anderson, Phys. Rev., 93, 596, 1954